NAVAL POSTGRADUATE SCHOOL
Monterey, California

THESIS

NONCOHERENT DETECTION OF BFSK SIGNALS WITH

LINEAR AND NONLINEAR DIVERSITY COMBINING

OVER RICIAN FADING CHANNELS WITH PARTIAL

BAND INTERFERENCE

by

Ahmet Cem Karaagac

March 1991

Thesis Advisor:	Clark Robertson
Co-Advisor :	Tri T. Ha

Approved for public release; distribution is unlimited.

91 1121 021

91-16115

Unclassified

Security Classification of this page

REPORT DOCUMENTATION PAGE

1a Report Security Classification Unclassified		1b Restrictive Markings		
2a Security Classification Authority Unclassified		3 Distribution Availability of Report Approved for public release; distribution is unlimited.		
2b Declassification/Downgrading Schedule				
4 Performing Organization Report Number(s)		5 Monitoring Organization Report Number(s)		
6a Name of Performing Organization Naval Postgraduate School	6b Office Symbol (If Applicable) EC	7a Name of Monitoring Organization Naval Postgraduate School		
6c Address (city, state, and ZIP code) Monterey, CA 93943-5000		7b Address (city, state, and ZIP code) Monterey, CA 93943-5000		
8a Name of Funding/Sponsoring Organization	8b Office Symbol (If Applicable)	9 Procurement Instrument Identification Number		
8c Address (city, state, and ZIP code)		10 Source of Funding Numbers		

Program Element Number	Project No	Task No	Work Unit Accession No

11 Title (Include Security Classification) NONCOHERENT DETECTION OF BFSK SIGNALS WITH LINEAR AND NONLINEAR DIVERSITY COMBINING OVER RICIAN FADING CHANNELS WITH PARTIAL BAND INTERFERENCE (Unclassified)

12 Personal Author(s) Karaagac, Ahmet C.

13a Type of Report Master's Thesis	13b Time Covered From To	14 Date of Report (year, month,day) March 1991	15 Page Count 146

16 Supplementary Notation The views expressed in this thesis are those of the author and do not reflect the official policy or position of the Department of Defense or the U.S. Government

17 Cosati Codes

Field	Group	Subgroup

18 Subject Terms (continue on reverse if necessary and identify by block number)

19. Abstract (Continue on reverse if necessary and identify by block number) A performance analysis of Binary Orthogonal Frequency Shift Keying (BFSK) Fast Frequency Hopped (FFH) receivers implemented with both square-law and envelope detectors is performed. Bit error probabilities of the two types of receivers for linear combining , noise-normalization combining, and self-normalization combining under worst-case partial-band interference with nonselective Rician fading and thermal noise are compared. The analysis is repeated for the case of no interference to point out the effect of fading. A study of nonlinear diversity combining receivers (self-normalization and noise-normalization) is also performed for a system model that is free from thermal noise. Envelope and square-law detectors for particular types of nonlinear combining investigated do not differ in performance, but this is not true for linear combining detectors. The visible superiority of envelope detectors for linear combining is noted. Nonlinear combining receivers achieve a diversity and performance improvement compared to linear combining receivers.

20 Distribution/Availability of Abstract Unclassified	21 Abstract Security Classification [X] unclassified/unlimited [ ] same as report [ ] DTIC users	
22a Name of Responsible Individual Robertson, Clark.	22b Telephone (Include Area code) 408-646-2383	22c Office Symbol EC/RC

DD FORM 1473, 84 MAR   83 APR edition may be used until exhausted   security classification of this page

All other editions are obsolete   Unclassified

NONCOHERENT DETECTION OF BFSK SIGNALS WITH LINEAR AND NONLINEAR
DIVERSITY COMBINING OVER RICIAN FADING CHANNELS WITH PARTIAL-BAND
INTERFERENCE

by

Ahmet Cem Karaagac
Lieutenant JG, Turkish Navy
B.S., Turkish Naval Academy, 1985

Submitted in partial fulfillment
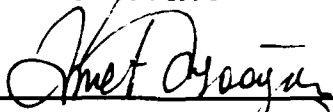of the requirements for the degree of

MASTER OF SCIENCE IN ELECTRICAL ENGINEERING

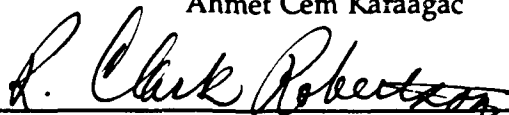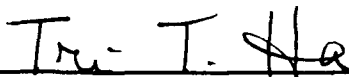from the

NAVAL POSTGRADUATE SCHOOL

March 1991
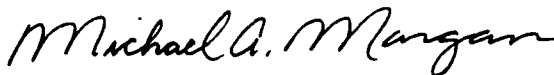
Author: _____

Ahmet Cem Karaagac

Approved by: _____

Clark Robertson, Thesis Advisor

_____

Tri T. Ha, Co-Advisor

_____

Michael A. Morgan, Chairman

Department of Electrical and Computer Engineering

ii

ABSTRACT

A performance analysis of Binary Orthogonal Frequency Shift Keying (BFSK) Fast Frequency Hopped (FFH) receivers implemented with both square-law and envelope detectors is performed. Bit error probabilities of the two types of receivers for linear combining, noise-normalization combining, and self-normalization combining under worst-case partial-band interference with nonselective Rician fading and thermal noise are compared. The analysis is repeated for the case of no interference to point out the effect of fading. A study of nonlinear diversity combining receivers (self-normalization and noise-normalization) is also performed for a system model that is free from thermal noise. Envelope and square-law detectors for particular types of nonlinear combining investigated do not differ in performance, but this is not true for linear combining detectors. The visible superiority of envelope detectors for linear combining is noted. Nonlinear combining receivers achieve a diversity and performance improvement compared to linear combining receivers.

iii

TABLE OF CONTENTS

I. INTRODUCTION

Previous studies have proven that Fast Frequency Hopped (FFH) Spread-spectrum communication systems are alternatives to conventional systems under the presence of multipath fading and/or partial-band interference.

Difficulties in synchronous carrier recovery in a multipath fading environment enables noncoherent orthogonal FFH Binary Frequency Shift Keying (FFH-BFSK) modulation to be an attractive choice [Ref. 1]. At the receiver, demodulation of the dehopped signal is performed by a circuit implemented with bandpass filter and envelope detector arrays. Envelope and square-law detectors are used interchangeably. Their performances have been proven to be identical for some cases, and have been accepted as identical for the others. An envelope detector is easier to implement, while a square-law detector is easier to obtain analytical result for. This assumption of identical performance is examined for FFH-BFSK orthogonal noncoherent modulation systems with L-fold diversity and both linear (ordinary FFH-BFSK) and nonlinear combining. For the latter case, two systems are analyzed:

1. Noise-normalization (Adaptive Gain Control (AGC) [Ref. 2]) combining in which noise and interference statistics are assumed to be known or predicted.

2. Self-normalization combining which does not require the noise and interference statistics to be known.

In order to make the research applicable to satellite-to-mobile applications a Rician fading channel is assumed.

The performances of the systems are also inspected under the absence of interference to emphasize the effect of fading. As a special case both of the nonlinear combining systems are analyzed under the absence of the thermal noise to show the effect of the thermal noise on the performances of the systems.

Chapter II presents background information, and a description of the models, and evaluation of the bit error rates are given in Chapter III. In Chapter IV, numerical results are presented. Conclusion are given in Chapter V.

II. BACKGROUND INFORMATION

The behavior of envelope and square-law detectors are analyzed with a model similar to that presented in [Ref. 1] and [Ref. 3].

FFH-BFSK communication systems employing a diversity level of L, communicating over a channel of bandwidth W, are assumed to be effected by an interference source. The interference is assumed to be an additive narrow-band Gaussian process over an equally probable portion γ of the channel bandwidth W. The BFSK modulator represents a binary input 1 with the frequency f_1 and a binary input 0 with that of f_2, in a binary symmetric channel model scheme. The bit duration of T_b is equally divided into L chips. The bit rate is $R_b = 1/T_b$, and the hopping rate is $R_h = L/T_b = LR_b$. The binary signal is passed through a baseband filter of bandwidth $R_h + R_b$. The output of the baseband filter modulates the signal generated by a frequency hop synthesizer. The frequency hop synthesizer is driven by a pseudorandom code generator. The hopping frequency f_h is a discrete uniform process taking one of the N possible levels where $N = W/R_h$. The modulated signal is filtered by a baseband filter of bandwidth R_h, upconverted by a RF oscillator, and transmitted.

If the cell bandwidth is small compared to the channel coherence bandwidth, the fading process can be modelled as frequency nonselective; furthermore, if the channel bandwidth is large enough to assign a minimum spacing between two consecutive hopping frequencies that is large compared to the coherence bandwidth of the channel, each cell fades independently. Under these assumptions the amplitude of the dehopped signal is modelled as a Rician random variable. The intensity of the fading is assumed to be constant for the entire bandwidth, as a result, the statistics of the L Rician random variables affecting the L hops of a bit are equal.

The interference is assumed to be additive white Gaussian noise. Whether the interference is a deliberate jammer or a coincidental narrowband process, it is not always possible to maximize the negative impact on the performance of the communication link when the finite energy is spread over the entire bandwidth. Reference 4 shows that for the linear combining square-law detector, especially with relatively high diversity levels (when the number of hops per bit is greater than 2), it is not an effective jamming strategy to distribute the total jamming power uniformly over the entire bandwidth even when the signal and the interference energies are equal at the receiver RF circuit. When the jamming power is not distributed uniformly over the entire bandwidth, there exists a certain portion (γ) of bandwidth that maximize the Bit Error Rate (BER) as a function of the variables:

4

1. Interference energy.

2. Thermal noise energy.

3. Detector type.

4. Hopping rate.

5. Severity of fading.

The average power spectral density (PSD) of the narrowband interference is $N_I/2$ when spread over the entire bandwidth W; therefore, the conditional partial-band interference PSD is $N_I/2\gamma$ if it is present, zero otherwise.

III. SYSTEM AND WAVEFORM ANALYSIS

A. DESCRIPTION OF THE WAVEFORMS

The interference power is uniformly distributed over γW Hz of the total system bandwidth W. The received signal after the kth dehopping, where k is an integer taking a value from 1 to L, is represented as:

$$r_k(t) = \begin{cases} s_k(t) + n_k(t) + i_k(t) & \text{with probability } \gamma \\ s_k(t) + n_k(t) & \text{with probability } (1-\gamma) \end{cases} \quad (1)$$

$$(k-1)\tau_h < t \leq k\tau_h$$

where $s_k(t)$ is the information carrying signal affected by fading, $n_k(t)$ is the thermal noise component, and $i_k(t)$ is the interference noise component. The information carrying signal in the kth hop interval is:

$$s_k(t) = \begin{cases} a_k\sqrt{2S} \cos(2\pi f_1 t + \theta_k) & \text{binary 1 is sent} \\ a_k\sqrt{2S} \cos(2\pi f_2 t + \phi_k) & \text{binary 0 is sent} \end{cases} \quad (2)$$

where θ_k and ϕ_k are random phases uniformly distributed over $(0, 2\Pi)$. The average signal power is $a_k^2 S$, and a_k is a Rician random variable. Channel fading is assumed to be slow compared to the hoptime, but each hop is assumed to be independent. The statistics of a_k are assumed to be identical for each chip of a bit. The probability density function of a_k is:

6

$$f_{A_k}(a_k) = \frac{a_k}{\sigma^2} \, e^{-(a_k^2+A^2)/(2\sigma^2)} \, I_0\left(\frac{A}{\sigma^2} \, a_k\right) \qquad a_k \geq 0 \qquad (3)$$

where A^2 is the signal strength of the nonfaded (direct) component and $2\sigma^2$ is the mean-squared value of the Rayleigh-faded (diffuse) component. $I_0(.)$ Represents the modified Bessel function of zero order.

B. DESCRIPTION OF THE SYSTEMS, AND ANALYSIS OF THE SYSTEM PERFORMANCES UNDER MULTIPATH FADING, PARTIAL-BAND INTERFERENCE AND THERMAL NOISE.

1. Linear Combining Receivers

a. Envelope Detector

A linear combining envelope detector receiver is depicted in Fig. 1. Assuming that a binary 1 is sent, we obtain the sampled detector outputs contaminated with only wideband thermal noise as:

$$x_{1k} = \sqrt{(a_k \sqrt{2S} \cos\theta_k + n_{c_{1k}})^2 + (a_k \sqrt{2S} \sin\theta_k + n_{s_{1k}})^2}$$

$$x_{2k} = \sqrt{n_{c_{2k}}^2 + n_{c_{2k}}^2} \qquad (4)$$

and with narrowband interference added as:

$$x_{1k} = \sqrt{(a_k \sqrt{2S} \cos\theta_k + n_{c_{1k}} + i_{c_{1k}})^2 + (a_k \sqrt{2S} \sin\theta_k + n_{s_{1k}} + i_{s_{1k}})^2}$$

$$x_{2k} = \sqrt{(n_{c_{2k}} + i_{c_{2k}})^2 + (n_{s_{2k}} + i_{s_{2k}})^2} \qquad (5)$$

where n_{cjk}, n_{sjk}, $j=1,2$ are independent thermal noise components in the channels at the sampling instants $t=k\tau_h$ (where $\tau_h=1/R_h$). Both are assumed to be independent zero mean Gaussian random variables with equal variances $\sigma_N^2=N_0B$, where B is the cell bandwidth which is equal to the hopping rate R_h. The interference components i_{cjk}, i_{sjk}, are both narrowband zero mean Gaussian random variables with a variance of $\sigma_I^2 = N_IB/\gamma$. Equation (4) and (5) can be represented as

$$X_{1k} = \sqrt{(a_k\sqrt{2S}\cos\theta_k + v_{1k})^2 + (a_k\sqrt{2S}\sin\theta_k + v_{2k})^2}$$
$$X_{2k} = \sqrt{v_{3k}^2 + v_{4k}^2} \tag{6}$$

where v_{ik}s $(i=1,2\ 3,4)$ are independent zero mean Gaussian random variables with equal variances σ_k^2:

$$\sigma_k^2 = \begin{cases} \sigma_N^2 = N_0B & \text{with probability } (1-\gamma) \\ \\ \sigma_T^2 = \sigma_N^2 + \sigma_I^2 = (N_0 + N_I/\gamma)B & \text{with probability } \gamma \end{cases} \tag{7}$$

Narrowband interference, when present, is assumed to affect both channels. The conditional probability density functions for X_{1k} and X_{2k} are given in Ref. 5:

$$f_{X_{1k}/A_k}(X_{1k}/a_k) = \frac{X_{1k}}{\sigma_k^2} e^{-\frac{(x_{1k}^2 + 2Sa_k^2)}{2\sigma_k^2}} I_0\left(\frac{\sqrt{2S}}{\sigma_k^2} a_k X_{1k}\right) \quad X_{1k} \geq 0 \tag{8}$$

$$f_{X_{2k}/A_k}(X_{2k}/a_k) = f_{X_{2k}}(X_{2k}) = \frac{X_{2k}}{\sigma_k^2} e^{-\frac{x_{2k}^2}{2\sigma_k^2}} \quad X_{2k} \geq 0$$

The unconditional probability density function of the envelope of the output of channel one, $f_{X1k}(x_{1k})$, is obtained by integrating:

$$f_{X_{1k}}(x_{1k}) = \int_0^\infty f_{X_{1k}/A_k}(x_{1k}/a_k) \, f_{A_k}(a_k) \, da_k \qquad (9)$$

to get

$$f_{X_{1k}}(x_{1k}) = \frac{x_{1k}}{\sigma_k^2} \, e^{-\left(\frac{x_{1k}^2}{2\sigma_k^2}\right)} e^{-\left(\frac{A^2}{2\sigma^2}\right)} \int_0^\infty \frac{a_k}{\sigma^2} \, e^{-\left(\frac{2S}{2\sigma_k^2} + \frac{1}{2\sigma^2}\right)}$$

$$\times \left[I_0\left(\frac{A}{\sigma^2} \, a_k\right) I_0\left(\frac{\sqrt{2S}}{\sigma_k^2} x_{1k} a_k\right) \right] da_k$$

$$(10)$$

Without loss of generality, S is normalized to unity, and equation (10) is evaluated to obtain

$$f_{X_{1k}}(x_{1k}) = \frac{x_{1k}}{\sigma_k^2} \, \frac{e^{-\rho_k/(1+\xi_k)}}{1+\xi_k} \, e^{-x_{1k}^2/[2\sigma_k^2(1+\xi_k)]}$$

$$\times \left[I_0\left(\frac{\sqrt{2}\,A}{\sigma_k^2(1+\xi_k)} \, x_{1k}\right) \right] \quad x_{1k} \geq 0$$

$$(11)$$

where $\rho_k = A^2/\sigma_k^2$ is the signal-to-noise ratio of the nonfaded (direct) component of the kth hop of a bit and $\xi_k = 2\sigma^2/\sigma_k^2$ is the signal-to-noise ratio of the Rayleigh faded (diffuse) component. It is possible to normalize A^2 to unity and equation (11) becomes

9

$$f_{X_{1k}}(x_{1k}) = \frac{\rho_k}{1+\xi_k} x_{1k} e^{-\rho_k/(1+\xi_k)} e^{-\rho_k x_{1k}^2/[2(1+\xi_k)]}$$

$$\times \left[I_0\left(\frac{\sqrt{2}\rho_k}{1+\xi_k} x_{1k} \right) \right] \qquad x_{1k} \geq 0$$

(12)

The bit error probability for the receiver in Fig. 1 in the presence of partial-band interference is

$$P(E) = \sum_{l=0}^{L} \binom{L}{l} \gamma^l (1-\gamma)^{L-l} P(e/l)$$

(13)

where $P(e/l)$ is the conditional bit error probability when l of L hops of a bit have interference, and is given as

$$P(e/l) = Pr(x_1 \leq x_2/l) = \int_0^\infty f_{X_1}(x_1/l) \left[\int_{x_1}^\infty f_{X_2}(x_2/l)\, dx_2 \right] dx_1$$

(14)

where both x_1 and x_2 are the sum of L independent random variables, l of which are interfered. Thus,

$$f_{X_1}(x_1/l) = f_{x_{1k}^{(1)}}^{*l}(x_{1k}^{(1)}) * f_{x_{1k}^{(0)}}^{*(L-l)}(x_{1k}^{(0)})$$

$$f_{X_2}(x_2/l) = f_{x_{2k}^{(1)}}^{*l}(x_{2k}^{(1)}) * f_{x_{2k}^{(0)}}^{*(L-l)}(x_{2k}^{(0)})$$

(15)

where *m is m-fold linear convolution, and the superscript (1) and (0) denote the random variables with and without interference, respectively. In the following, the superscripts are attached only to the names of the functions, not to the variables and the constants.

Analytic solutions for $f_{x1}(x_1/l)$ and $f_{x2}(x_2/l)$ include nested infinite summations which make $P(E)$ tedious to obtain

10

numerically. The following approach is preferred for numeric results.

Define

$$\overline{f}_{X_{1k}}^{(1)}(x_{1k}) = \begin{cases} f_{X_{1k}}^{(1)}(x_{1k}) & x_{1k} \leq M \\ 0 & x_{1k} > M \end{cases} \tag{16}$$

and

$$\overline{f}_{X_{1k}}^{(0)}(x_{1k}) = \begin{cases} f_{X_{1k}}^{(0)}(x_{1k}) & x_{1k} \leq M \\ 0 & x_{1k} > M \end{cases} \tag{17}$$

where $M = \max \{ M_1, M_2 \}$ and

$$\int_0^{M_1} f_{X_{1k}}^{(1)}(x_{1k}) \cdot dx_{X_{1k}} \triangleq 1 \qquad and \qquad \int_0^{M_2} f_{X_{1k}}^{(0)}(x_{1k}) \cdot dx_{1k} \triangleq 1 \tag{18}$$

For the linear combining detector, $M=M_2$. Define

$$\overline{f}_{X_{2k}}^{(0)}(x_{2k}) = \begin{cases} f_{X_{2k}}^{(0)}(x_{2k}) & x_{2k} \leq N \\ 0 & x_{2k} > N \end{cases} \tag{19}$$

and

$$\overline{f}_{X_{2k}}^{(1)}(x_{2k}) = \begin{cases} f_{X_{2k}}^{(1)}(x_{2k}) & x_{2k} \leq N \\ 0 & x_{2k} > N \end{cases} \tag{20}$$

where $N=\max\{N_1,N_2\}$,

$$\int_0^{N_1} f_{X_{2k}}^{(1)}(x_{2k}) \, dx_{2k} \triangleq 1 \qquad and \qquad \int_0^{N_2} f_{X_{2k}}^{(0)}(x_{2k}) \cdot dx_{2k} \triangleq 1 \tag{21}$$

and M/N is chosen as integer. It is easier to explain the method used when M=N. Define

$$f_{X_{1k}}^{(1)} = \overline{f}_{X_{1k}}^{(1)}(X_{1k})\Big|_{X_{1k}=(n-1)\cdot\Delta} \qquad where \quad \frac{M}{\Delta}+1 \ge n \ge 1 \qquad (22)$$

where Δ is the distance between samples that are taken from the pdfs.

$$f_{X_{1k}}^{(0)}(n) = \overline{f}_{X_{1k}}^{(0)}(X_{1k})\Big|_{X_{1k}=(n-1)\cdot\Delta}$$

$$f_{X_{2k}}^{(0)}(n) = \overline{f}_{X_{2k}}^{(0)}(X_{2k})\Big|_{X_{2k}=(n-1)\cdot\Delta} \qquad (23)$$

$$f_{X_{2k}}^{(1)}(n) = \overline{f}_{X_{2k}}^{(1)}(X_{2k})\Big|_{X_{2k}=(n-1)\cdot\Delta}$$

Probability density function for x_1 and x_2 can be approximated as $f_{x1}^{\cdot}(n)$ and $f_{x2}^{\cdot}(n)$ where

$$f_{X_1}^{\cdot}(n) = \textbf{IDFT}\Big([\textbf{DFT}(f_{X_{1k}}^{(1)}(n))]^1 \times [\textbf{DFT}(f_{X_{1k}}^{(0)}(n))]^{L-1} \Big)\cdot\Delta^{L-1} \qquad (24)$$

DFT and IDFT are Discrete Fourier Transform and the Inverse Discrete Fourier Transform respectively. Numeric values are obtained using the Fast Fourier Transform (FFT) and the Inverse Fast Fourier Transform (IFFT). In implementing the analyses of a K point FFT (where K is an integer power of 2), K is chosen such that $K>ML/\Delta+1$, and remaining samples of the functions between $M/\Delta+1$ and K are padded with zeros. Redefine

$$f_{X_{1k}}^{(1)}(n) = \begin{cases} \overline{f}_{X_{1k}}^{(1)}(X_{1k})\Big|_{X_{1k}=(n-1)\cdot\Delta} & \frac{M}{\Delta}+1\ge n \ge 1 \\[2mm] 0 & K>\frac{ML}{\Delta}+1\ge n> \frac{M}{\Delta}+1 \end{cases} \qquad (25)$$

and the other functions can be redefined similarly. The probability of bit error is obtained by integrating equation

12

(14) numerically and substituting into equation (13) for L=2,4,6,8. For L=1 (slow FH), the exact result is obtained as

$$P(E/L=1) = \gamma \frac{e^{-\rho_k^{(1)}/(2+\xi_k^{(1)})}}{2+\xi_k^{(1)}} + (1-\gamma) \frac{e^{-\rho_k^{(0)}/(2+\xi_k^{(0)})}}{2+\xi_k^{(0)}} \tag{26}$$

b. Square-Law Detector

The linear combining square-law detector is depicted in Figure 2. Assuming that a binary 1 is sent when there is not interference, we obtain the sampled detector outputs as

$$x_{1k} = (a_k\sqrt{2S}\cos\theta_k + n_{c_{1k}})^2 + (a_k\sqrt{2S}\sin\theta_k + n_{s_{1k}})^2$$

$$x_{2k} = (n_{c_{2k}}^2 + n_{s_{2k}}^2) \tag{27}$$

and when there is interference

$$x_{1k} = (a_k\sqrt{2S}\cos\theta_k + n_{c_{1k}} + i_{c_{1k}})^2 + (a_k\sqrt{2S}\sin\theta_k + n_{s_{1k}} + i_{s_{1k}})^2$$

$$x_{2k} = (n_{c_{2k}} + i_{c_{2k}})^2 + (n_{s_{2k}} + i_{s_{2k}})^2 \tag{28}$$

All the variables are as defined for the envelope detector. Using equation (8) and equation (9), we obtain the probability density functions for x_{1k} and x_{2k} via a transformation of $x=y^2$, where x represents x_{1k} or x_{2k} and y stands for x_{1k} and x_{2k}, in equations (8) and (9), respectively. Hence

13

$$f_{X_{1k}}(X_{1k}) = \frac{1}{\sigma_k^2} \frac{1}{2(1+\xi_k)} I_0\left(\frac{\sqrt{2\rho_k X_{1k}}}{\sigma_k(1+\xi_k)}\right) e^{-\frac{1}{1+\xi_k}\left(\frac{x_k}{2\sigma_k^2}+\rho_k\right)} \qquad X_{1k} \geq 0$$

(29)

$$f_{X_{2k}}(X_{2k}) = \frac{1}{2\sigma_k^2} e^{-X_{2k}/2\sigma_k^2} \qquad\qquad X_{2k} \geq 0$$

(30)

The characteristic functions of the decision random variables x_{1k} and x_{2k} are

$$C_{X_{1k}}(s) = \int_{-\infty}^{\infty} f_{X_{1k}}(X_{1k}) \; e^{-X_{1k}s} \; dX_{1k}$$

(31)

$$C_{X_{1k}}(s) = \int_0^{\infty} \frac{1}{\sigma_k^2} \frac{1}{2(1+\xi_k)} e^{-\rho_k/(1+\xi_k)} e^{-X_{1k}/(2\sigma^2(1+\xi_k))}$$

$$\times \left[I_0\left(\frac{\sqrt{2\sigma_k}\sqrt{X_{1k}}}{\sigma_k(1+\xi_k)}\right) e^{-sX_{1k}}\right] dX_{1k}$$

Substituting $x_{1k}=u^2$ and $dx_{1k}=2udu$ into equation (31) and integrating, one obtains

$$C_{X_{1k}}(s) = \int_0^{\infty} \frac{1}{\sigma_k^2(1+\xi_k)} e^{-\rho_k/(1+\xi_k)} u \; e^{-u^2\left(s+\frac{1}{2\sigma_k^2(1+\xi_k)}\right)} I_0\left(\frac{\sqrt{2\rho_k}}{\rho_k(1+\xi_k)} u\right) du$$

(32)

The result yields [Ref. 6]

$$C_{X_{1k}}(s) = \frac{e^{-\rho_k/(1+\xi_k)}}{\sigma_k^2(1+\xi_k)} \frac{1}{2\left(s+\frac{1}{2\sigma_k^2(1+\xi_k)}\right)} e^{\left(\frac{\rho_k}{2\sigma_k^2(1+\xi_k)^2} \frac{1}{s+\frac{1}{2\sigma_k^2(1+\xi_k)}}\right)}$$

(33)

14

Define $x_1^{(1)}$ as the sum of 1 interfered random variables and $x_1^{(0)}$ as the sum of remaining L-1 random variables that are not interfered, and c as an integer assuming a value of either 1 or L-1 for the superscripts (1) and (0) respectively.   Then

$$f_{X_1}^{(i)}(x_1) = \mathcal{L}^{-1}\left\{[C_{X_{1k}}(s)]^c\right\} \quad \text{for } i=0,1 \tag{34}$$

which is

$$f_{X_1}^{(i)}(x_1) = \mathcal{L}^{-1}\left\{\frac{e^{-\rho_k c/(1+\xi_k)}}{\sigma_k^{2c}(1+\xi_k)^c} \frac{e^{\left(\frac{\rho_k c}{2\sigma_k^2(1+\xi_k)^2}\frac{1}{s+\frac{1}{2\sigma_k^2(1+\xi_k)}}\right)}}{2^c\left(s+\frac{1}{2\sigma_k^2(1+\xi_k)}\right)^c}\right\} \tag{35}$$

Using [8 Campbell-Foster Pairs 650.0] we obtain

$$f_{X_1}^{(i)}(x_1) = \frac{e^{-c\rho_k/(1+\xi_k)}}{2^{\frac{c+1}{2}}\sigma_k^{c+1}(1+\xi_k)} \frac{1}{(\rho_k c)^{\frac{c-1}{2}}} x_1^{(c-1)/2}$$

$$\times I_{c-1}\left(\frac{\sqrt{2\rho_k c}\sqrt{x_1}}{\sigma_k(1+\xi_k)}\right)e^{-x_1/2\sigma_k^2(1+\xi_k)} \tag{36}$$

and

$$C_{X_{2k}}(s) = \frac{\rho_k}{2}\int_0^{\infty} e^{-\left(\frac{\rho_k}{2}+s\right)x_{2k}}dx_{2k} = \frac{\rho_k}{2\left(s+\frac{\rho_k}{2}\right)} \tag{37}$$

15

The characteristic function for the random variable x_2 which is the sum of 1 interfered and L-1 noninterfered random variables, is

$$C_{X_2}(s) = \left(\frac{\rho_k^{(1)}}{2}\right)^1 \left(\frac{\rho_k^{(0)}}{2}\right)^{(L-1)} \frac{1}{\left(s+\frac{\rho_k^{(1)}}{2}\right)^1} \frac{1}{\left(s+\frac{\rho_k^{(0)}}{2}\right)^{(L-1)}} \tag{38}$$

This can be separated as

$$C_{X_2}(s) = \frac{A_{11}}{s+\frac{\rho_k^{(1)}}{2}} + \frac{A_{12}}{\left(s+\frac{\rho_k^{(1)}}{2}\right)^2} + \ldots + \frac{A_{11}}{\left(s+\frac{\rho_k^{(1)}}{2}\right)^1}$$

$$+ \frac{A_{21}}{s+\frac{\rho_k^{(0)}}{2}} + \frac{A_{22}}{\left(s+\frac{\rho_k^{(0)}}{2}\right)^2} + \ldots + \frac{A_{2,L-1}}{\left(s+\frac{\rho_k^{(0)}}{2}\right)^{(L-1)}} \tag{39}$$

where

$$A_{1j} = \frac{1}{(1-j)!} \cdot \frac{d^{(1-j)}}{ds^{(1-j)}} \left[\frac{1}{\left(s+\frac{\rho_k^{(0)}}{2}\right)^{(L-1)}}\right]\Bigg|_{s=-\frac{\rho_k^{(1)}}{2}} \qquad 1 \le j \le 1 \tag{40}$$

which yields

$$A_{1j} = (-1)^{(1-j)} \binom{L-j-1}{1-j} \frac{2^{L-j}}{\left(\rho_k^{(0)} - \rho_k^{(1)}\right)^{(L-j)}} \qquad 1 \le j \le 1, \quad 1 \ne L \text{ and } 1 \ne 0 \tag{41}$$

16

$$A_{2j} = \frac{1}{(L-j-1)!} \frac{d^{(L-1-j)}}{ds^{(L-j-1)}} \left[\frac{1}{\left(s + \frac{\rho_k^{(1)}}{2} \right)^l} \right] \Bigg|_{s = -\frac{\rho_k^{(0)}}{2}} \qquad 1 \le j \le L-1 \tag{42}$$

A_{2j} is verified to be

$$A_{2j} = (-1)^{-l} \binom{L-j-1}{L-1-j} \frac{2^{L-j}}{\left(\rho_k^{(0)} - \rho_k^{(1)} \right)^{L-j}} \qquad 1 \le j \le L-1 \tag{43}$$

.

.

The probability density function for the decision variable x_2 is obtained by taking the inverse Laplace transform of the characteristic function $C_{x2}(s)$

$$f_{X_2}(X_2) = \sum_{j=1}^{l} \frac{\left(\rho_k^{(1)} \right)^l}{2^j} \left(\rho_k^{(0)} \right)^{L-l} (-1)^{l-j} \binom{L-j-1}{l-j}$$

$$\times \left[\frac{1}{\left(\rho_k^{(0)} - \rho_k^{(1)} \right)^{(L-j)}} \frac{X_2^{(j-1)}}{(j-1)!} e^{-(\rho_k^{(1)} x_2/2)} \right]$$

$$+ \sum_{j=1}^{L-l} \frac{\left(\rho_k^{(1)} \right)^l}{2^j} \left(\rho_k^{(0)} \right)^{L-l} (-1)^l \binom{L-j-1}{L-1-j}$$

$$\times \left[\frac{1}{\left(\rho_k^{(0)} - \rho_k^{(1)} \right)^{(L-j)}} \frac{X_2^{j-1}}{(j-1)!} e^{-(\rho_k^{(0)} x_2)/2} \right] \tag{44}$$

.

.

and when l=L and l=0

$$f_{X_2}(X_2) = \frac{\left(\rho_k^{(1)} \right)^L}{2^L (L-1)!} X_2^{L-1} e^{-(\rho_k^{(1)} x_2)/2} \qquad l = L \tag{45}$$

$$f_{X_2}(X_2) = \frac{\left(\rho_k^{(0)} \right)^l}{2^l (L-1)!} x^{l-1} e^{-(\rho_k^{(0)} x_2)/2} \qquad l = 0$$

17

The probability of bit error is

$$P(E) = \sum_{l=0}^{L} \binom{L}{l} \gamma^l (1-\gamma)^{(L-l)} P(e/l) \tag{46}$$

where

$$P(e/l) = \int_0^{\infty} f_{X_1}(x_1) \int_{x_1}^{\infty} f_{X_2}(x_2) \, dx_2 \, dx_1 \tag{47}$$

and

$$f_{X_1}(x_1) = f_{X_1}^{(1)}(x_1) * f_{X_1}^{(0)}(x_1) \tag{48}$$

It is tedious to derive P(e/l) by using the exact solution for equation (21) except for the cases l=0 and l=L; hence, numerical analysis is preferred. As before,

$$f_{X_1}^{(i)}(x_1) = \mathbf{IDFT}\left[\left(\mathbf{DFT}(f_{X_1}^{(1)}(n))\right) \times \left(\mathbf{DFT}(f_{X_1}^{(0)}(n))\right)\right] \cdot \Delta \tag{49}$$

is defined where

$$f_{X_1}^{(i)}(n) = \overline{f}_{X_1}^{(i)}(x_1)\Big|_{x_1 = (n-1) \cdot \Delta} \qquad \frac{M}{\Delta} + 1 \geq n \geq 1 \tag{50}$$

and

$$\overline{f}_{X_1}^{(i)}(x_1) = \begin{cases} f_{X_1}^{(i)}(x_1) & M \geq x_1 \geq 0 \\ 0 & otherwise \end{cases} \tag{51}$$

where M is the maximum of the reasonable limits of $f_{x1}^{(1)}(x_1)$ or $f_{x1}^{(0)}(x_1)$ in order to have the areas under these probability

density functions as unity. The sampling distance is Δ. The remaining part of the procedure is as explained previously for the envelope detector. Also

$$P(E/L{=}1) = \frac{\gamma}{2+\xi_k^{(1)}}\, e^{-\rho_k^{(1)}/(2+\xi_k^{(1)})} + \frac{(1-\gamma)}{2+\xi_k^{(0)}}\, e^{-\rho_k^{(0)}/(2+\xi_k^{(0)})} \qquad (52)$$

This result is the same as the one obtained for the envelope linear combining detector.

When the signal is completely diffuse (Rayleigh fading: $\rho_k^{(i)} \to 0$) the probability density function for a single hop is

$$f_{X_{1k}}(x_{1k}) = \beta_k e^{-\beta_k x_{1k}} \qquad \text{where } \beta_k = \frac{1}{2(\sigma_k^2 + 2\sigma^2)} \qquad (53)$$

and the characteristic function for the random variable x_1 is

$$C_{X_1}(s) = \left(\frac{\beta_1}{s+\beta_1}\right)^1 \left(\frac{\beta_o}{s+\beta_o}\right)^{L-1} \qquad \text{where } \beta_o = \beta_k^{(0)}, \ \beta_1 = \beta_k^{(1)} \qquad (54)$$

which yields

$$f_{X_1}(x_1/1) = \sum_{j=1}^{1} \frac{(-1)^{1-j}\beta_1^1\beta_o^{L-1}}{(\beta_o-\beta_1)^{L-j}} \binom{L-j-1}{1-j} \frac{x_1^{j-1}e^{-\beta_1 x_1}}{(j-1)!}$$

$$+ \sum_{j=1}^{L-1} \frac{(-1)^1\beta_1^1\beta_o^{L-1}}{(\beta_o-\beta_1)^{L-j}} \binom{L-j-1}{L-1-j} \frac{x_1^{j-1}e^{-\beta_o x_1}}{(j-1)!}$$

$$\hspace{11cm} (55)$$

$$f_{X_1}(x_1/L) = \frac{\beta_1^L x_1^{L-1}e^{-\beta_1 x_1}}{(L-1)!} \qquad\qquad f_{X_1}(x_1/1{=}0) = \frac{\beta_o^L x_1^{L-1}e^{-\beta_o x_1}}{(L-1)!}$$

19

The probability density function for x_2 is found in a similar manner

$$f_{X_2}(x_2/l) = \sum_{m=1}^{l} \frac{(-1)^{l-m}\alpha_1^l\alpha_o^{L-l}}{(\alpha_o-\alpha_1)^{L-m}}\binom{L-m-1}{l-m}\frac{x_2^{m-1}e^{-\alpha_1 x_2}}{(m-1)!}$$

$$+ \sum_{m=1}^{L-l} \frac{(-1)^l\alpha_1^l\alpha_o^{L-l}}{(\alpha_o-\alpha_1)^{L-m}}\binom{L-m-1}{L-l-m}\frac{x_2^{m-1}e^{-\alpha_o x_2}}{(m-1)!}$$

$$f_{X_2}(x_2/L) = \frac{\alpha_1^L x_2^{L-1}e^{-\alpha_1 x_2}}{(L-1)!} \qquad f_{X_2}(x_2/l=0) = \frac{\alpha_o^L x_2^{L-1}e^{-\alpha_o x_2}}{(L-1)!} \tag{56}$$

where

$$\alpha_o = \frac{1}{2\sigma_k^{(0)2}} \qquad \alpha_1 = \frac{1}{2\sigma_k^{(1)2}} \tag{57}$$

After some algebra the conditional bit error probabilities when l=0 and when l=L are found to be

$$P(e/l=0) = \sum_{k=0}^{L-1}\binom{2L-k-2}{L-1}\frac{\alpha_o^{L-k}\beta_o^L}{(\beta_o+\alpha_o)^{2L-k-1}}$$

$$P(e/L) = \sum_{k=0}^{L-1}\binom{2L-k-2}{L-1}\frac{\alpha_1^{L-k}\beta_1^L}{(\beta_1+\alpha_1)^{2L-k-1}} \tag{58}$$

In general

20

$$P(e/1) = \sum_{j=1}^{1} \frac{(-1)^{1-j}\beta_1^1\beta_o^{L-1}}{(\beta_o-\beta_1)^{L-j}}\binom{L-j-1}{1-j}\sum_{m=1}^{1}\frac{(-1)^{1-m}\alpha_1^1\alpha_o^{L-1}}{(\alpha_o-\alpha_1)^{L-m}}\binom{L-m-1}{1-m}$$

$$\times\left[\sum_{t=0}^{m-1}\binom{m+j-t-2}{j-1}\frac{1}{\alpha_1^{t+1}(\alpha_1+\beta_1)^{(m+j-t-1)}}\right]$$

$$+\sum_{j=1}^{1}\frac{(-1)^{1-j}\beta_1^1\beta_o^{L-1}}{(\beta_o-\beta_1)^{L-1}}\binom{L-j-1}{1-j}\sum_{m=1}^{L-1}\frac{(-1)^1\alpha_1^1\alpha_o^{L-1}}{(\alpha_o-\alpha_1)^{L-m}}\binom{L-m-1}{1-1}$$

$$\times\left[\sum_{t=0}^{m-1}\binom{m+j-t-2}{j-1}\frac{1}{\alpha_o^{t+1}(\beta_1+\alpha_o)^{m+j-t-1}}\right]$$

$$+\sum_{j=1}^{L-1}\frac{\beta_1^1\beta_o^{L-1}}{(\beta_o-\beta_1)^{L-1}}\binom{L-j-1}{1-1}\sum_{m=1}^{1}-\frac{(-1)^1\alpha_1^1\alpha_o^{L-1}}{(\alpha_o-\alpha_1)^{L-m}}\binom{L-m-1}{1-m}$$

$$\times\left[\sum_{t=0}^{m-1}\binom{m+j-t-2}{j-1}\frac{1}{\alpha_1^{t+1}(\beta_o+\alpha_1)^{m+j-t-1}}\right]+\sum_{j=1}^{L-1}\frac{\beta_1^1\beta_o^{L-1}}{(\beta_o-\beta_1)^{L-1}}\binom{L-j-1}{1-1}$$

$$\times\left[\sum_{m=1}^{L-1}\frac{\alpha_1^1\alpha_o^{L-1}}{(\alpha_o-\alpha_1)^{L-m}}\binom{L-m-1}{1-1}\sum_{t=0}^{m-1}\binom{m+j-t-2}{j-1}\frac{1}{\alpha_o^{t+1}(\beta_o+\alpha_o)^{m+j-t-1}}\right] \tag{59}$$

2. Self-Normalization Receivers

a. Envelope Detector

The self-normalization combining scheme [Ref. 1] is a method of obtaining the predecision variables by normalizing the outputs of the envelope detectors of Fig. 1 with the sum

of the detector outputs. The receiver is depicted in Fig. 3.
Equations (11) and (8) are revisited

$$f_{X_{1k}}(x_{1k}) = \frac{x_{1k}}{2S\sigma^2+\sigma_k^2}\, e^{-A^2S/(2\sigma^2S+\sigma_k^2)}\, e^{-x_{1k}^2/[2(2\sigma^2+\sigma_k^2)]}\, I_0\!\left(\frac{\sqrt{2SA}}{2S\sigma^2+\sigma_k^2}\, x_{1k}\right)$$

(60)

$$f_{X_{2k}}(x_{2k}) = \frac{x_{2k}}{\sigma_k^2}\, e^{-x_{2k}/2\sigma_k^2} \qquad\qquad x_{2k}\geq 0$$

We define z_{1k} and v_{1k} as

$$z_{1k} = \frac{x_{1k}}{x_{1k}+x_{2k}} \qquad 0\leq z_{1k}\leq 1$$

(61)

$$v_{1k} = x_{1k}+x_{2k} \qquad 0\leq v_{1k} <\infty$$

The Jacobian of the transformation is

$$J = \begin{vmatrix} \dfrac{\partial z_{1k}}{\partial x_{1k}} & \dfrac{\partial z_{1k}}{\partial x_{2k}} \\[2mm] \dfrac{\partial v_{1k}}{\partial x_{1k}} & \dfrac{\partial v_{1k}}{\partial x_{2k}} \end{vmatrix} = \frac{1}{v_{1k}}$$

(62)

Equation (61) can be inverted to yield $x_{1k}=v_{1k}z_{1k}$ and $x_{2k}=v_{1k}(1-z_{1k})$. Since x_{1k} and x_{2k} are independent random variables, their joint probability density function is

$$f_{X_{1k},X_{2k}}(x_{1k}\ ,\ x_{2k}) = f_{X_{1k}}(x_{1k}) \times f_{X_{2k}}(x_{2k})$$

(63)

$$f_{X_{1k},X_{2k}}(x_{1k}\ ,\ x_{2k}) = \frac{x_{1k}\, x_{2k}}{2\sigma_k^2\beta_k^2}\, e^{-A^2S/\beta_k^2}\, e^{-x_{1k}^2/2\beta_k^2}\, e^{-x_{2k}^2/2\sigma_k^2}\, I_0\!\left(\frac{\sqrt{2SA}}{\beta_k^2}\, x_{1k}\right)$$

where $\beta_k^2=\sigma_k^2+2S\sigma^2$. Hence

$$f_{Z_{1k},V_{1k}}(z_{1k},v_{1k}) = |\,J\,|.\ f_{X_{1k},X_{2k}}(v_{1k}.z_{1k}\ ,v_{1k}.(1-z_{1k}))$$

(64)

The probability density function for z_{ik} is now obtained as

22

$$f_{z_{1k}}(z_{1k}) = \int_0^\infty f_{z_{1k}, v_{1k}}(z_{1k}, v_{1k}) \, . \, dv_{1k} \qquad (65)$$

Substituting equation (63) into equation (65), we get

$$f_{z_{1k}}(z_{1k}) = \frac{e^{-A^2 S/\beta_k^2}}{2\sigma_k^2 \beta_k^2}$$

$$\times \int_0^\infty z_{1k}(1-z_{1k}) \, v_{1k}^3 \, e^{-\frac{1}{2}\left(\frac{z_{1k}^2}{\beta_k^2} + \frac{(1-z_{1k})^2}{\sigma_k^2}\right) \cdot v_{1k}^2} \, I_0\left(\frac{\sqrt{2S}A z_{1k}}{\beta_k^2} \, v_{1k}\right) . \, dv_{1k} \qquad (66)$$

Making the necessary substitutions into the equation in Ref. 6 on page 394

$$\int_0^\infty J_0(at) \, e^{-p^2 t^2} \, t^{\mu-1} \, dt = \sum_{m=0}^\infty \frac{(-1)^m}{m! \, \Gamma(m+1)} \, \frac{\Gamma\left(\frac{\mu}{2}+m\right)}{2p^{\mu+2m}} \qquad (67)$$

where $\Gamma(.)$ is the Gamma function and $J_0(.)$ is the Bessel function of the first kind of order zero, we can evaluate equation (66). Since $\Gamma(m)=(m-1)!$ for m an integer

$$f_{z_{1k}}(z_{1k}) = \frac{e^{-A^2 S/\beta_k^2}}{2\sigma_k^2 \beta_k^2} \, z_{1k}(1-z_{1k})$$

$$\times \sum_{m=0}^\infty \frac{2(m+1)}{m!} \left(\frac{SA^2}{\beta_k^4}\right)^m \frac{z_{1k}^{2m}}{\left(\frac{z_{1k}^2}{\beta_k^2} + \frac{(1-z_{1k})^2}{\sigma_k^2}\right)^{m+2}} \qquad (68)$$

which simplifies into

23

$$f_{Z_{1k}}(z_{1k}) = \frac{e^{-A^2S/\beta_k^2}}{\sigma_k^2\beta_k^2} (1-z_{1k}) \cdot z_{1k} \frac{2}{\left(\dfrac{z_{1k}^2}{\beta_k^2} + \dfrac{(1-z_{1k})^2}{\sigma_k^2}\right)^2}$$

$$\times \left[\sum_{m=0}^{\infty} \frac{m+1}{m!} \left(\frac{SA^2 z_{1k}^2}{\beta_k^4\left(\dfrac{z_{1k}^2}{\beta_k^2} + \dfrac{(1-z_{1k})^2}{\sigma_k^2}\right)}\right)^m\right] \qquad (69)$$

Using

$$\frac{d(ye^y)}{dy} = \sum_{m=0}^{\infty} \frac{m+1}{m!} y^m = e^y(y+1) \qquad (70)$$

and replacing for y

$$y = \frac{SA^2 z_{1k}^2}{\beta_k^4\left(\dfrac{z_{1k}^2}{\beta_k^2} + \dfrac{(1-z_{1k})^2}{\sigma_k^2}\right)} \qquad (71)$$

we obtain the pdf of z_{1k} as

$$f_{Z_{1k}}(z_{1k}) = \frac{2e^{-SA^2/\beta_k^2}}{\sigma_k^2\beta_k^2} \frac{z_{1k}(1-z_{1k})}{\left(\dfrac{z_{1k}^2}{\beta_k^2} + \dfrac{(1-z_{1k})^2}{\sigma_k^2}\right)^2}$$

$$\times \left(1 + \frac{SA^2 z_{1k}^2}{\beta_k^4\left(\dfrac{z_{1k}^2}{\beta_k^2} + \dfrac{(1-z_{1k})^2}{\sigma_k^2}\right)}\right) \times e^{\left(\frac{SA^2 z_{1k}^2}{\beta_k^4\left(\frac{z_{1k}^2}{\beta_k^2} + \frac{(1-z_{1k})^2}{\sigma_k^2}\right)}\right)} \qquad 0 \le z_{1k} \le 1 \qquad (72)$$

24

Substituting $\xi_k = 2\sigma^2/\sigma_k^2$, $\rho_k = A^2/\sigma_k^2$, and $S=1$ in equation (72), we get

$$f_{z_{1k}}(z_{1k}) = \frac{2\ e^{-\rho_k/(1+\xi_k)}\ (z_{1k}(1-z_{1k}))}{\left(z_{1k}^2 + (1-z_{1k})^2\ (1+\xi_k)\right)^2}$$
$$\times \left(1 + \frac{\rho_k z_{1k}^2}{(1+\xi_k)\left[z_{1k}^2 + (1-z_{1k})^2\ (1+\xi_k)\right]}\right) \times e^{-\left(\frac{\rho_k\ z_{1k}^2}{(1+\xi_k)\ (z_{1k}^2 + (1-z_{1k})^2\ (1+\xi_k))}\right)} \quad (73)$$

Recalling equation (13) for probability of bit error

$$P(E) = \sum_{l=0}^{L} \binom{L}{l} \gamma^l\ (1-\gamma)^{L-l}\ P(e/l) \quad (74)$$

and using

$$\sum_{l=0}^{L} (z_{1k}+z_{2k}) = z_1 + z_2 = L$$

$$P(e/l) = P(\ z_2 > z_1\ /l) \quad (75)$$

we get the partial probability of bit error, when l of L chips contain interference noise energy, as

$$P(e/l) = P\left(z_1 < \frac{L}{2}/l\right) \quad (76)$$

The results for probability bit error are obtained numerically in a similar fashion to that previously explained. The probability of bit error for L=1 is found to be the same as in equation (26).

b. Square-Law Detector

The square-law self-normalization detector is depicted in Figure 4. P(E) is derived for L=2,4,6,8 using the equation from reference 1

$$f_{Z_{1k}}(z_{1k}) = \frac{\rho_k z_{1k} + (1+\xi_k)[1+\xi_k(1-z_{1k})]}{[1+\xi_k(1-z_{1k})]^3} \; e^{-\rho_k(1-z_{1k})/[1+\xi_k(1-z_{1k})]} \tag{77}$$

in the method previously explained. For L=1, P(E) is derived analytically, and the same result as in equation (26) is obtained.

3. Noise-Normalization Combining Receivers

a. Envelope Detector

The noise-normalization combining scheme normalizes the outputs of the envelope detectors of Figure 1 with the noise power (square-rooted) obtained from the output of the noise only channel (noise power prediction channel) at the sampling instants to form the predecision variables z_{1k} and z_{2k} (depicted in Figure 5). The probability density functions for z_{1k} and z_{2k} can be derived applying a linear transformation to the pdfs of the linear combining detectors x_{1k} and x_{2k}, such as $z_{1k}=x_{1k}/\sigma_k$ $z_{2k}=x_{2k}/\sigma_k$. The results for $f_{z1k}(z_{1k})$ and $f_{z2k}(z_{2k})$ yield

$$f_{z_{1k}}(z_{1k}) = \frac{e^{-\rho_k/(1+\xi_k)}}{(1+\xi_k)} \; z_{1k} \; e^{-z_{1k}^2/[2(1+\xi_k)]} \; I_0\left(\frac{\sqrt{2\rho_k}}{1+\xi_k} z_{1k}\right) \qquad z_{1k} \geq 0$$

$$\tag{78}$$

$$f_{z_{2k}}(z_{2k}) = z_{2k} \; e^{-z_{2k}^2/2} \qquad\qquad z_{2k} \geq 0$$

26

The probability of bit error is obtained with a method similar to that used in the linear combining envelope detector case. An exact result is derived for the probability of bit error of a single hop per bit (slow FH). The result is the same as in the equation (26).

b. Square-Law Detector

The square-law noise-normalization detector is depicted in Figure 6. The decision is made by a comparison circuit which accepts as inputs the sum of the random variables that are obtained by normalizing the outputs of the detectors with the output of the noise power measurement channel. Assuming a binary one is sent, we get the pdfs for single hop random variables [Ref. 3]

$$f_{z_{1k}}(z_{1k}) = \frac{1}{2(1+\xi_k)} \, e^{-(z_{1k}+2\rho_k)/[2(1+\xi_k)]} \, I_0\left(\frac{\sqrt{2\rho_k z_{1k}}}{1+\xi_k}\right) \quad z_{1k} \geq 0$$

(79)

$$f_{z_{2k}}(z_{2k}) = \frac{e^{-z_{2k}/2}}{2} \quad z_{2k} \geq 0$$

The pdfs for the random variables $z_1^{(1)}$ and $z_1^{(0)}$, where (1) and (0) represent the portion having interference and the portion not having interference, are

$$f_{z_1^{(i)}}(z_1^{(i)}) = \frac{\beta_k^{(i)} z_{1k}^{(c_i-1)/2}}{(2c_i\rho_k^{(i)})^{(c_i-1)/2}} \, e^{-\left[\beta_k^{(i)}\left(z_1^{(i)}+2c_i\rho_k^{(i)}\right)\right]} \, I_{c_i-1}\left(2\beta_k^{(i)}2c_i\rho_k^{(i)}z_1^{(i)}\right)$$

(80)

$$f_{z_2}(z_2) = \frac{(z_2/2)^{L-1}}{2(L-1)!} \, e^{-(z_2/2)}$$

27

where c_i is 1 if i=1 or L-1 if i=0, and

$$\beta_k^{(i)} = \frac{1}{2(1+\xi_k^{(i)})} \tag{81}$$

The probability of bit error for L=2,4,6,8 is obtained in a similar fashion as for the previous cases, and P(E/L=1) is found to be the same as in the equation (26).

When the signal is completely diffuse $(\rho_k^{(i)} \to 0)$, and the characteristic function from reference 3, replacing $\beta_1 = \beta_k^{(1)}$, and $\beta_0 = \beta_k^{(2)}$, is

$$C_{Z_1}(s/1) = \left(\frac{\beta_1}{s+\beta_1}\right)^1 \left(\frac{\beta_0}{s+\beta_0}\right)^{L-1} \tag{82}$$

This can be inverted to yield

$$f_{Z_1}(z_1/1) = \sum_{j=1}^{1} \frac{(-1)^{1-j}\beta_1^1\beta_0^{L-1}}{(\beta_0-\beta_1)^{L-j}} \binom{L-j-1}{1-j} \frac{z_1^{j-1}e^{-\beta_1 z_1}}{(j-1)!}$$

$$+ \sum_{j=1}^{L-1} \frac{(-1)^{-1}\beta_1^1\beta_0^{L-1}}{(\beta_0-\beta_1)^{L-j}} \binom{L-j-1}{L-1-j} \frac{z_1^{j-1}e^{-\beta_0 z_1}}{(j-1)!} \quad L>1>0 \tag{83}$$

$$f_{Z_1}(z_1/L) = \frac{\beta_1^L}{(L-1)!} z_1^{L-1}e^{-\beta_1 z_1} \ , \ \ f_{Z_1}(z_1/1=0) = \frac{\beta_0}{(L-1)!} z_1^{L-1}e^{-\beta_0 z_1} \tag{84}$$

and

$$f_{Z_2}(z_2) = \frac{z_2^{L-1}}{2^L(L-1)!} e^{-z_2/2} \tag{85}$$

Now

$$P(e/1) = \int_0^\infty f_{z_1}(z_1)\,dz_1 \int_{z_1}^\infty f_{z_2}(z_2)\,dz_2 \tag{86}$$

Since

$$\int e^{ay} y^N dy = e^{ay} \sum_{k=0}^{N} \frac{(-1)^k y^{N-k}}{a^{k+1}} \frac{N!}{(N-k)!} \quad \text{for } N \text{ is integer} \tag{87}$$

then

$$P(e/1) = \int_0^\infty f_{z_1}(z_1) \left[e^{-z_2/2} \sum_{k=0}^{L-1} \frac{z_1^{L-1-k}}{2^{L-1-k}(L-k-1)!} \right] dz_1 \tag{88}$$

Replacing $f_{z_1}(z_1)$ in the equation above and solving for $1=L$, we get

$$\tag{89}$$

$$P(e/L) = \frac{\beta_1^l}{(L-1)!} \int_0^\infty \sum_{k=0}^{L} \frac{e^{-(\beta_1+\frac{1}{2})z_1} z_1^{l-1-k}}{2^{L-k-1}(L-k-1)!}\,dz_1$$

$$= \frac{\beta_1^L}{(L-1)!} \sum_{k=0}^{L-1} \frac{1}{2^{L-k-1}(L-k-1)!} \left[\sum_{t=0}^{2L-k-2} \frac{(-1)(2L-k-2)!\, z_1^{2L-k-t-2}}{(\beta_1+\frac{1}{2})^{t+1}(2L-k-t-2)!} \right] \Bigg|_{z_1=0}^{\infty}$$

The upper limit of the function yields 0, while the lower limit has value only at $t=2L-k-2$; hence,

$$P(e/L) = \sum_{k=0}^{L-1} \binom{2L-k-2}{L-1} \frac{(2L)^L}{(2\beta_1+1)^{2L-k-1}} \tag{90}$$

Similarly

$$P(e/1=0) = \sum_{k=0}^{L-1} \binom{2L-k-2}{L-1} \frac{(2\beta_o)^L}{(2\beta_1+1)^{2L-k-1}} \tag{91}$$

29

finally

$$
P(e/1) = \sum_{j=1}^{1} \frac{(-1)^{1-j}\beta_1^l\beta_o^{L-1}}{(\beta_o-\beta_1)^{1-j}} \binom{L-j-1}{1-j} \sum_{k=0}^{L-1} \binom{1-k+j-2}{j-1} \frac{1}{2^{1-1-k}(\beta_1+\frac{1}{2})^{L-k+j}}
$$

$$
+ \sum_{j=1}^{L-1} \frac{(-1)^{1}\beta_1^l\beta_o^{L-1}}{(\beta_o-\beta_1)^{L-j}} \binom{L-j-1}{L-j-1} \sum_{k=0}^{L-1} \binom{L-k+j-2}{j-1} \frac{1}{2^{L-1-k}(\beta_1+\frac{1}{2})^{L-k+j-1}}
$$

(92)

C. SYSTEM PERFORMANCES UNDER MULTIPATH FADING AND THERMAL NOISE (NEGLECTING THE EFFECT OF PARTIAL-BAND INTERFERENCE)

1. Envelope Detector

An analysis for envelope detector for three kinds of receivers previously discussed is similar to that used in the partial-band interference analysis. In the absence of partial-band interference, the performance of a noise-normalization detector is easily proven equal to the performance of the linear combining version of the same detector. Hence

$$
X_1 = \sum_{k=1}^{L} X_{1k} \qquad X_2 = \sum_{k=1}^{L} X_{2k}
$$

(93)

$$
z_1 = \sum_{k=1}^{L} z_{1k} = \sum_{k=1}^{L} \frac{X_{1k}}{\sigma_k} = \frac{X_1}{\sigma_k}
$$

30

Similarly $z_2 = x_2/\sigma_k$, and for linear combining

$$P(E) = \int_0^\infty f_{X_1}(x_1) \cdot dx_1 \int_{x_1}^\infty f_{X_2}(x_2) \cdot dx_2 \qquad (94)$$

is equal to

$$P(E) = \int_0^\infty f_{Z_1}(z_1) \cdot dz_1 \int_{z_1}^\infty f_{Z_2}(z_2) \cdot dz_2 \qquad (95)$$

if the substitutions $x_1 = \sigma_k z_1$, $dx_1 = \sigma_k \cdot dz_1$ and $x_2 = \sigma_k z_2$, $dx_2 = \sigma_k \cdot dz_2$ are made, where recall that $f_{Z1}(z_1)dz_1 = f_{X1}(\sigma_k \cdot z_1) \cdot dx_1$ and $f_{Z2}(z_2)dz_2 = f_{X2}(\sigma_k \cdot z_2) \cdot dx_2$ for the linear transformation. This proof can be applied to wideband (uniform) interference. The probability of bit error for $L=1$ can be extracted from that of with-interference results, and it is

$$P(E/L=1) = \frac{e^{-\rho_k/(2+\xi_k)}}{2+\xi_k} \qquad (96)$$

2. Square-Law Detector

a. Self-Normalization Combining

Results are obtained numerically except for $L=1$. $P(E/L=1)$ is found the same as for equation (96).

b. Noise-Normalization Combining

The probability density function for x_1 is derived by replacing $c=L$ in equation (80) to obtain

$$f_{X_1}(x_1) = \frac{\beta_k \, x_1^{(L-1)/2}}{(2L\rho_k)^{(L-1)/2}} \, e^{-[\beta_k(x_1+2L\rho_k)]} \, I_{L-1}(2\beta_k\sqrt{2L\rho_k x_1}) \qquad x_1 \geq 0 \quad (97)$$

The pdf for x_2 is the same as in equation (38) where $\beta_k = 1/2(1+\xi_k)$, and the probability of bit error is

$$P(E) = \int_0^\infty f_{X_1}(x_1) \, [\int_{x_1}^\infty f_{X_2}(x_2) \, dx_2] \, . \, dx_1 \qquad (98)$$

Substituting equation (80) and equation (97) into equation (98) and integrating the inner integral, we get

$$P(E) = \frac{\beta_k \, e^{-2\beta_k L\rho_k}}{2^L (2L\rho_k)^{(L-1)/2}}$$

$$\times \left[\sum_{i=0}^{L-1} 2^i \int_0^\infty \frac{e^{-(\beta_k+\frac{1}{2})x_1}}{(L-i-1)!} \, x_1^{(L-1)/2} \, x_1^{(L-i-1)} \, I_{L-1}(2\beta_k\sqrt{2L\rho_k x_1}) \, dx_1 \right] \qquad (99)$$

The result of the integration is an infinite sum and numeric integration is preferred instead. For slow FH ($L=1$), the result is obtained from previous analysis and found to be the same as in equation (96).

32

c. Linear Combining

The probability density function for x_1 is obtained from equation (36) by substituting $c=L$

$$f_{X_1}(x_1) = \frac{e^{-L\rho_k/(1+\xi_k)}}{2^{(L+1)/2} \sigma_k^{L+1} (1+\xi_k)} \frac{1}{(\rho_k L)^{(L-1)/2}} x_1^{(L-1)/2}$$

$$\times I_{L-1}\left(\frac{\sqrt{2\rho_k L x_1}}{\rho_k(1+\xi_k)}\right) e^{-x_1/2\sigma^2(1+\xi_k)} \quad x_1 \geq 0$$

(100)

The pdf for x_2 is derived using the characteristic function method

$$f_{X_2}(x_2) = \mathscr{L}^{-1}\left\{\left(\mathscr{L}\left\{\frac{\rho_k}{2} \cdot e^{-\rho_k x_2/2}\right\}\right)^L\right\} \quad when \ A^2=1$$

(101)

which yields

$$f_{X_2}(x_2) = \left(\frac{\rho_k}{2}\right)^L \mathscr{L}^{-1}\left\{\frac{1}{\left(s+\frac{\rho_k}{2}\right)^L}\right\}$$

(102)

which reduces to

$$f_{X_2}(x_2) = \left(\frac{\rho_k}{2}\right)^L \frac{x_2^{L-1}}{(L-1)!} e^{-\rho_k x_2/2} \quad x_2 \geq 0$$

(103)

Substituting equation (102) and equation (103) into the well known equation for the probability of bit error for noncoherent BFSK, we get

33

$$P(E) = \int_0^\infty f_{X_1}(x_1) \left[\int_{X_1}^\infty f_{X_2}(x_2) \, dx_2 \right] dx_1$$

Evaluation of the inner integral yields

$$P(E) = \frac{e^{-L\rho_k/(1+\xi_k)}}{2^{(L+1)/2} \sigma_k^{L+1} (1+\xi_k)(\rho_k L)^{(L-1)/2}}$$

(104)

$$\times \sum_{k=0}^{L-1} \frac{\rho_k}{2^k \, k!} \int_0^\infty x_1^{(L-1)/2} \, x_1^k \, e^{-\frac{x_1}{2}\left(\rho_k + \frac{1}{\rho_k^2(1+\xi_k)}\right)} \, I_{L-1}\left(\frac{\sqrt{2\rho_k L x_1}}{\rho_k(1+\xi_k)} \right) dx_1$$

Replacing $x_1 = \sigma_k^2 z_1$ and $dx_1 = \sigma_k^2 dz_1$ in equation (104), we obtain equation (99). As a result, we see that noise-normalization combining for the square-law detector detection procedure has no performance improvement as compared to linear combining in the absence of partial-band interference or jamming. $P(E/L=1)$ is found to be the same as in the previous cases.

D. PERFORMANCE ANALYSIS IN THE ABSENCE OF THERMAL NOISE

The neglect of thermal noise ($N_o \rightarrow 0$) is a basic simplifying assumption in work regarding partial-band interference and fading. This analysis is implemented for the nonlinear combining detectors; it is found impractical to obtain accurate results for the linear combining detectors when thermal noise is neglected.

34

1. Envelope Detector

a. Self-Normalization Combining

Recall equation (72) for the pdf of a single hop

$$
f_{z_{1k}}(z_{1k}) = \frac{2e^{-\rho_k/(1+\xi_k)}(1+\xi_k)z_{1k}(1-z_{1k})}{[z_{1k}^2+(1-z_{1k})^2(1+\xi_k)]^2}
$$

$$
\times\left(1+\frac{\rho_k z_{1k}^2}{(1+\xi_k)[z_{1k}^2+(1-z_{1k})^2(1+\xi_k)]}\right)\times e^{\left(\frac{\rho_k z_{1k}^2}{(1+\xi_k)[z_{1k}^2+(1-z_{1k})^2(1+\xi^k)]}\right)} \tag{105}
$$

With no thermal noise, and for the sake of simplicity letting B=1, we have

$$
\sigma_k^2 = \begin{cases} 0 & \text{when the hop is free of interference} \\ \dfrac{N_I}{\gamma} & \text{when the hop has interference} \end{cases} \tag{106}
$$

If the random variable z_{1k} is not contaminated with interference, the parameters ρ_k and ξ_k in the probability density function of the particular random variable go to infinity in the limit. Define the condition set C as

$$
C = \begin{cases} \rho_k \to \infty \\ \xi_k \to \infty \\ (1-z_{1k})(1+\xi_{1k}) \to \infty \\ z_{1k} \to 1 \end{cases} \tag{107}
$$

where the third condition can take place if and only if the order of ξ_{1k} is greater than the order of $1/(1-z_{1k})$ as z_{1k} approaches to 1. By a simple limit operation

$$\lim_C f_{Z_{1k}}(z_{1k}) \to \infty \qquad (108)$$

We now redefine the pdf for z_{1k} under the declared condition as

$$f_{Z_{1k}}(z_{1k}) = \delta(1-z_{1k}) \qquad (109)$$

where $\delta(.)$ is delta function. Recall that the probability density function of the sum of statistically independent random variables is the convolution of the probability density functions of the random variables included in the sum. The convolution operation with a delta function is implemented simply by shifting the function involved on the horizontal axis as much as the distance of the delta function from the origin. Every single cell in the combination that does not have interference shifts the resultant pdf by one unit to the right. The conditional probability of bit error when 1 of L hops have interference power is thus

$$P(e/l) = \int_0^{L/2} \left[f_{Z_{1k}^{*l}(z_1)} * \delta(z_1-(L-l)) \right] . dz_1 \qquad (110)$$

Hence

$$P(e/l) = \begin{cases} \int_{L-l}^{L/2} f_{Z_{1k}}^{*l}(z_1) . dz_1 & \text{when } l > L/2 \\ 0 & \text{when } l \le L/2 \end{cases} \qquad (111)$$

and the probability of bit error becomes

36

$$P(E) = \begin{cases} \displaystyle\sum_{l=\frac{L}{2}+1}^{L} \binom{L}{l} P(e/l) \; \gamma^l (1-\gamma)^{(L-l)} & L \text{ is even} \\[20pt] \displaystyle\sum_{l=\frac{L+1}{2}}^{L} \binom{L}{l} P(e/l) \; \gamma^l \; (1-\gamma)^{(L-l)} & L \text{ is odd} \end{cases} \tag{112}$$

Numerical results are obtained with the method previously explained. For single hop per bit FH, the probability of bit error is obtained as

$$P(E/L=1) = \gamma \frac{e^{-\rho_k^{(1)}/(2+\xi_k^{(1)})}}{2+\xi_k^{(1)}} \tag{113}$$

b. Noise Normalization Combining

Recall equation (78) for envelope detector noise-normalization combining pdf for signal-containing random variable z_{1k}

$$f_{z_{1k}}(z_{1k}) = \frac{e^{-\rho_k/(1+\xi_k)}}{1+\xi_k} \; z_{1k} \; e^{-z_{1k}^2/[2(1+\xi_k)]} \; I_0\!\left(\frac{\sqrt{2\rho_k}}{1+\xi_k} z_{1k}\right) \quad z_{1k} \geq 0 \tag{114}$$

and z_{2k} from equation (78)

$$f_{z_{2k}}(z_{2k}) = z_{2k} \; e^{z_{2k}^2/2} \quad z_{2k} \geq 0 \tag{115}$$

If we replace B=1 for simplicity and if N_o approaches 0, then ξ_k and ρ_k approach to infinity, and

$$\sigma_k^2 = \begin{cases} 0 & \text{without interference} \\[10pt] \dfrac{N_I}{\gamma} & \text{with interference} \end{cases} \tag{116}$$

37

We separate equation (114) into 3 parts

$$f_{z_{1k}}(z_{1k}) = e^{-\rho_k/(1+\xi_k)} \quad \times \quad \frac{z_{1k}}{1+\xi_k} \quad \times \quad \frac{I_0\left(2\sqrt{\frac{\rho_k}{1+\xi_k}}\sqrt{\frac{z_{1k}^2}{2(1+\xi_k)}}\right)}{e^{z_{1k}^2/[2(1+\xi_k)]}} \tag{117}$$

$$\text{(1)} \qquad\qquad \text{(2)} \qquad\qquad\qquad \text{(3)}$$

Defining

$$x = \frac{z_{1k}^2}{2(1+\xi_k)} \qquad\qquad a = \sqrt{\frac{\rho_k}{1+\xi_k}} \tag{118}$$

and recalling

$$I_0(2a\sqrt{x}) = \sum_{m=0}^{\infty} \frac{a^{2m} x^m}{(m!)^2} \qquad e^x = \sum_{m=0}^{\infty} \frac{x^m}{m!} \tag{119}$$

we find that the first part assumes a finite value as $\sigma_k^2 \to 0$. The order of $I_0(2a\sqrt{x})$ is equal to the order of e^x, so the third part may also converge as well. The second part is infinite as $z_{1k} \to \infty$. Defining the condition set C as

$$C = \left\{ \begin{array}{c} \rho_k^2 \to 0 \\ \rho_k^2 z_{1k} \to \infty \end{array} \right\} \tag{120}$$

so $\lim_c f_{z1k}(z_{1k}) \to \infty$, we have

$$f_{z_{1k}}^{(0)}(z_{1k}) = \lim_{M \to \infty} \delta(M - z_{1k}) \tag{121}$$

which is an impulse at the infinity. The probability density function for the random variable z_{2k} is finite for all z_{2k}.

The convolution operation of a function with an impulse at the infinity yields zero for finite values of z_{1k}. Therefore, for every bit including even a single chip that is not contaminated by the interference, the conditional probability of bit error is zero. It is only necessary to evaluate $P(e/l=L)$ and

$$P(E) = \gamma^L P(e/l=L) \tag{122}$$

The results are obtained numerically except for L=1, which is found to be the same as in the self-normalization case.

2. Square-Law Detector

a. Self-Normalization Combining

Recall equation (77). Separating it into two parts, we have

$$f_{z_{1k}}(z_{1k}) = \frac{\rho_k z_{1k} + (1+\xi_k)[1+\xi_k(1-z_{1k})]}{[1+\xi(1-z_{1k})]^3} \times e^{-\rho_k(1-z_{1k})/[1+\xi_k(1-z_{1k})]} \tag{123}$$

$$\qquad\qquad\qquad (1) \qquad\qquad\qquad\qquad (2)$$

and the condition set C is defined as

$$C = \left\{ \begin{array}{l} \rho_k \to \infty \\ \xi_k \to \infty \\ z_{1k} \to 1 \\ \xi_k(1-z_{1k}) \to A \end{array} \right\} \tag{124}$$

where A stands for any finite real value. Under this condition set the limit

$$\lim_{c} f_{Z_{1k}}(z_{1k}) \to \infty \tag{125}$$

The second part is finite and nonzero, and the first part goes to infinity (the denominator is finite, the numerator approaches infinity in the limit); hence the probability density function for a single chip which does not include interference is

$$f_{Z_{1k}}^{(0)}(z_{1k}) = \delta(1-z_{1k}) \tag{126}$$

The performance analysis is carried out numerically, and results for equation (112) are obtained using the equation (123).

b. Noise-Normalization Combining

Equation (80)

$$f_{Z_{1k}}(z_{1k}) = \frac{e^{-z_{1k}/2}}{2} \qquad z_{1k} \geq 0 \tag{127}$$

gives a finite result for all finite values of z_{2k}. Separating equation (81) into three parts and rewriting it for c noninterfered hops, we have

$$f_{Z_1}^{(0)}(z_1) = e^{-c\rho_k^{(0)}/(1+\xi_k^{(0)})} \times \frac{z_1^{(c-1)/2}}{c^{(c-1)/2} 2^{(c+1)/2} (1+\xi_k^{(0)}) (\rho_k^{(0)})^{(c-1)/2}}$$

$$\times \frac{I_{c-1}\left(2\sqrt{\frac{c\rho_k^{(0)}}{1+\xi_k^{(0)}}}\sqrt{\frac{z_1}{2(1+\xi_k^{(0)})}}\right)}{e^{z_1/2(1+\xi_k^{(0)})}} \tag{128}$$

We derive a condition set C as

$$
C = \begin{cases}
(\sigma_k^{(0)})^2 \to 0 \\
\rho_k^{(0)} \to \infty \\
\xi_k^{(0)} \to \infty \\
z_1^{(0)} \to \infty
\end{cases}
\tag{129}
$$

Defining

$$
x = \sqrt{\frac{z_1}{2(1+\xi_k^{(0)})}} \qquad a = \sqrt{\frac{c\rho_k^{(0)}}{1+\xi_k^{(0)}}}
\tag{130}
$$

and recalling the series expansion for the modified Bessel function with an integer order $(c-1)$ and for the exponential function

$$
I_{c-1}(2ax) = \sum_{m=0}^{\infty} \frac{a^{2m+c-1}x^{2m}x^{c-1}}{m!\,(m+c-1)!}, \qquad e^{x^2} = \sum_{m=0}^{\infty} \frac{x^{2m}}{m!}
\tag{131}
$$

we see that the limit of the first part of equation (129) under the condition set C has a finite nonzero value. In addition the third part, which has a form of $I_{c-1}(2ax)/(e^{x^2})$, does not converge (the order of $I_{c-1}(.)$ is equal to or greater than the order of e^{x^2}; so if $c \geq 2$ this may happen). Finally, the second part may approach infinity depending on the order of z_1 with respect to $1/\sigma_k^2$. Hence, $\lim_C f_{z_1}^{(0)}(z_1) \to \infty$, and

$$
f_{z_1}(z_1) =_{M \to \infty} \delta(M-z_1) \quad \textit{for } c=L-1 \geq 2
\tag{132}
$$

Rewriting this equation, we get

41

$$f_{Z_1}^{(0)}(z_1) = f_{Z_{1k}}^{(0)}(z_1) * f_{Z_{1k}}^{(0)}(z_1) \qquad when \ c=2 \qquad (133)$$

This is simply a two-fold convolution (auto-convolution) of $f_{Z1k}^{(0)}(z_1)$, and equation (132) is valid if and only if

$$f_{Z_{1k}}^{(0)}(z_{1k}) = \frac{M}{2} \to \delta\left(\frac{M}{2} - z_1\right) \quad is \ true \qquad (134)$$

Obviously, equation (132) is valid not only for $c \geq 2$ but also for $c=1$, and $P(E) = \gamma^L P(e/1=L)$ can be derived from equation (99) as

$$P(E) = \frac{\gamma^L \beta_k^{(1)} e^{-2\beta_k^{(1)} L \rho_k^{(1)}}}{2^L (2L\rho_k^{(1)})^{(L-1)/2}} \sum_{i=0}^{L-1} 2^i \int_0^\infty \frac{e^{-(\beta_k^{(1)} + \frac{1}{2})z_1}}{(L-i-1)!}$$

$$\times \left[z_1^{(L-1)/2} z_1^{(L-1-i)} \ I_{L-1}\left(2\beta_k^{(1)} \sqrt{2l\rho_k^{(1)} z_1}\right) \right] . dz_1 \qquad (135)$$

Results are obtained numerically by evaluating equation (134) when $L>1$. For $L=1$, numerical results can be found with equation (113).

IV. NUMERICAL RESULTS

Bit error probabilities for worst case interference ratios are obtained versus bit energy-to-interference density with the following parameters: a) detector type, b) direct-to-diffuse signal ratios ($DD=A^2/2\sigma^2$), and c) bit energy-to-noise power spectral density ratios (E_b/N_o). These results are shown in Figures 7 through 62. In the absence of interference, the results shown in Figures 63 through 82 are obtained. They illustrate BER as a function of E_b/N_o with the following parameters: a) detector type, b) direct-to-diffuse signal ratios. Figures 83-86 are an illustration of the performance of the various nonlinear combining receivers versus bit energy-to-interference power spectral density (E_b/N_I) ratios when there is no thermal noise contamination ($N_o \to 0$) and DD=10 (a moderate fading effect).

Worst case γ values are obtained by inspection, and it can be seen that for a particular detector (and normalization) type the worst case γ's are functions of the parameters: E_b/N_o, E_b/N_I, L and DD. For the linear combining analyses, we see that all of the parameters mentioned effect the worst case γ (γ_o) in an inverse manner. For nonlinear combining, γ_o is directly proportional to L, while the effect of the other parameters investigated on γ_o is the same as for linear combining. The relationship between γ_o and $A^2/2\sigma^2$ is very

loose. For strong fading, detector performance is not sensitive to γ [reference 1].

A. PERFORMANCE ANALYSIS FOR WORST CASE PARTIAL-BAND INTERFERENCE

1. Linear Combining Detectors

(1) E_b/N_o=13,35 dB and DD=0.01 (Figures 7 and 8)

There is not a visible difference between envelope and square-law detectors. Both have a great amount of diversity improvement for $E_b/N_I \geq 5$ dB. The optimum value of L is greater than 4 for the envelope detector with $E_b/N_I > 10$ dB and the square-law detector for $E_b/N_I > 15$ db. The square-law detector has a slightly better performance for these optimum L values when $E_b/N_I > 30$ Db.

(2) E_b/N_o=13.35 Db and DD=1 (Figures 9 and 10)

Both detectors show a diversity improvement. The optimum number of chips per bit is greater than 4 for the envelope detector with $E_b/N_I \geq 12$ dB and for the square-law detector with $E_b/N_I > 17$ dB. The square-law detector has a slightly better performance.

(3) E_b/N_o=13.35 dB and DD=10 (Figures 11 and 12)

The region of diversity improvement begins for the envelope detector with $E_b/N_I > 9$ dB and for the square-law detector with $E_b/N_I > 20$ dB. The optimum L=4 for the envelope

detector with $E_b/N_I>15$ dB, while the optimum L never exceeds 2 for the square-law detector. Performance of the envelope detector is better than the square-law detector for 25 dB>E_b/N_I>7 dB and equal for E_b/N_I>25 dB.

(4) E_b/N_o dB and DD=1000 (Figures 13 and 14)

The square-law detector does not exhibit diversity improvement in this case, but the envelope detector does. The performance of the envelope detector is much better than the performance of the square-law detector. Simulations with greater $A^2/2\sigma^2$ such as 10^6 for some values of E_b/N_I show that there is a diversity improvement for the envelope detector not only versus fading but also versus partial-band interference. There is not any difference between the values obtained for $A^2/2\sigma^2$=1000 and 10^6, so $A^2/2\sigma^2$=1000 represents the no fading condition (Similarly $A^2/2\sigma^2$=0.01 represents Rayleigh fading).

(5) E_b/N_o =16 dB and DD=0.01 (Figures 15 and 16)

Both detectors show a diversity improvement. For the optimum values of L, the performance of the envelope detector is better than that of the square-law detector up to E_b/N_I=35 dB. Comparing Figures 15 and 16 to Figures 63 and 64 (the latter two figures illustrate performance when there is no partial-band interference for the same values of E_b/N_o and DD), we see that both detectors (linear combining) have almost the same diversity improvement versus fading, but the envelope detector is better versus partial-band interference.

(6) E_b/N_o=16 dB and DD=1 (Figures 17 and 18)

Both detectors show diversity improvement, but the performance of envelope detector is superior.

(7) E_b/N_o=16 dB and DD=10 (Figures 19 and 20)

Diversity improvement is achieved by the envelope detector, but not by the square-law detector up to E_b/N_I>27 dB. The envelope detector performance is better.

(8) E_b/N_o=16 dB and DD=1000 (Figures 21 and 22)

The envelope detector show diversity improvement up to 3 dB, but no diversity improvement is reached by the square-law detector. The envelope detector performance is better.

(9) E_b/N_o=18 dB and DD=10 (Figures 23 and 24)

The envelope detector shows a diversity improvement, but the square-law detector does not up to E_b/N_I>33 dB. Note that the diversity improvement region for this particular value of $A^2/2\sigma^2$ is decreasing with increasing E_b/N_o for the square-law detector. If thermal noise is negligible, then partial-band interference has a more significant impact on system performance than fading, and no diversity improvement is obtained with the square-law detector.

(10) E_b/N_o=18 dB and DD=100 (Figures 25 and 26)

A diversity improvement is obtained for the envelope detector up to 3 dB but there is no diversity improvement for the square-law detector. The envelope detector is 3 dB (or as much as diversity improvement) better in performance. For a

particular value of L, it is much better than 3 db because of the diversity degradation for the square-law detector.

2. Self-Normalization Combining Detectors

(1) E_b/N_o=13.35 dB and DD=0.01 (Figures 27 and 28)

The performances of both of the detectors are almost the same. Some diversity improvement is obtained, but performance degradation is as much as 4 dB as compared to linear combining detectors.

(2) E_b/N_o=13.35 dB and DD=1 (Figures 29 and 30)

The performances are the same for both of the self-normalization detectors. These detectors show a diversity improvement, but performance is degraded up to 3.5 dB as compared to the linear combining detectors.

(3) E_b/N_o=13.35 dB and DD=10 (Figures 31 and 32)

The performances of both of detectors are much alike. Some diversity improvement for E_b/N_I>10 db is obtained. Some performance improvement is achieved by the square-law detector for 12 db<E_b/N_I<28 dB, but this improvement is because of the deficiency in the performance of the square-law linear combining detector. Both of the detectors suffer a performance degradation for E_b/N_I>28 db, and this degradation with respect to the linear combining envelope detector is 3 dB at E_b/N_I=40 dB.

(4) E_b/N_o=13.35 dB DD=1000 (Figures 33 and 34)

The performances of both of the detectors are the same. Diversity improvement is obtained for 10 dB < E_b/N_I < 38 dB. Performance improvement for both of the detectors with respect to the linear combining envelope detector is about 5 dB.

(5) E_b/N_I=16 dB and DD=0.01/1 (Figures 35, 36 and 37, 38)

The performances of both of the detectors are the same, with a diversity improvement but not a performance improvement (with respect to the linear combining envelope detector).

(6) E_b/N_I=16 dB DD=10 (Figures 39 and 40)

Both of the detectors have the same performance. Diversity improvement and performance improvement are obtained for E_b/N_I>10 dB. The maximum performance improvement with respect to the envelope linear combining detector is 7 dB.

(7) E_b/N_o=16 dB DD=1000 (Figures 41 and 42)

Performance of the both detectors is the same, a diversity and a performance improvement is obtained up to 20 dB.

(8) E_b/N_o=18 dB DD=1000 (Figures 43 and 44)

The detector performances are the same. Diversity improvement and performance improvement (up to 15 dB) are obtained.

3. Noise-Normalization Combining Detectors

(1) E_b/N_o=13.35 dB DD=0.01/1 (Figures 45, 46 and 47 48)

The performances of the two detectors are the same. Diversity improvement but no performance improvement is obtained.

(2) E_b/N_o=13.35 dB DD=10/1000 (Figures 49, 50 and 51, 52)

The detector performances are much alike. Diversity and performance improvement relative to the linear combining and the self-normalization combining detectors are obtained and maximized for moderate values of E_b/N_I.

(3) E_b/N_o=16 dB DD=0.01/1 (Figures 53, 54 and 55, 56)

The performances of the detectors are similar. A visible performance improvement is not obtained.

(4) E_b/N_o=16 dB DD=10 and 1000 (Figures 57, 58 and 59,60)

Optimum L is 4 or at most 6. The performances of the detectors are similar. Both have diversity and performance improvement.

(5) E_b/N_o=18 dB DD=10 (Figures 61 and 62)

Performance and diversity improvement are obtained.

49

B.   COMPARISION OF THE PERFORMANCES IN THE ABSENCE OF PARTIAL -BAND INTERFERENCE

Linear and noise-normalization combining detectors are analytically shown to have the same performance when the effect of the partial-band interference is eliminated. Self-normalization combining detectors have a very poor performance in this case. Even though they show a diversity improvement (gained versus fading), noncoherent combining losses are much more than for the linear and the noise-normalization combining detectors. All the detectors show a diversity improvement for moderate values of direct-to-diffuse signal ratios, but for the self-normalization combining detectors the improvement region begins at greater values of E_b/N_o. There is not a visible performance difference between the envelope and the square-law self-normalization combining detectors.   By comparing the performances of the envelope and the square-law linear (also noise-normalization) combining detectors, one can conclude that for the systems suffering from fading the square-law detector performs slightly better. For no or moderate amounts of fading, their performances are the same.

C.   PERFORMANCES OF THE NONLINEAR DETECTORS UNDER NO THERMAL NOISE

The nonlinear combining receivers are analyzed for $A^2/2\sigma^2=10$. The performances of both detectors for self-normalization combining (Figures 81 and 82) are found to be

the same. Diversity improvement is obtained for $E_b/N_I > 7$ dB. The self-normalization receivers show a visible performance degradation regarding as compared to the noise-normalization combining detectors (comparing Figures 81 and 82 with 79 and 80).

Performances of the two detectors for noise-normalization combining are compared in Figures 81 and 82 . No visible difference is found. Both have diversity improvement for $E_b/N_I > 7$ dB.

V. CONCLUSION

The linear combining receiver implemented with the envelope detector is seen to have a diversity improvement both versus fading and partial-band interference, while the linear combining square-law detector has a diversity improvement versus only fading. Performance differences are also emphasized by the decreasing effect of thermal noise. Under no interference or wideband (uniform) interference conditions, the performances of the two linear combining detectors are found to be the same versus fading.

Self-normalization combining receivers implemented with envelope and square-law detectors are seen to have the same performance. They have diversity and performance improvement compared to the linear combining receivers versus only partial-band interference. They are very sensitive to fading and thermal noise. Self-normalization can be a good choice for down-link communication under good weather conditions and partial-band interference.

The square-law and envelope detectors implemented with the noise-normalization combining scheme do not differ in performance. They have the best performance. Their performances approach the linear combining receivers under wideband or no interference conditions. When the signal is

completely diffuse there is not any performance improvement for the noise-normalization combining receivers with respect to a linear combining receiver implemented with an envelope detector.

For slow frequency hopping, all the possible detector and combining type combinations that are inspected have the same performance.
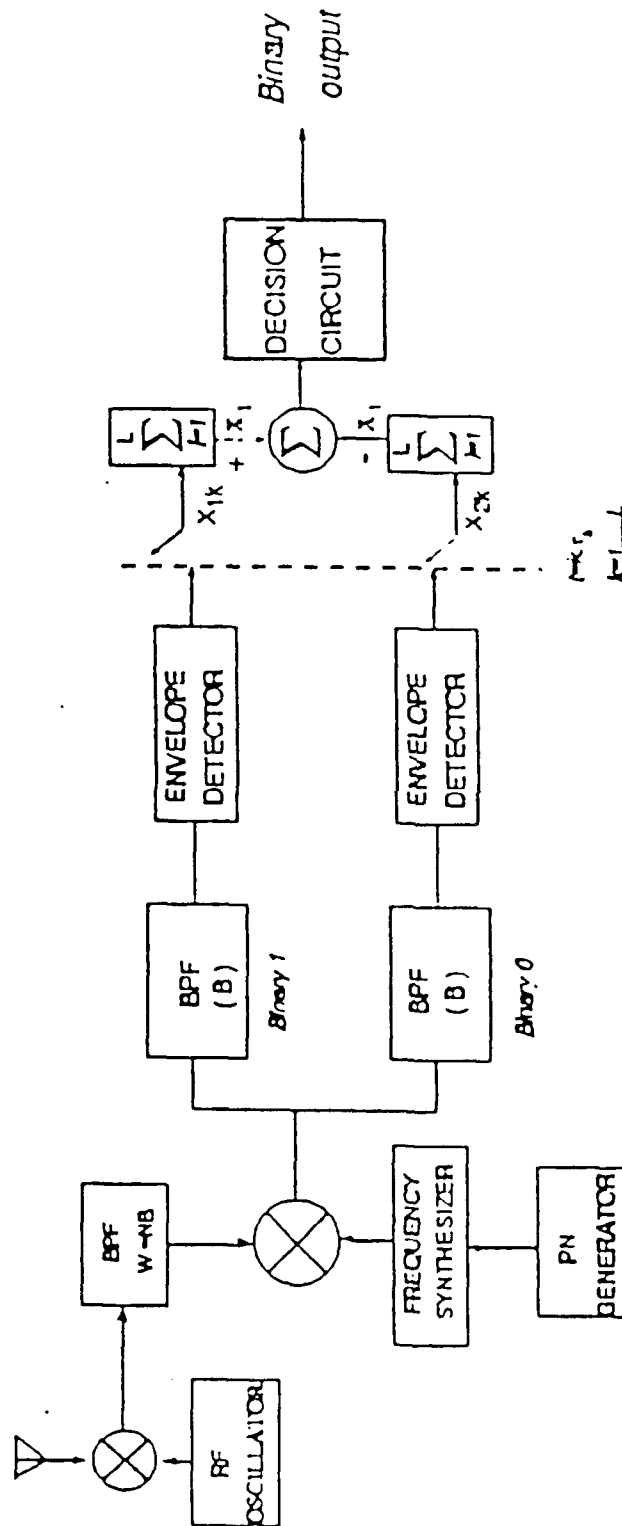
Figure 1. Envelope Detector Linear Combining
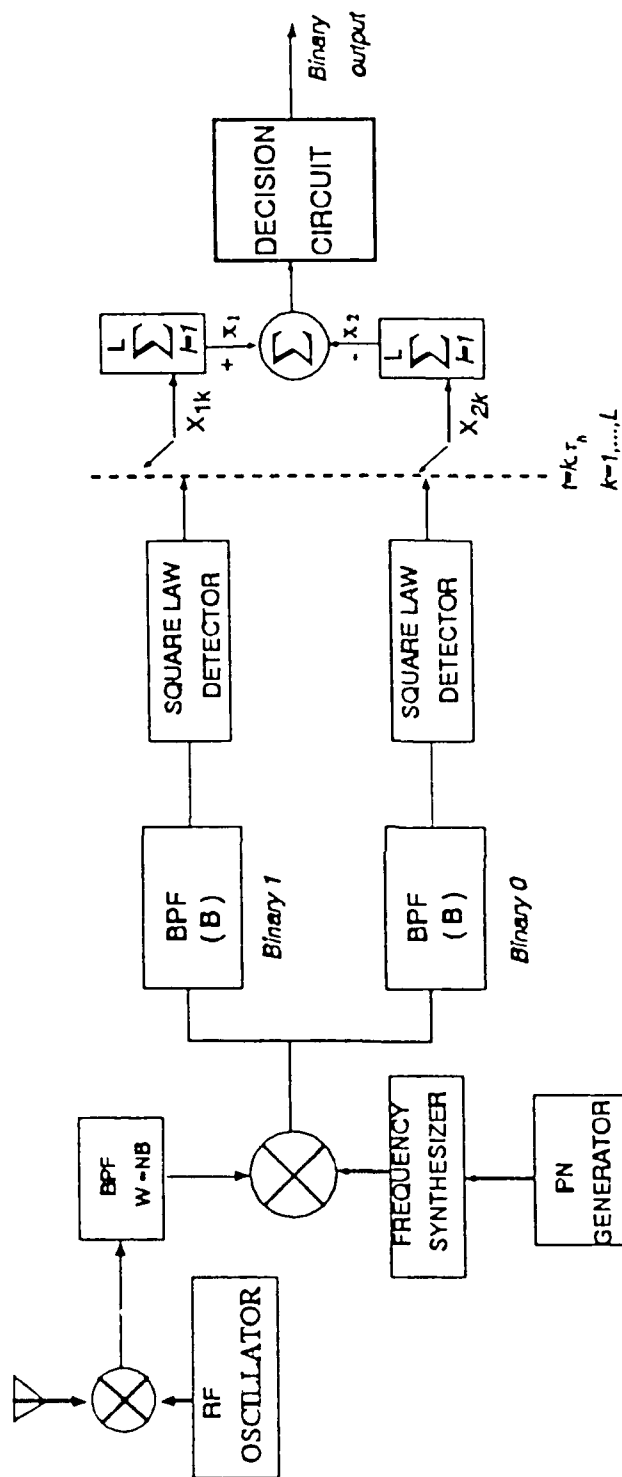
Figure 2. Square Law Detector Linear Combining
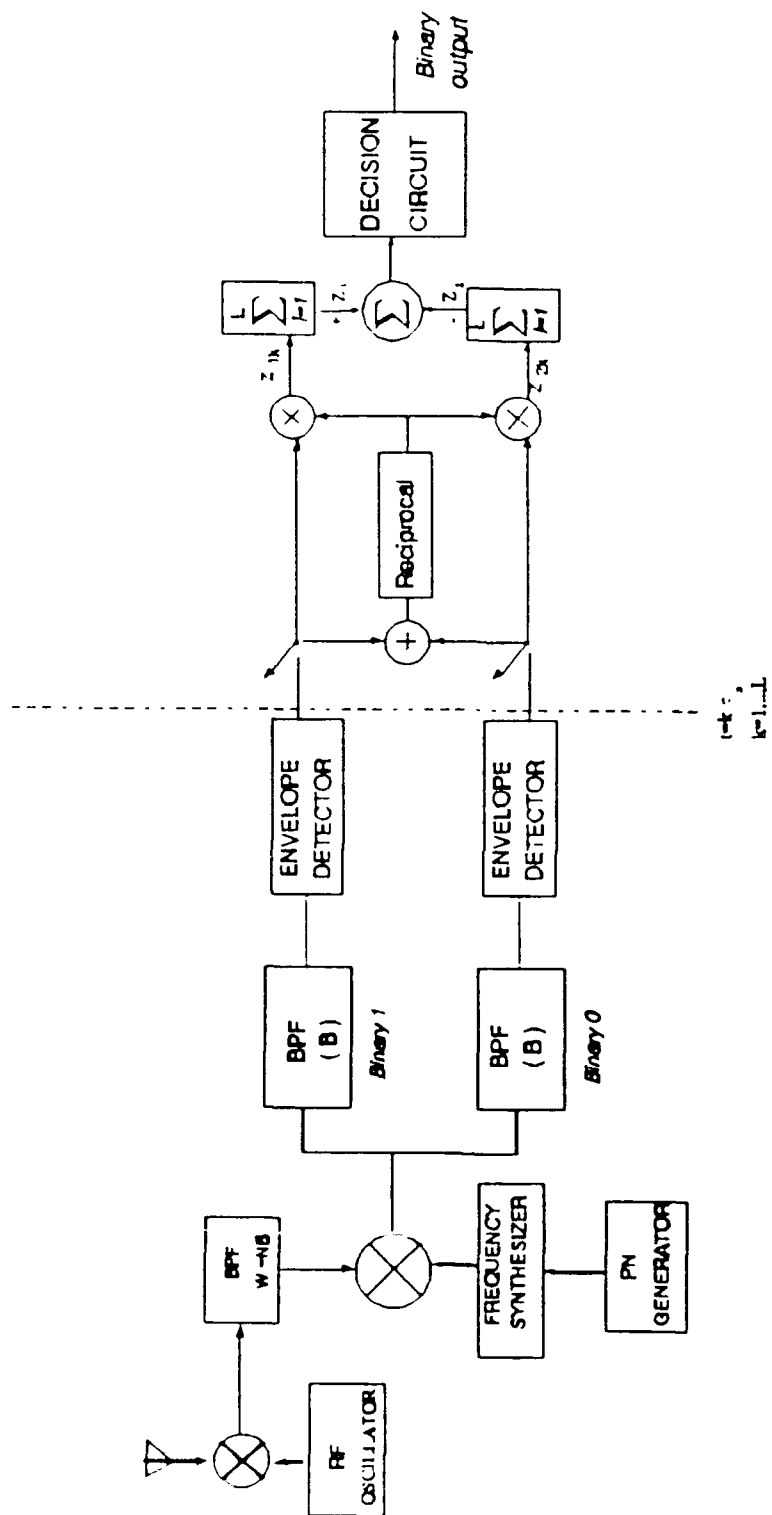
Figure 3. Envelope Detector Self-Normalization Combining

56
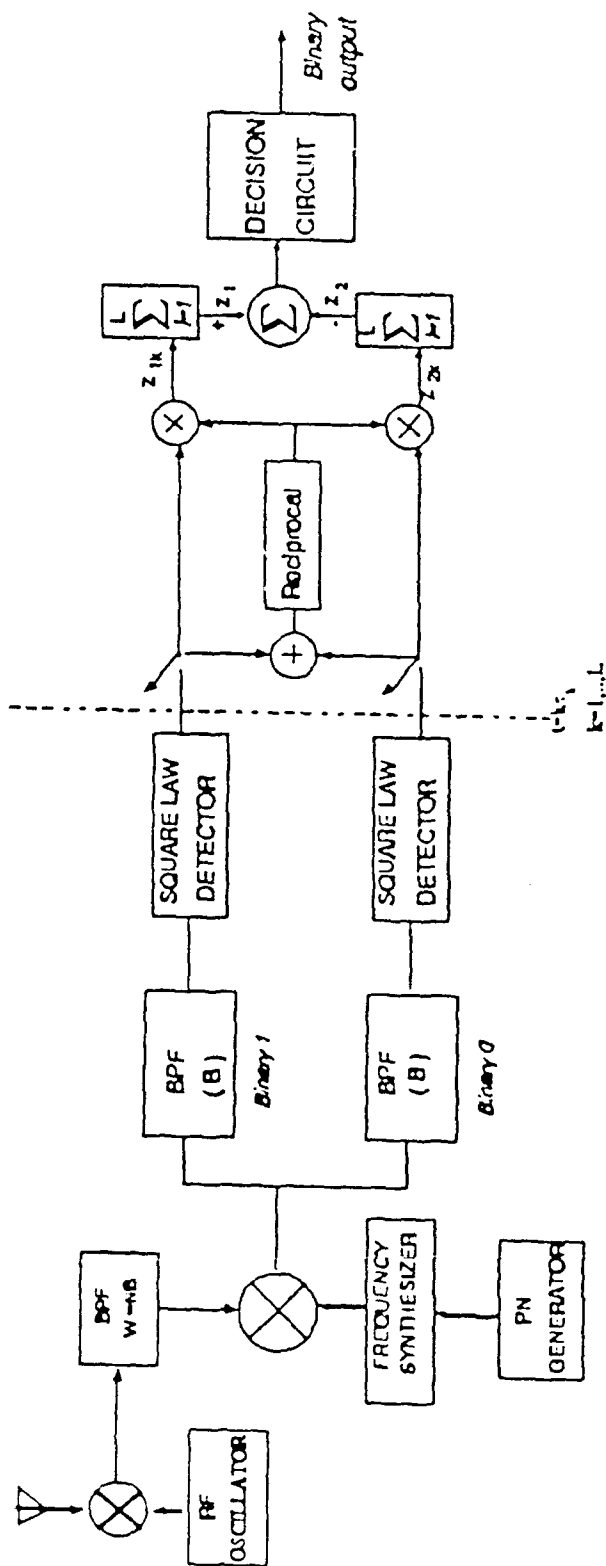
Figure 4. Square-Law Detector Self-Normalization Combining
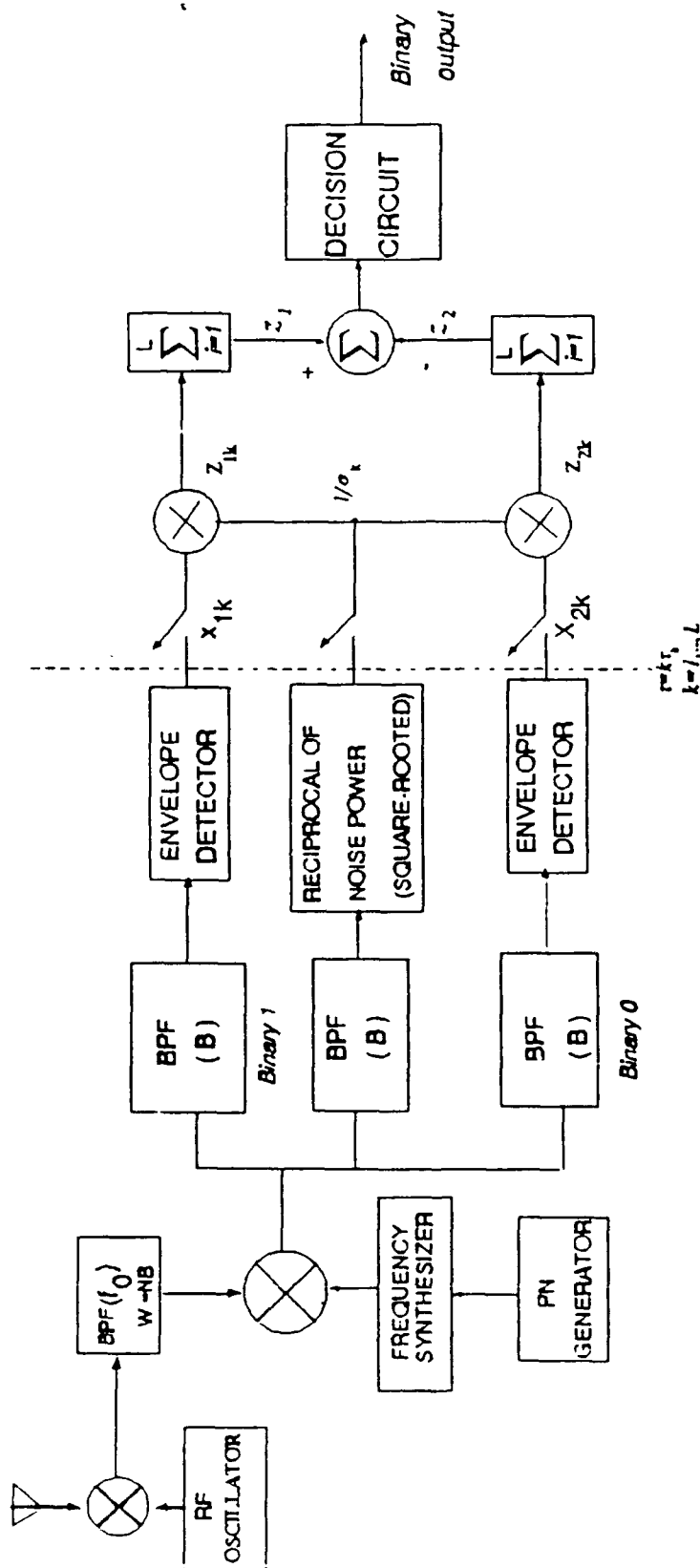
Figure 5. Envelope Detector Noise Normalization
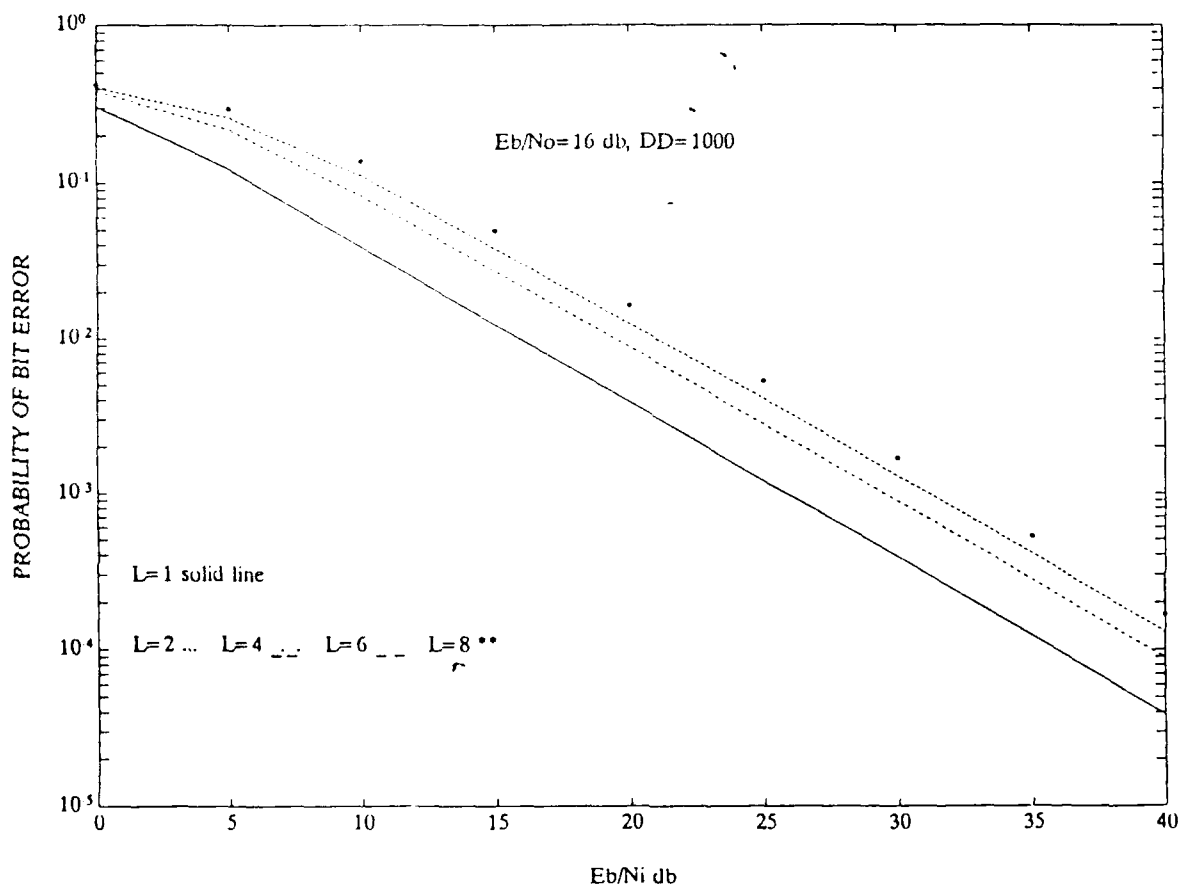
58
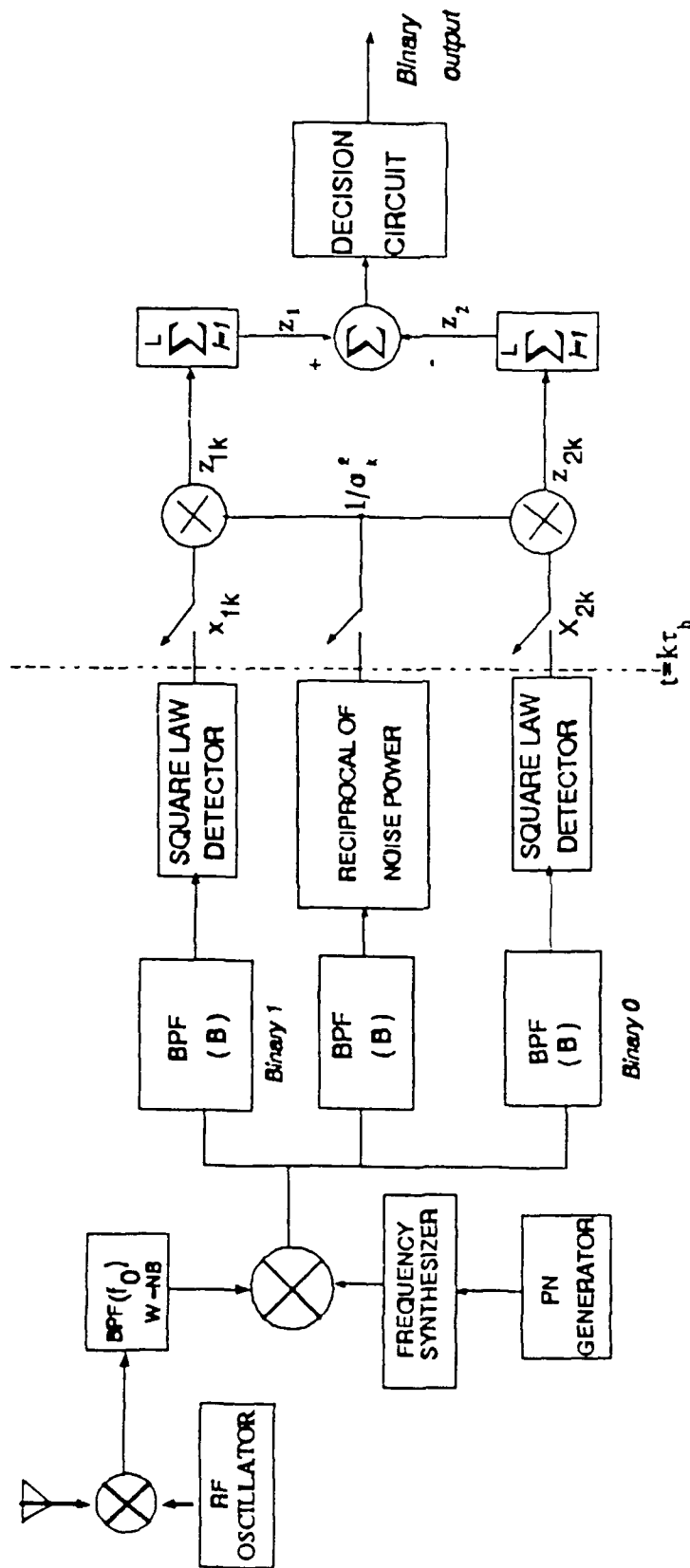
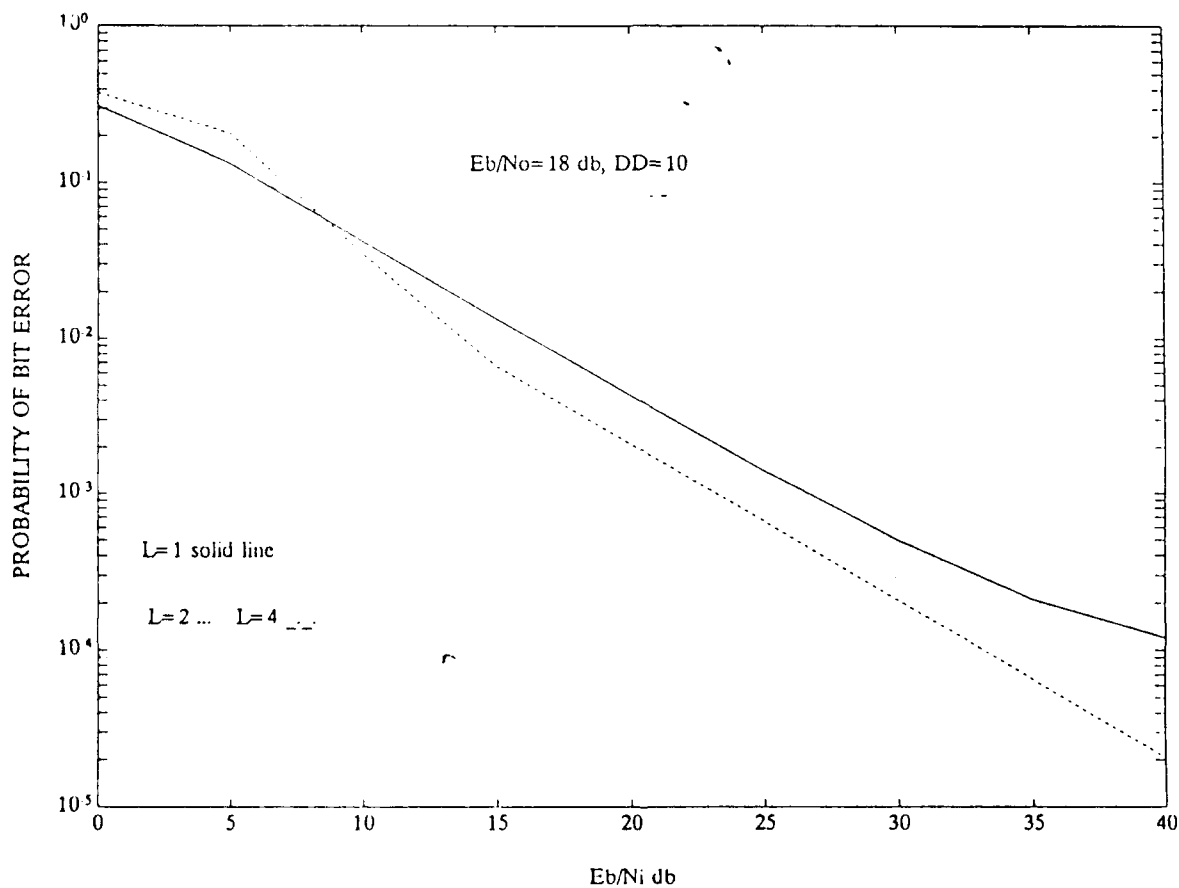*Figure 6. Square Law Detector Noise Normalization*
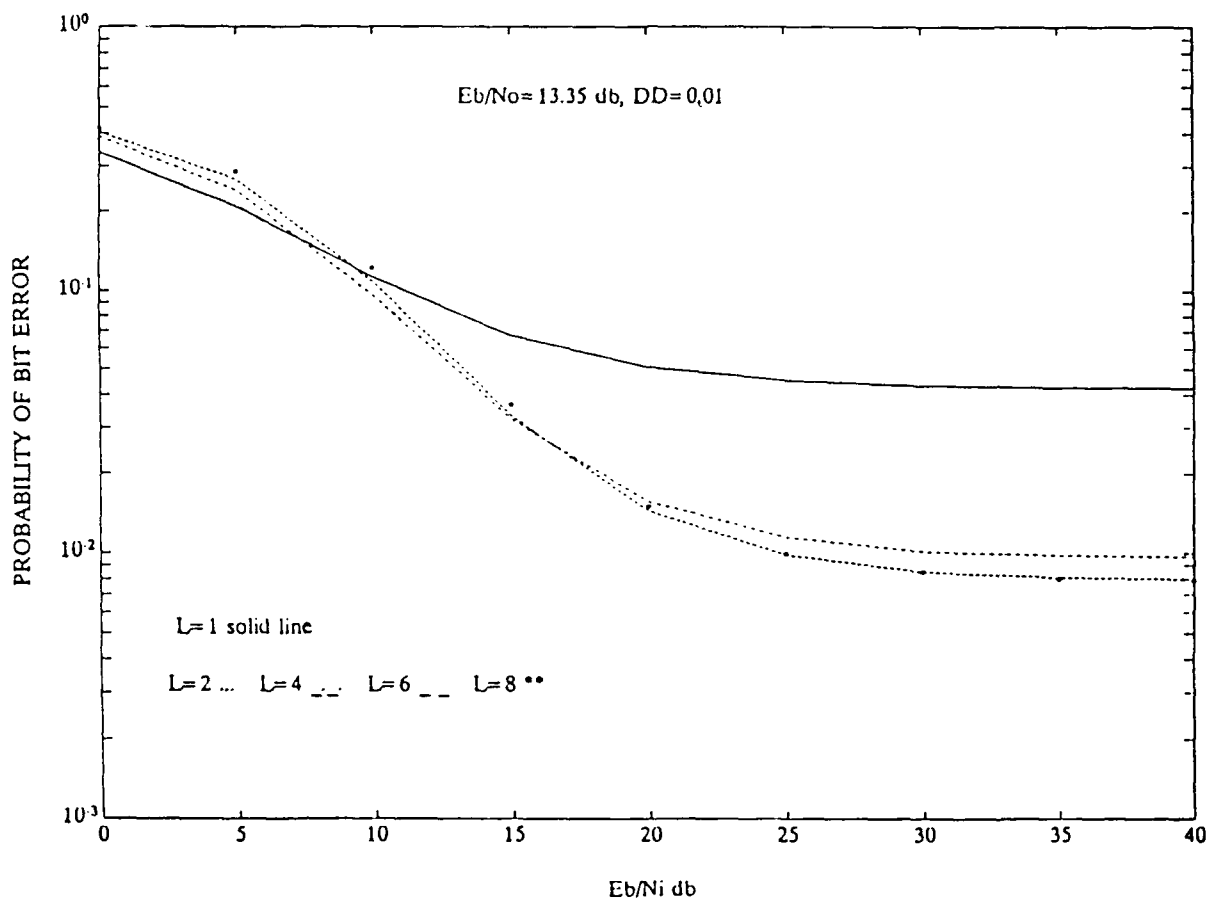
Figure 7. Envelope Detector Linear Combining: Worst case performance of the linear combining envelope detector receiver with diversity combining, partial-band interference, and thermal noise in a fading channel for a diffuse signal ($A^2/2\sigma^2=0.01$) and $E_b/N_o=13.35$ dB.
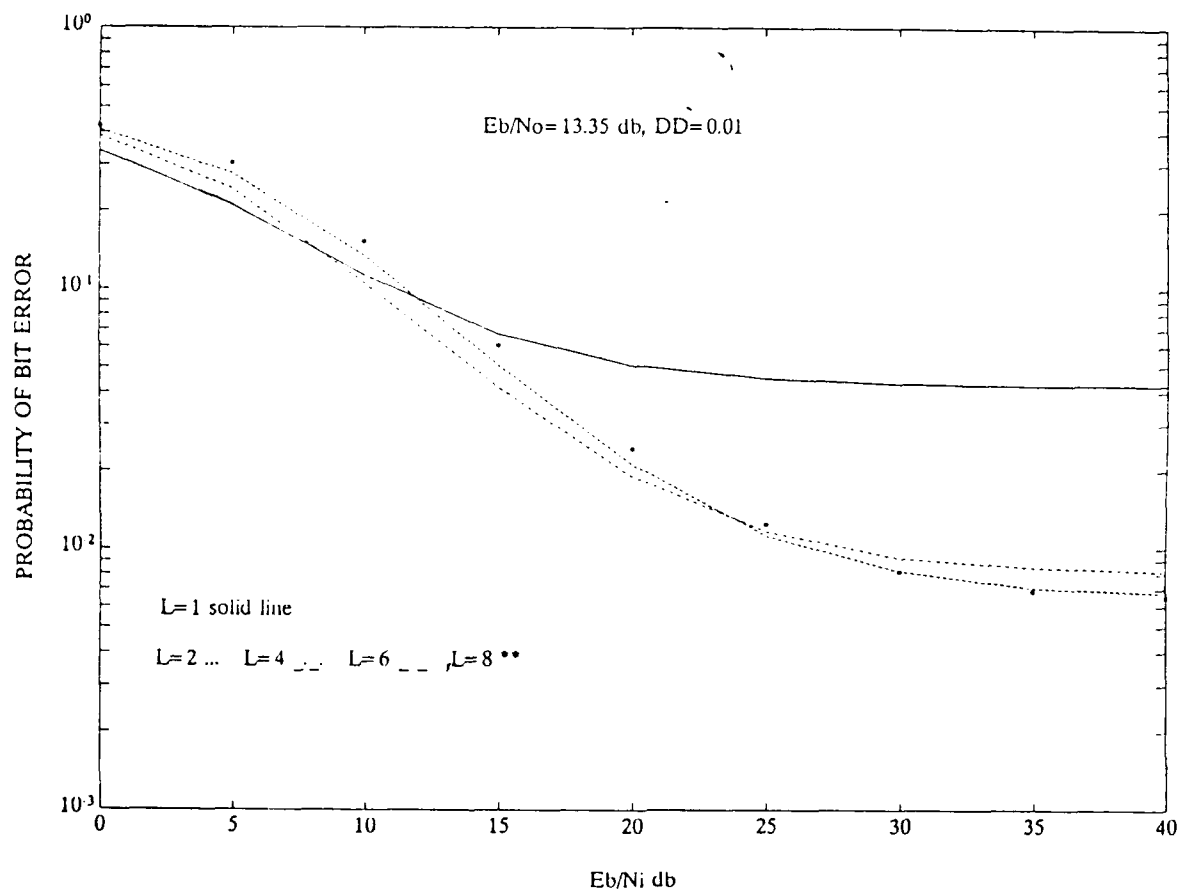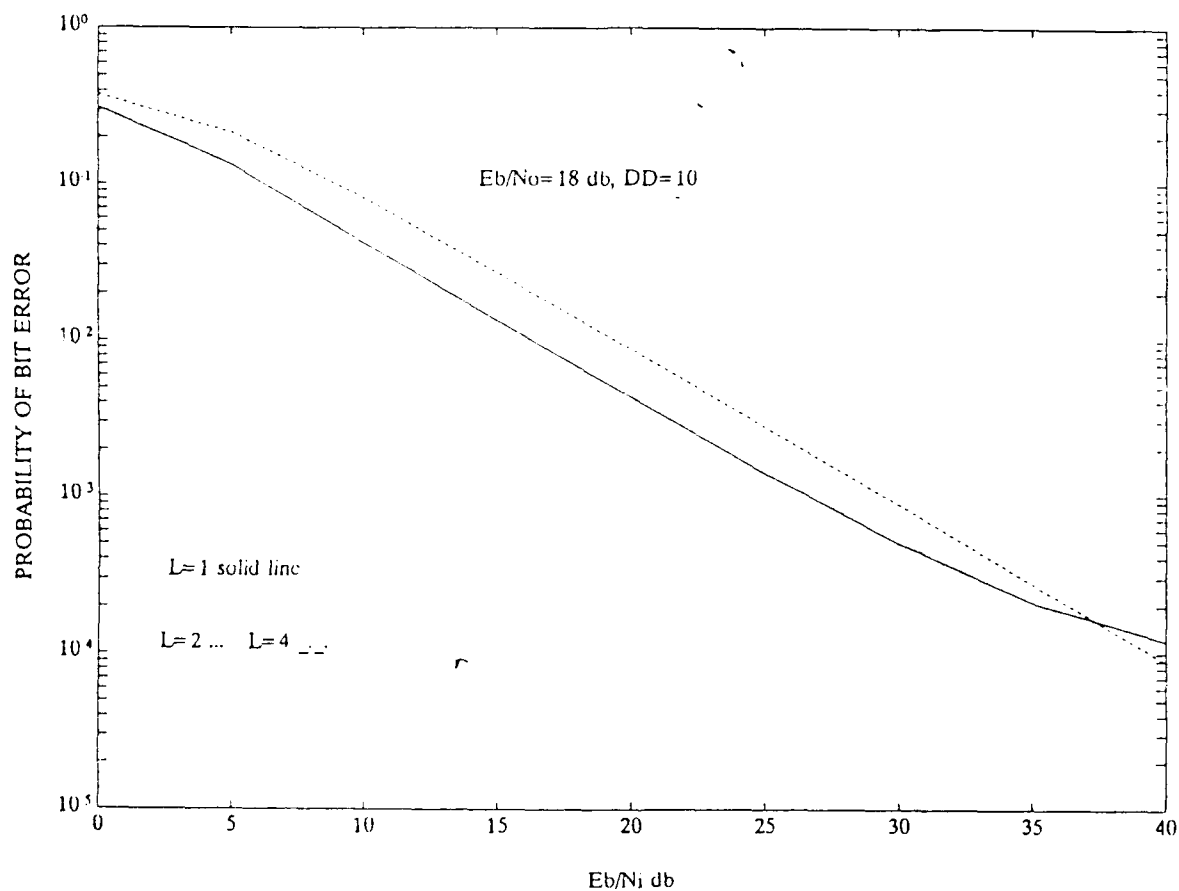
Figure 8. **Square-Law Detector Linear Combining:** Worst case
performance of the linear combining square-law detector
receiver with diversity combining, partial-band
interference, and thermal noise in a fading channel for a
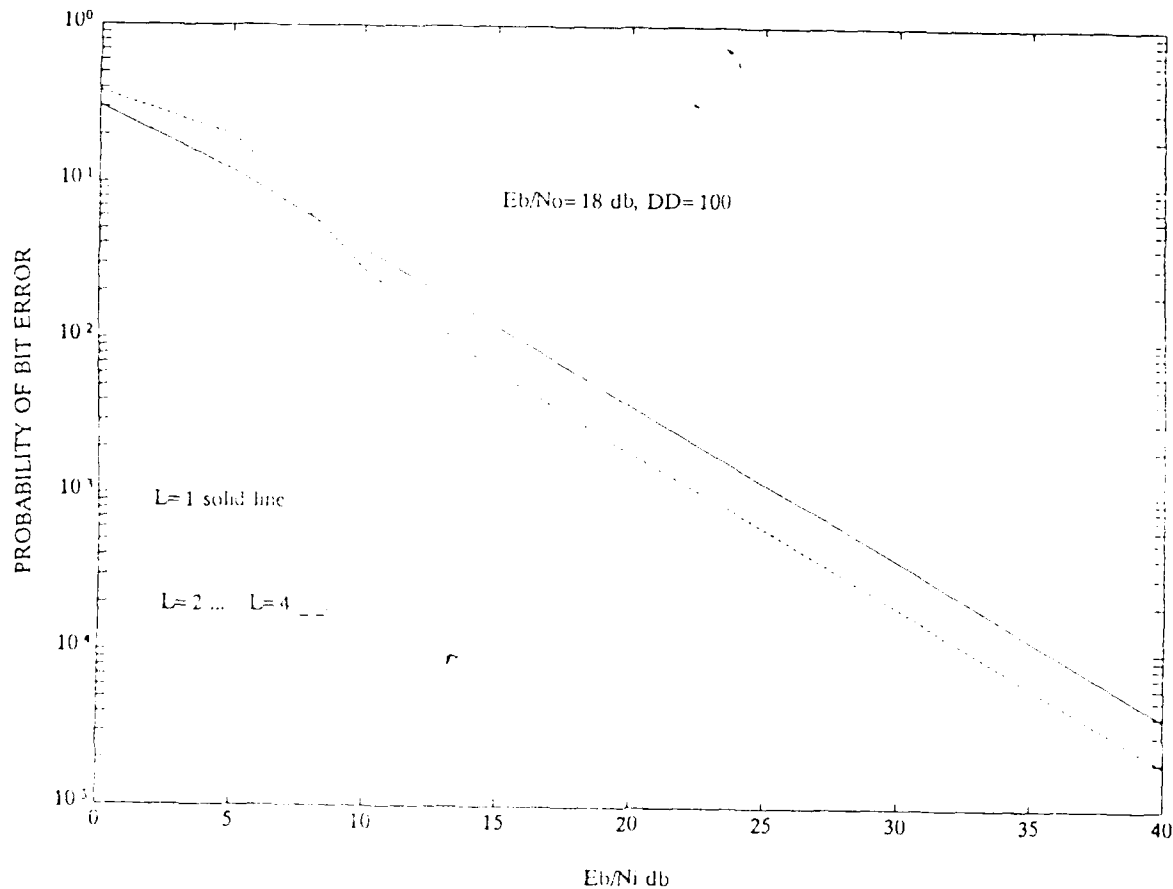diffuse signal ($A^2/2\sigma^2$=0.01) and E_b/N_o=13.35 dB.

61
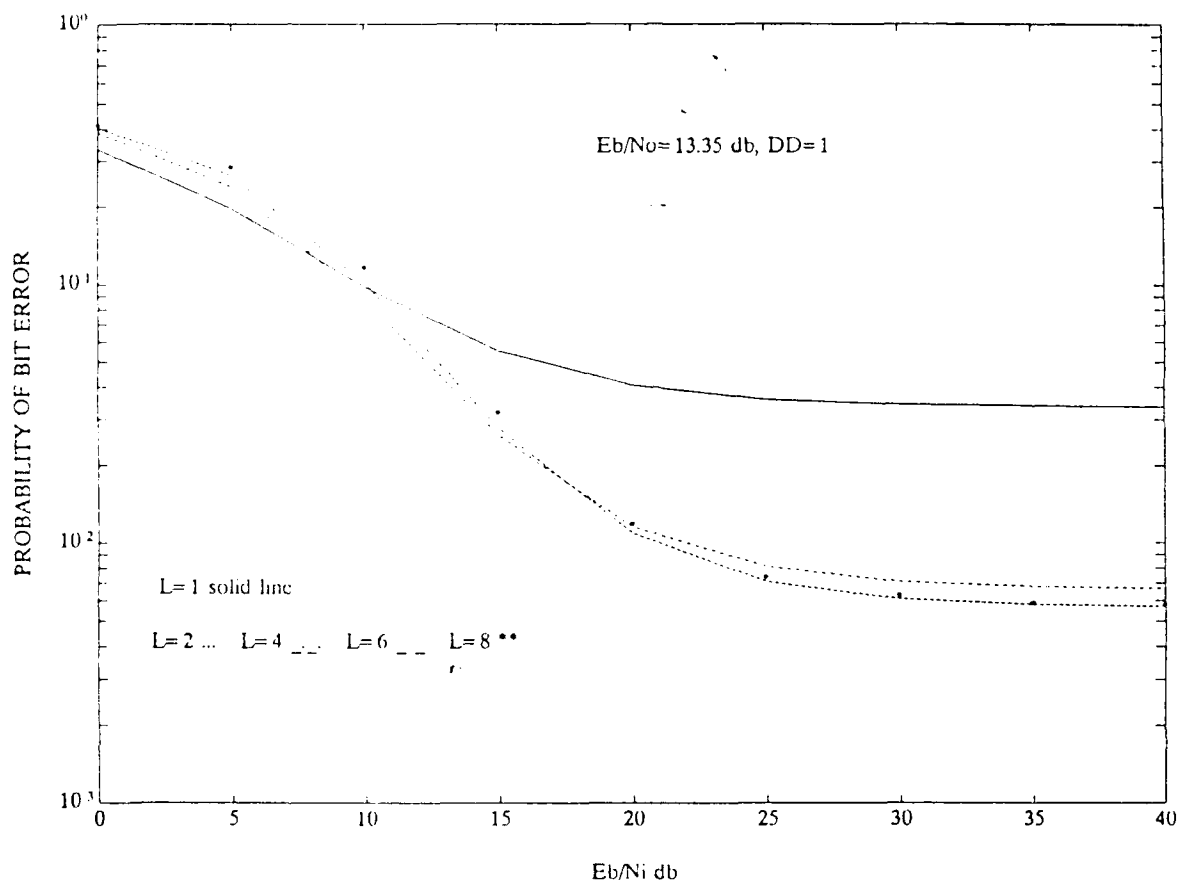
Figure 9. **Envelope Detector Linear Combining:** Worst case performance of the linear combining envelope detector receiver with diversity combining, partial-band interference, and thermal noise in a fading channel for a signal with equal direct and diffuse components $(A^2/2\sigma^2=1)$ and $E_b/N_o=13.35$ dB.
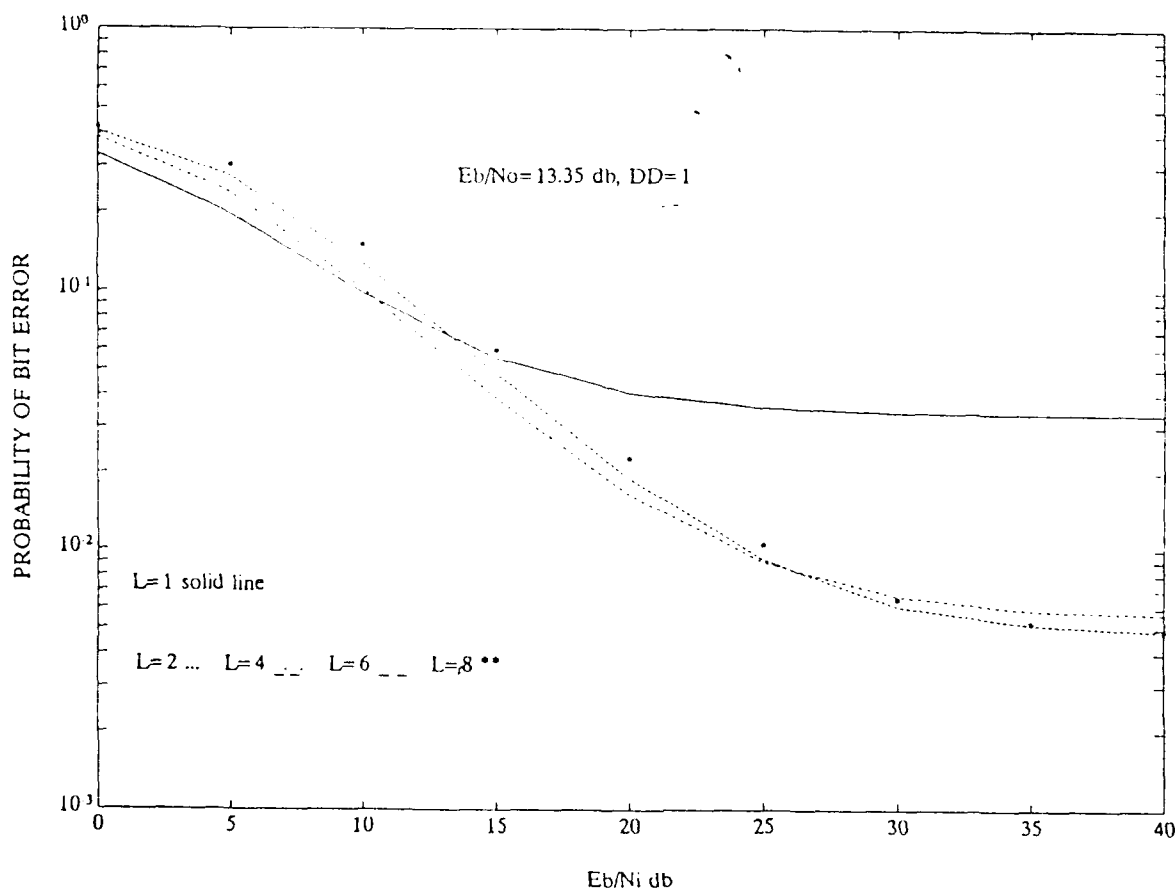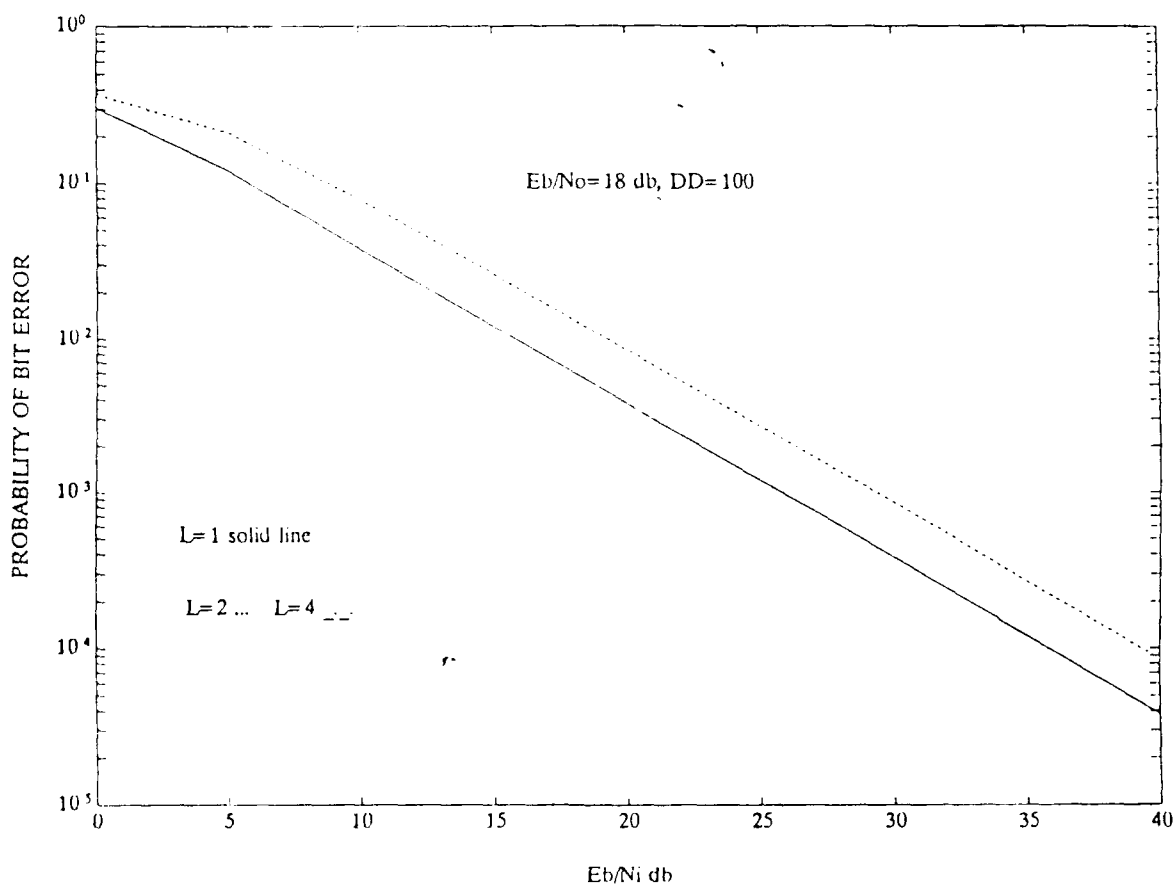
Figure 10. Square-Law Detector Linear Combining: Worst case performance of the linear combining square-law detector receiver with diversity combining, partial-band interference, and thermal noise in a fading channel for a signal with equal direct and diffuse components ($A_2/2\sigma^2 = 1$) and $E_b/N_o = 13.35$ dB.

63
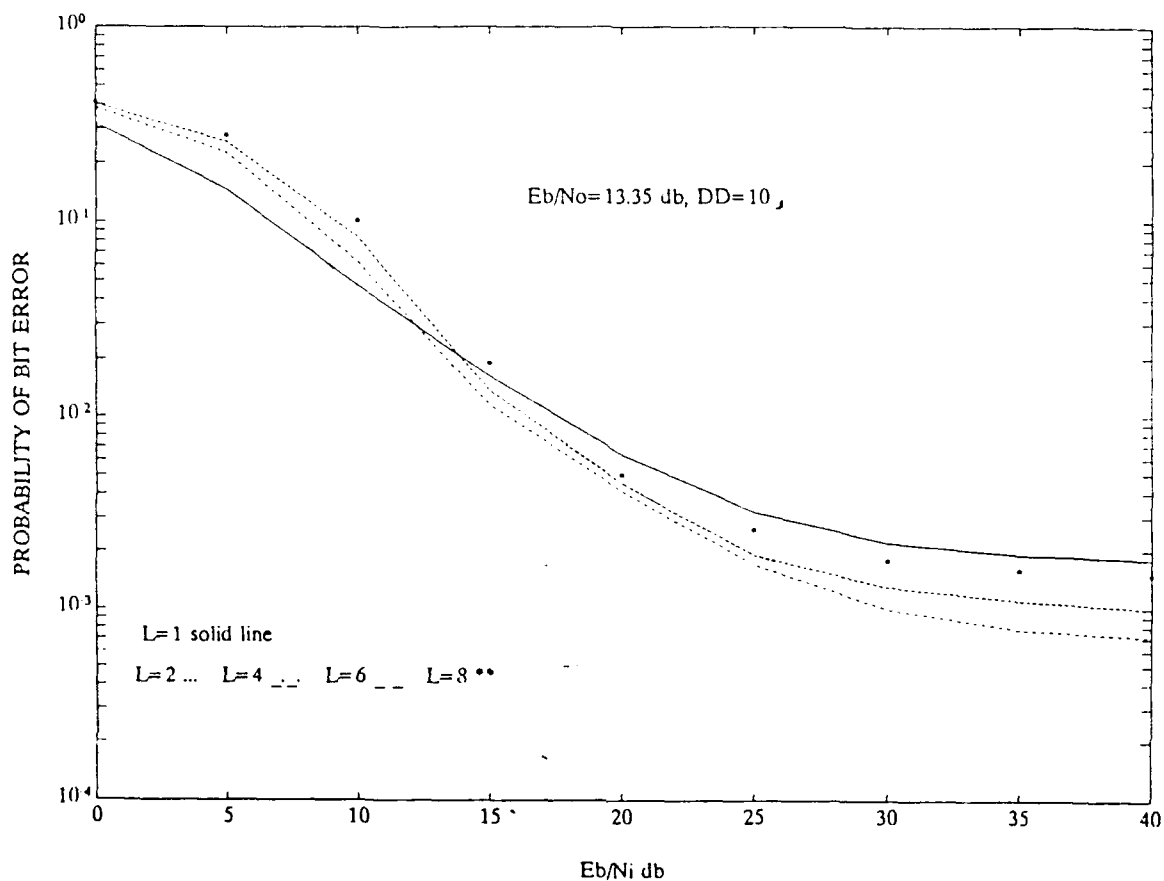
Figure 11. Envelope Detector Linear Combining: Worst case performance of the linear combining envelope detector receiver with diversity combining, partial-band interference, and thermal noise in a fading channel for a relatively strong direct signal component $(A^2/2\sigma^2=10)$ and $E_b/N_o=13.35$ dB.
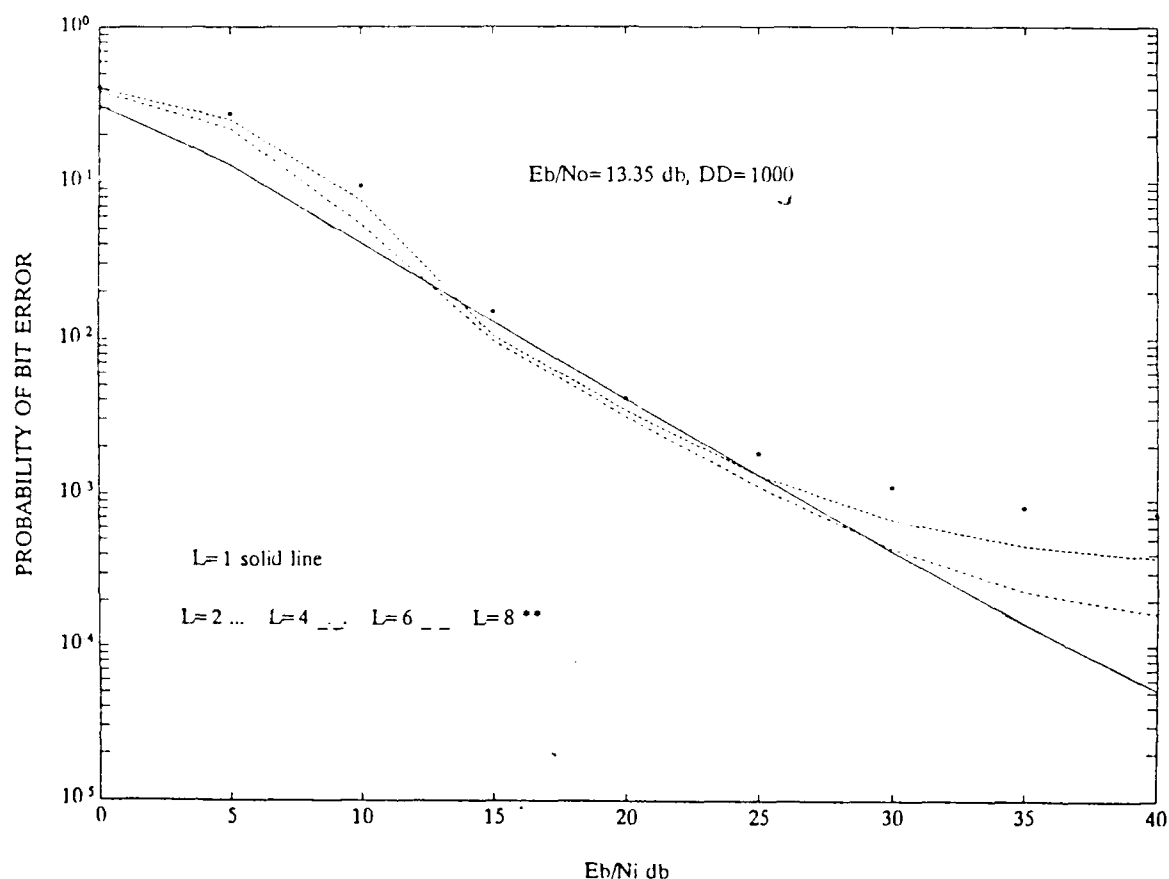
Figure 13. Envelope Detector Linear Combining: Worst case performance of the linear combining envelope detector receiver with diversity combining, partial-band interference, and thermal noise in a fading channel for a strong direct signal component ($A^2/2\sigma^2=1000$) and $E_b/N_o=13.35$ dB.

66

The figure shows a graph with the following labels:

- Y-axis: PROBABILITY OF BIT ERROR (10^0, 10^1, 10^2, 10^3, 10^4, 10^5)
- X-axis: Eb/Ni db (0, 5, 10, 15, 20, 25, 30, 35, 40)
- Eb/No=13.35 db, DD=1000
- L=1 solid line
- L=2 ... L=4 _._ L=6 _ _ L=8 **
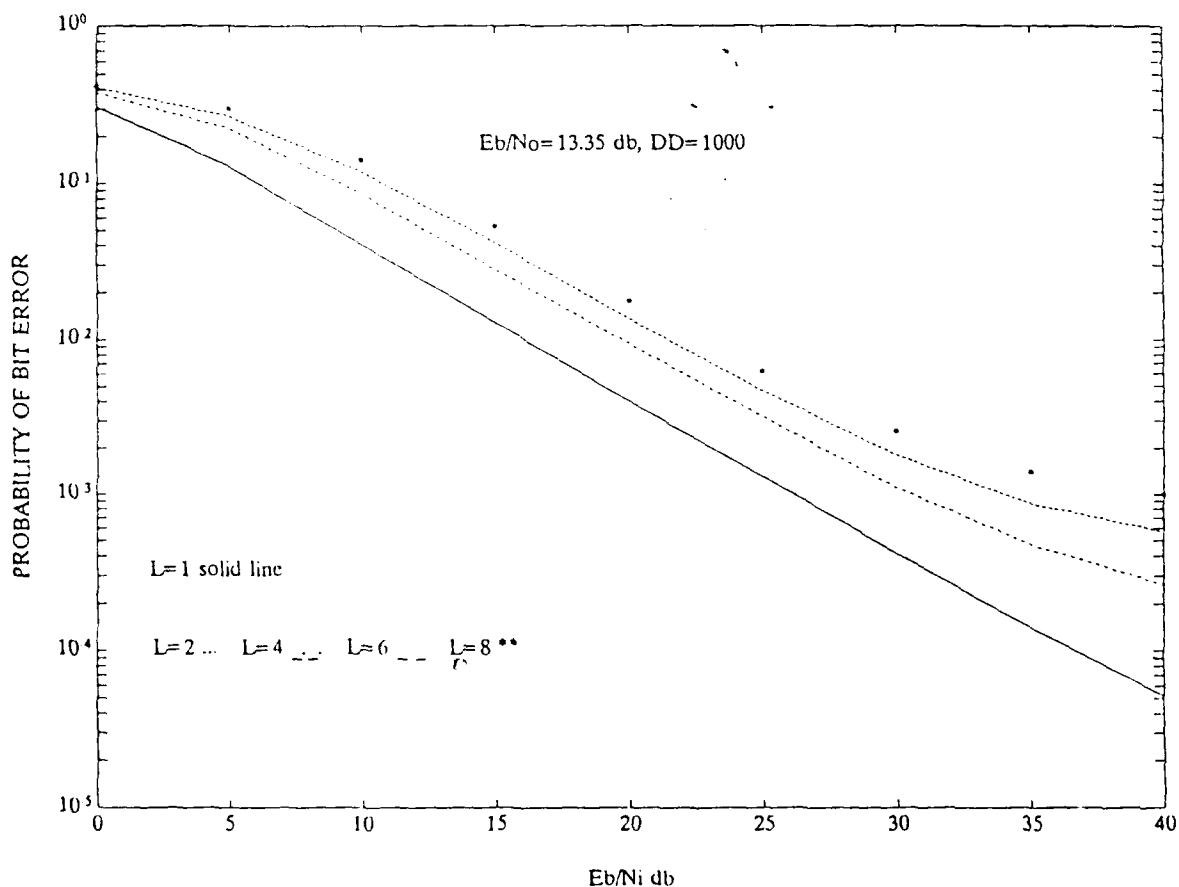
Figure 14. Square-Law Detector Linear Combining: Worst case performance of the linear combining square-law detector receiver with diversity combining, partial-band interference, and thermal noise in a fading channel for a strong direct signal component ($A^2/2\sigma^2=1000$) and $E_b/N_o=13.35$ dB.

67
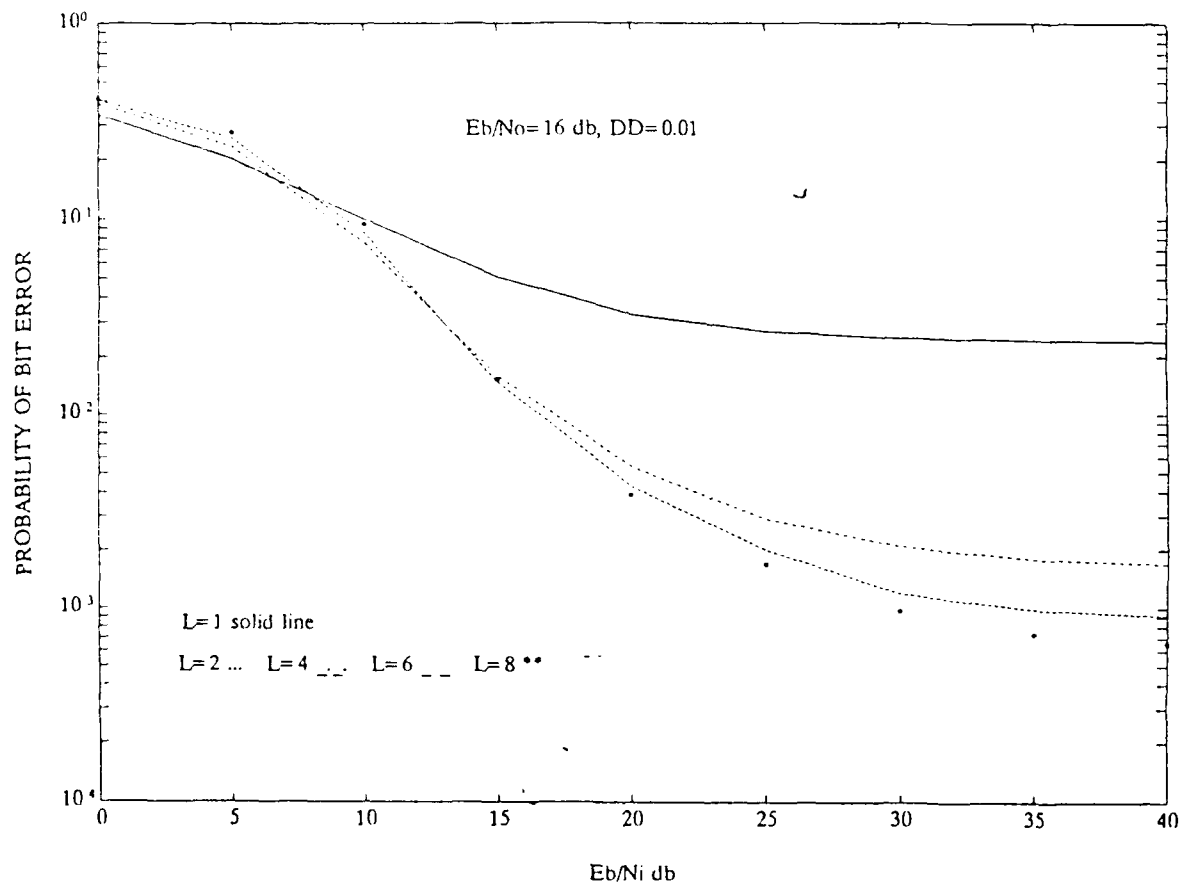
Figure 15. **Envelope Detector Linear Combining:** Worst case performance of the linear combining envelope detector receiver with diversity combining, partial-band interference, and thermal noise in a fading channel for a diffuse signal ($A^2/2\sigma^2=0.01$) and $E_b/N_o=16$ dB.
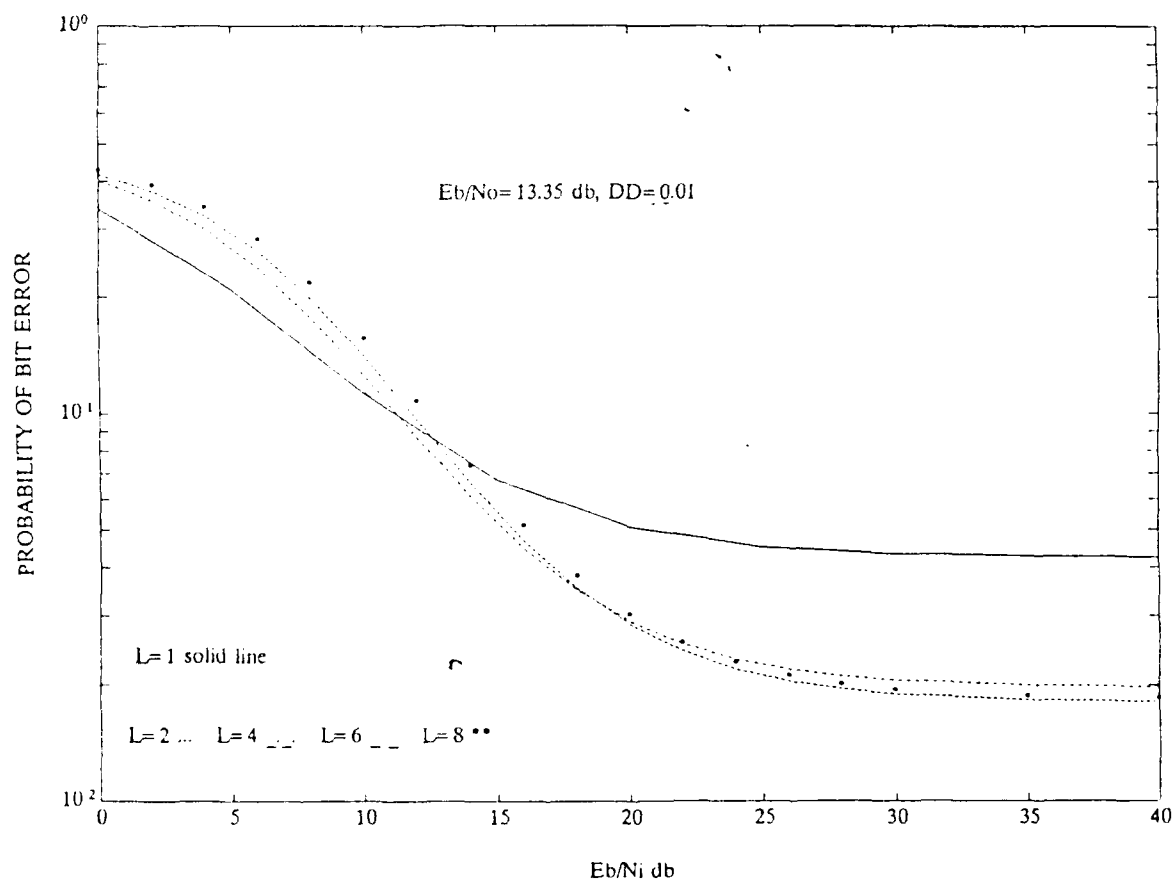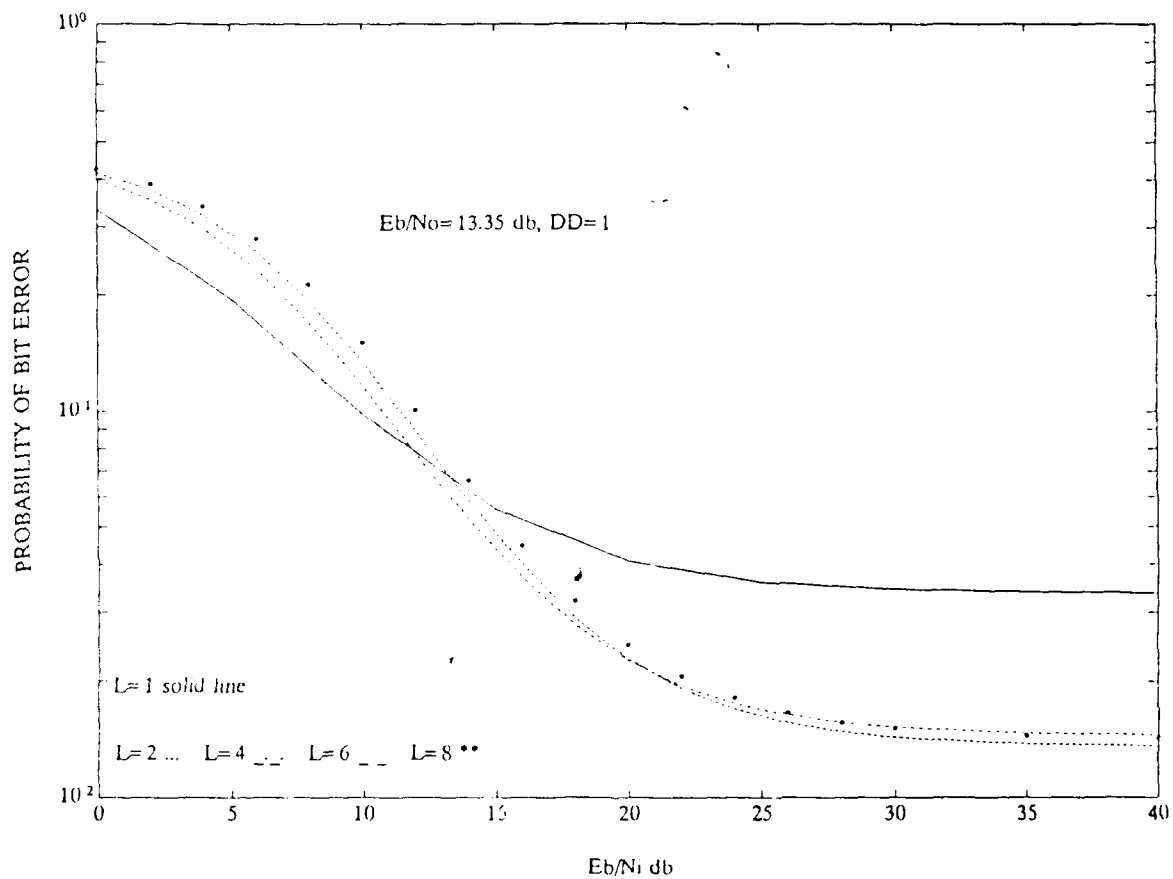
68
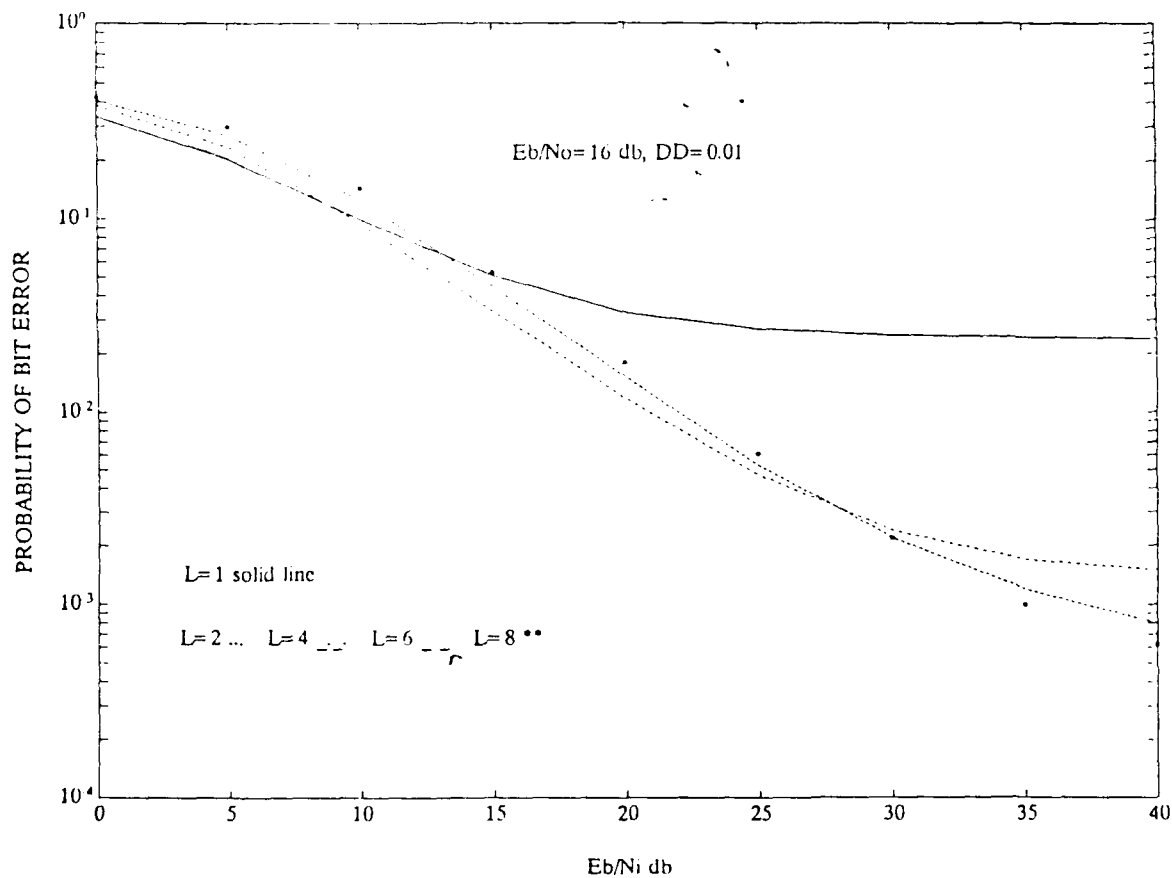
Figure 16. Square-Law Detector Linear Combining: Worst case performance of the linear combining square-law detector receiver with diversity combining, partial-band interference, and thermal noise in a fading channel for a diffuse signal ($A^2/2\sigma^2 = 0.01$) and $E_b/N_o = 16$ dB.

69
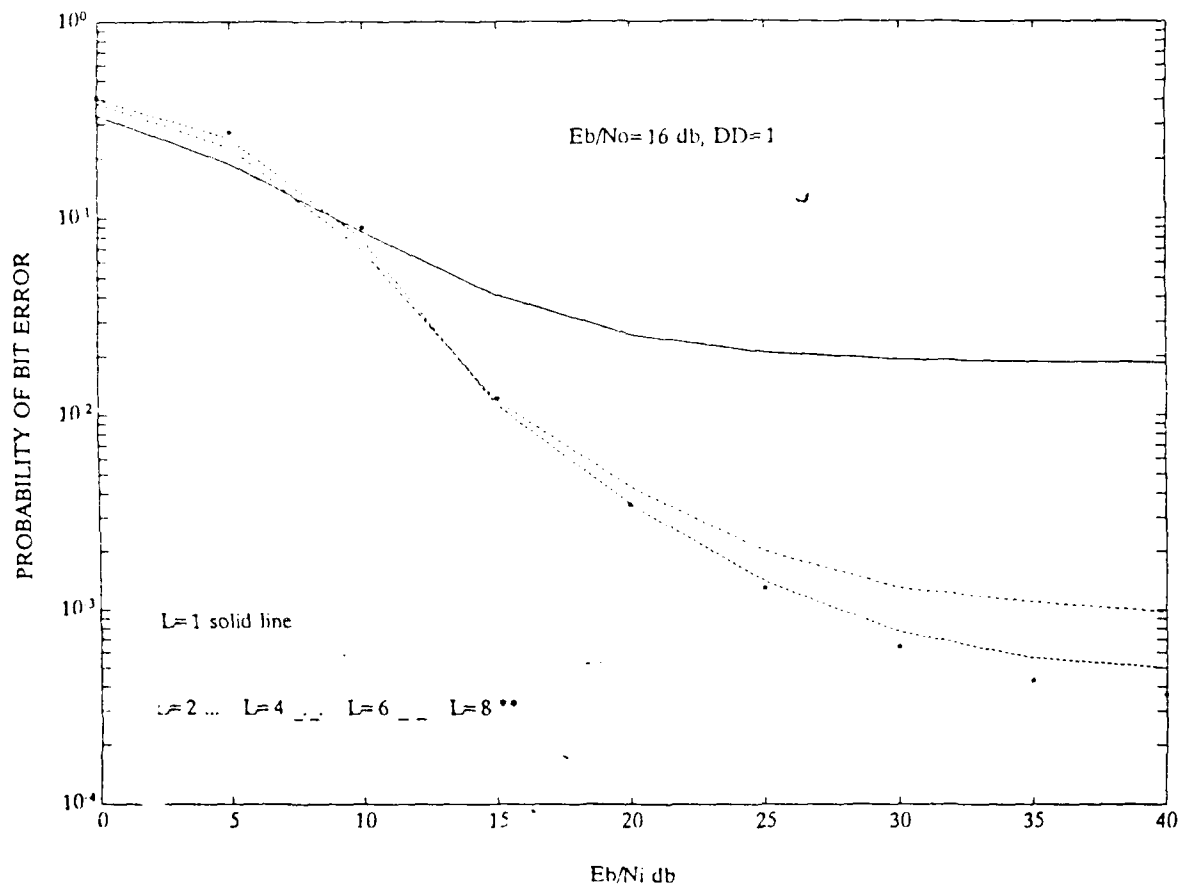
Figure 17. Envelope Detector Linear Combining: Worst case performance of the linear combining envelope detector receiver with diversity combining, partial-band interference, and thermal noise in a fading channel for a signal with equal direct and diffuse components ($A^2/2\sigma^2=1$) and $E_b/N_o=16$ dB.
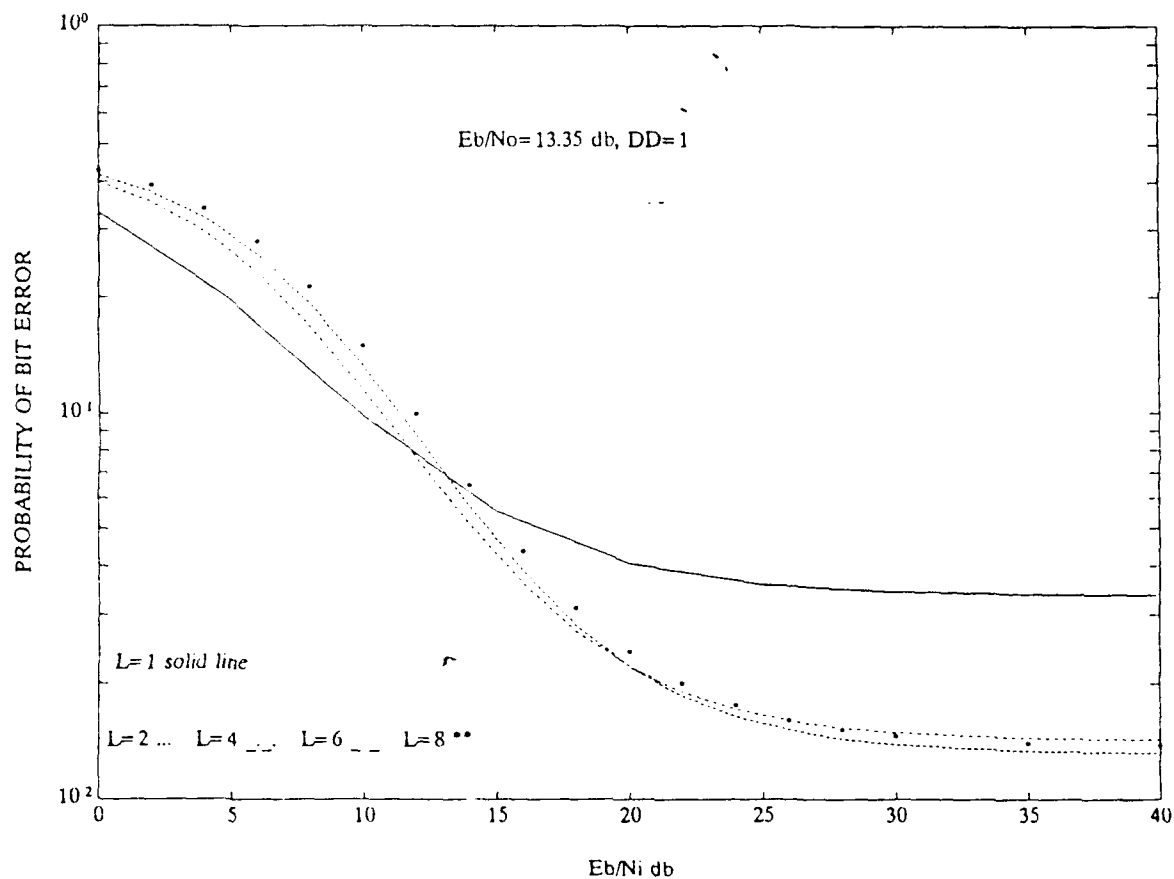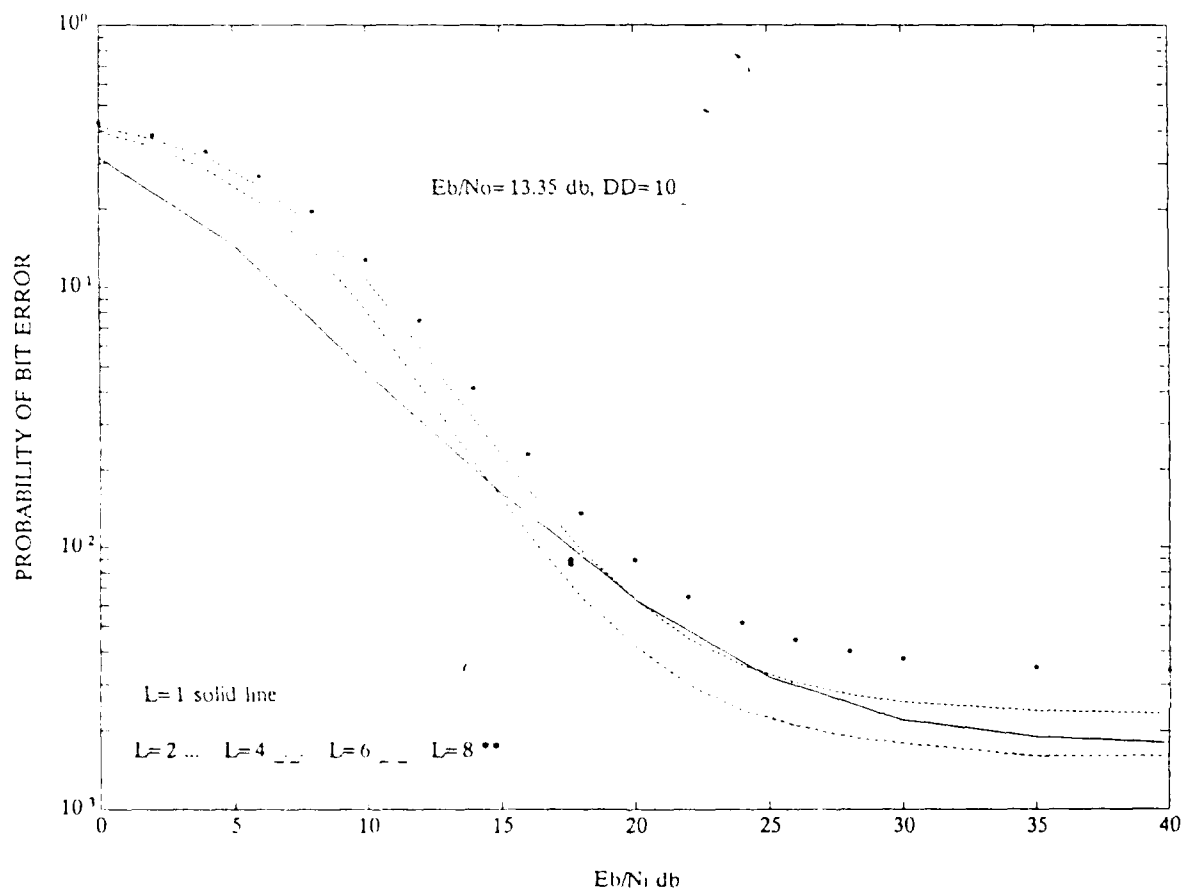
70
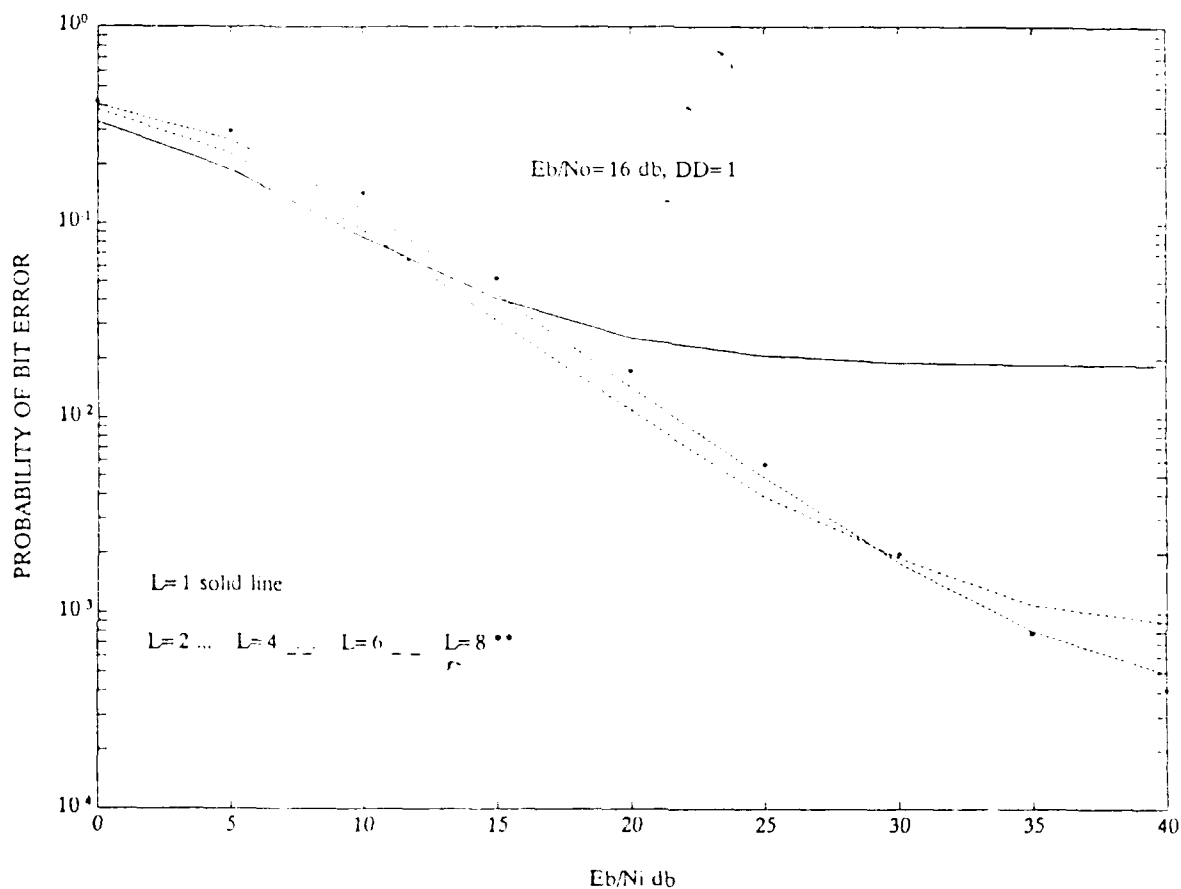
Figure 18. **Square-Law Detector Linear Combining:** Worst case performance of the linear combining square-law detector receiver with diversity combining, partial-band interference, and thermal noise in a fading channel for a signal with equal direct and diffuse components ($A^2/2\sigma^2=1$) and $E_b/N_o=16$ dB.
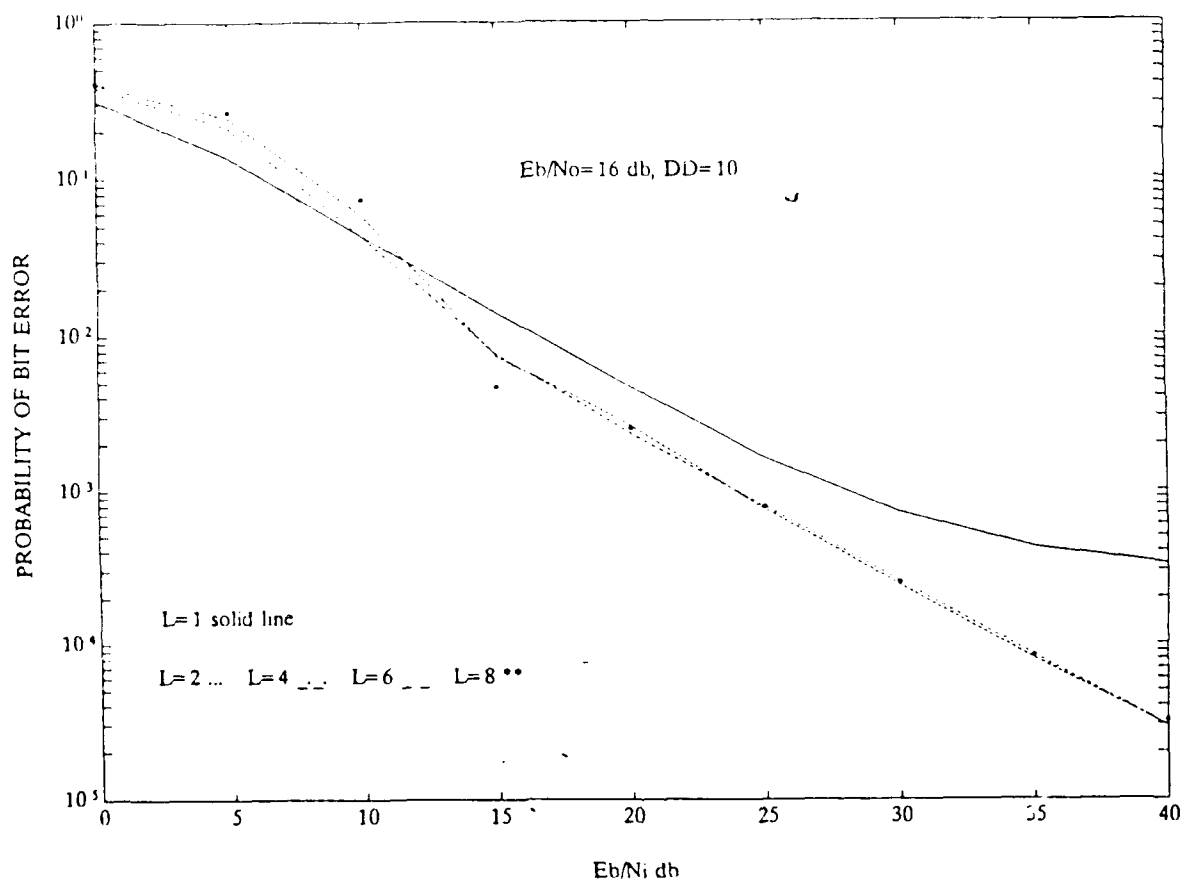
Figure 19. Envelope Detector Linear Combining: Worst case performance of the linear combining envelope detector receiver with diversity combining, partial-band interference, and thermal noise in a fading channel for a relatively strong direct signal component and $(A^2/2\sigma^2=10)$ $E_b/N_o=16$ dB.

72
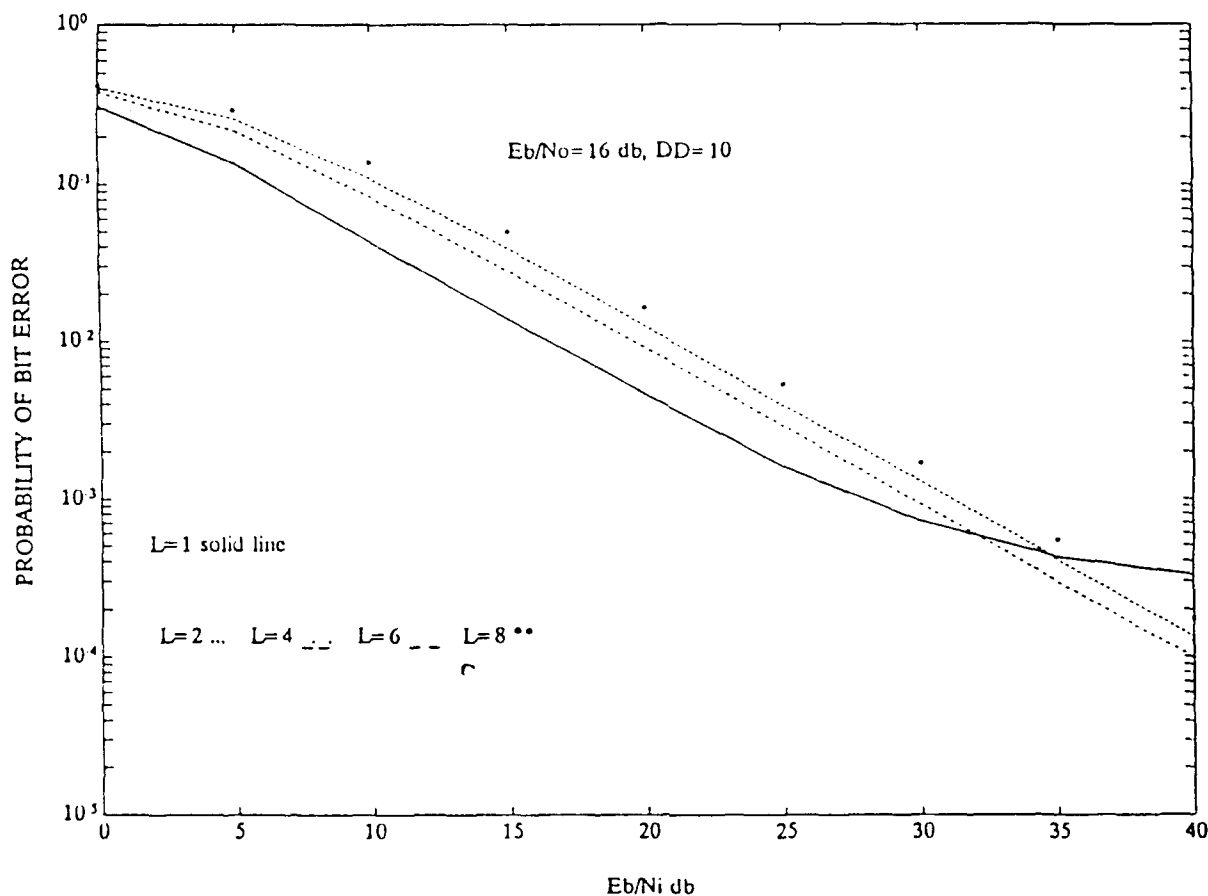
Figure 20. Square-Law Detector Linear Combining: Worst case performance of the linear combining square-law detector receiver with diversity combining, partial-band interference, and thermal noise in a fading channel for a relatively strong direct signal component ($A^2/2\sigma^2=10$) and $E_b/N_o=16$ dB.
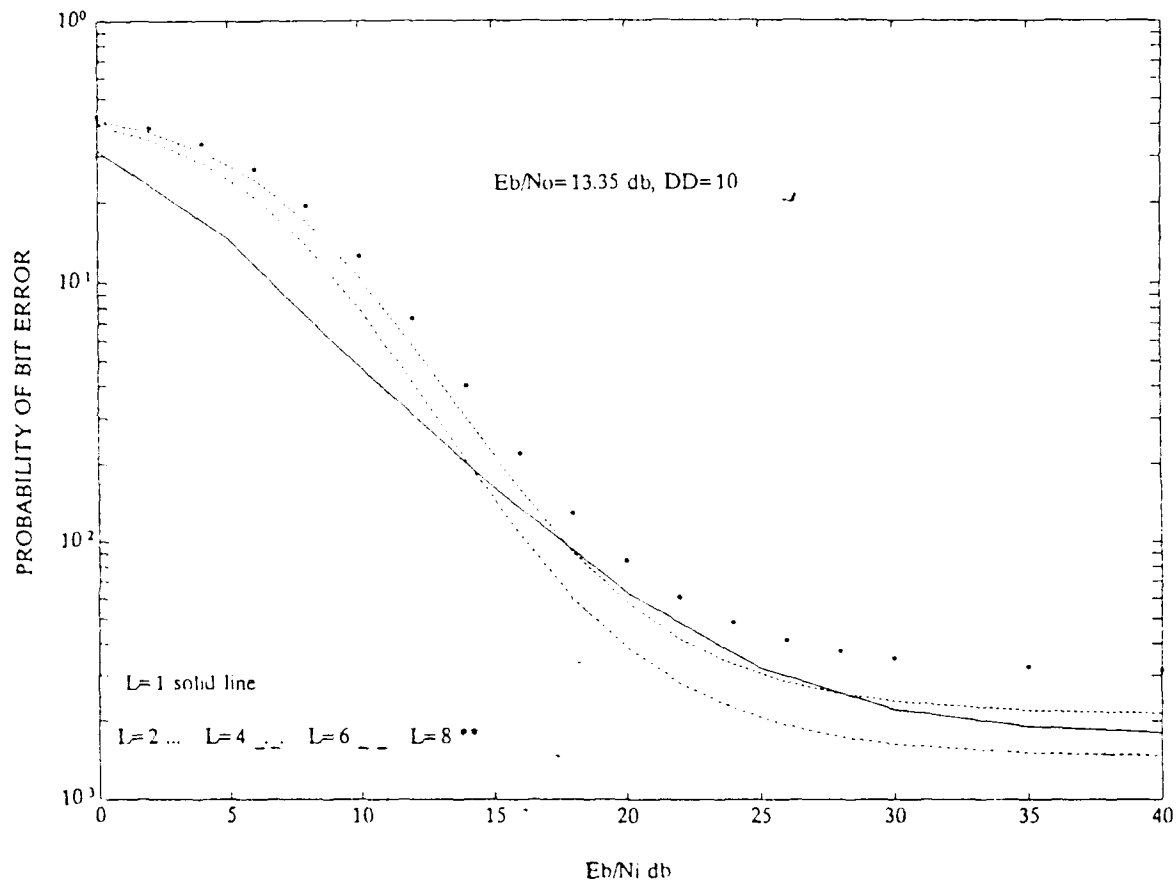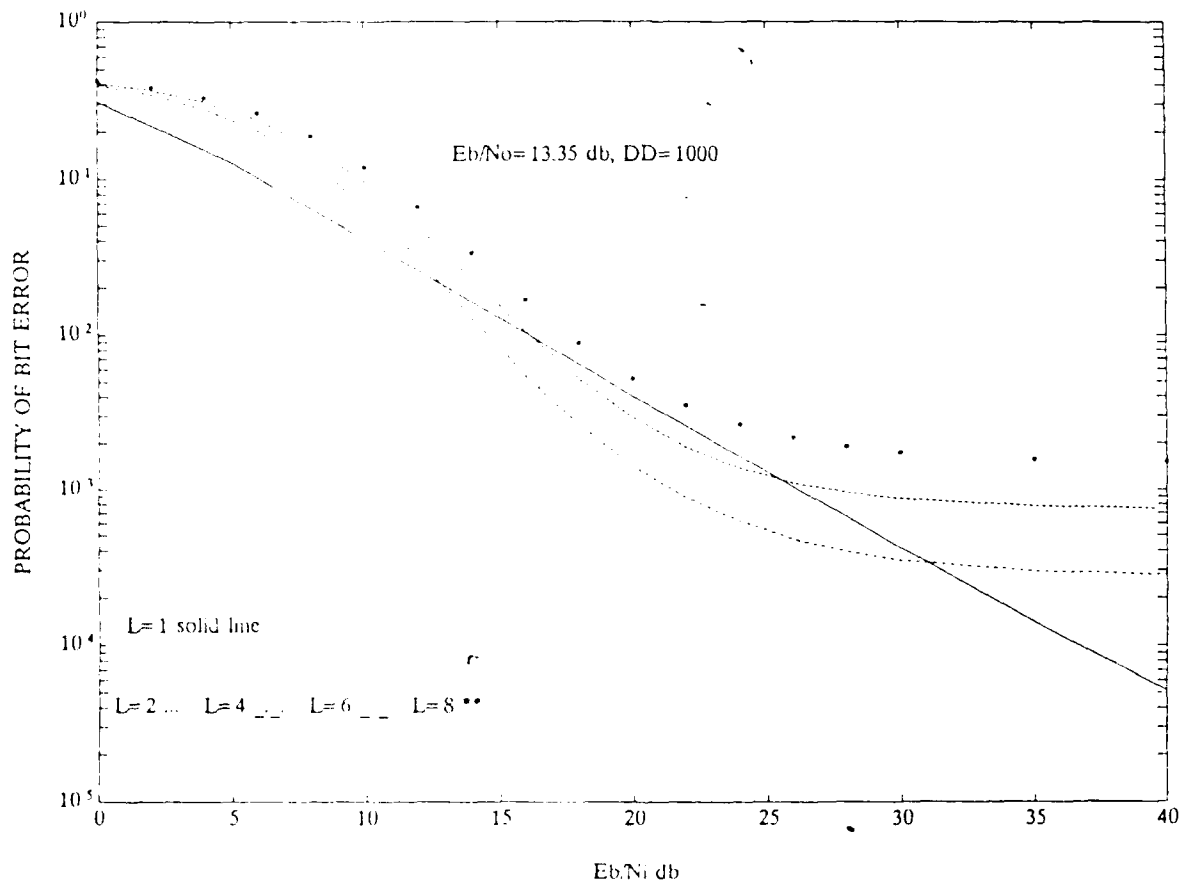
73
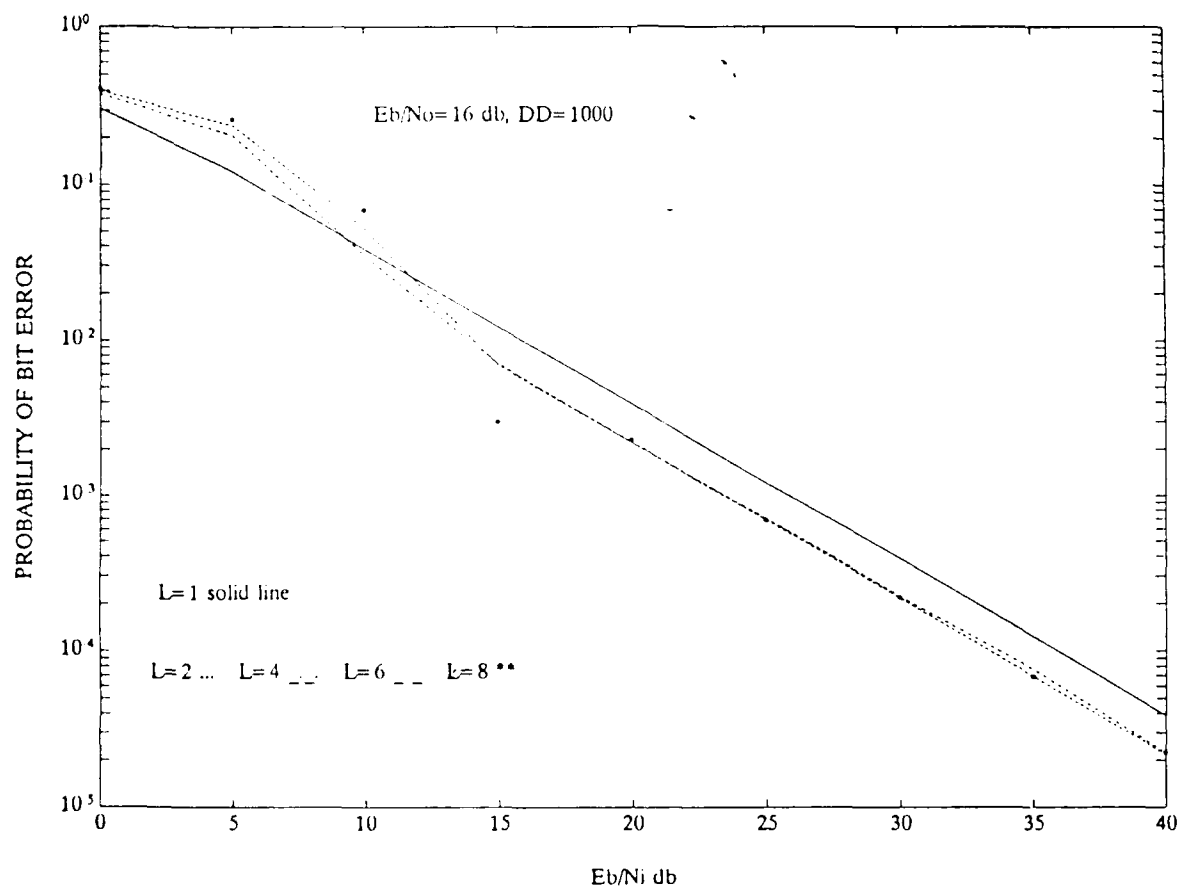
Figure 21. Envelope Detector Linear Combining: Worst case performance of the linear combining envelope detector receiver with diversity combining, partial-band interference, and thermal noise in a fading channel for a strong direct signal component ($A^2/2\sigma^2=1000$) and $E_b/N_o=16$ dB.

Figure 22. **Square-Law Detector Linear Combining:** Worst case performance of the linear combining square-law detector receiver with diversity combining, partial-band interference, and thermal noise in a fading channel for a strong direct signal component $(A^2/2\sigma^2=1000)$ and $E_b/N_o=16$ dB.
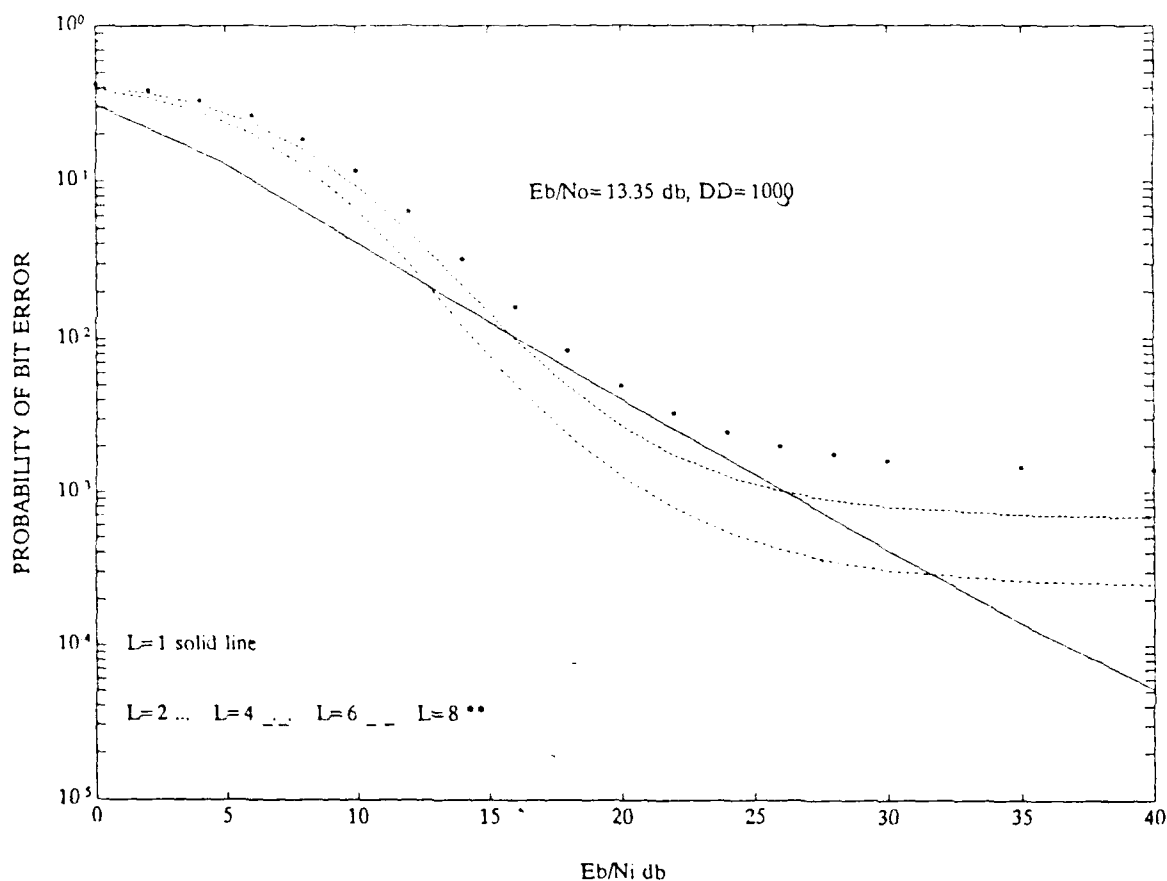
Figure 23. **Envelope Detector Linear Combining:** Worst case performance of the linear combining envelope detector receiver with diversity combining, partial-band interference, and thermal noise in a fading channel for a relatively strong direct signal component ($A^2/2\sigma^2=10$) and $E_b/N_o=18$ dB.
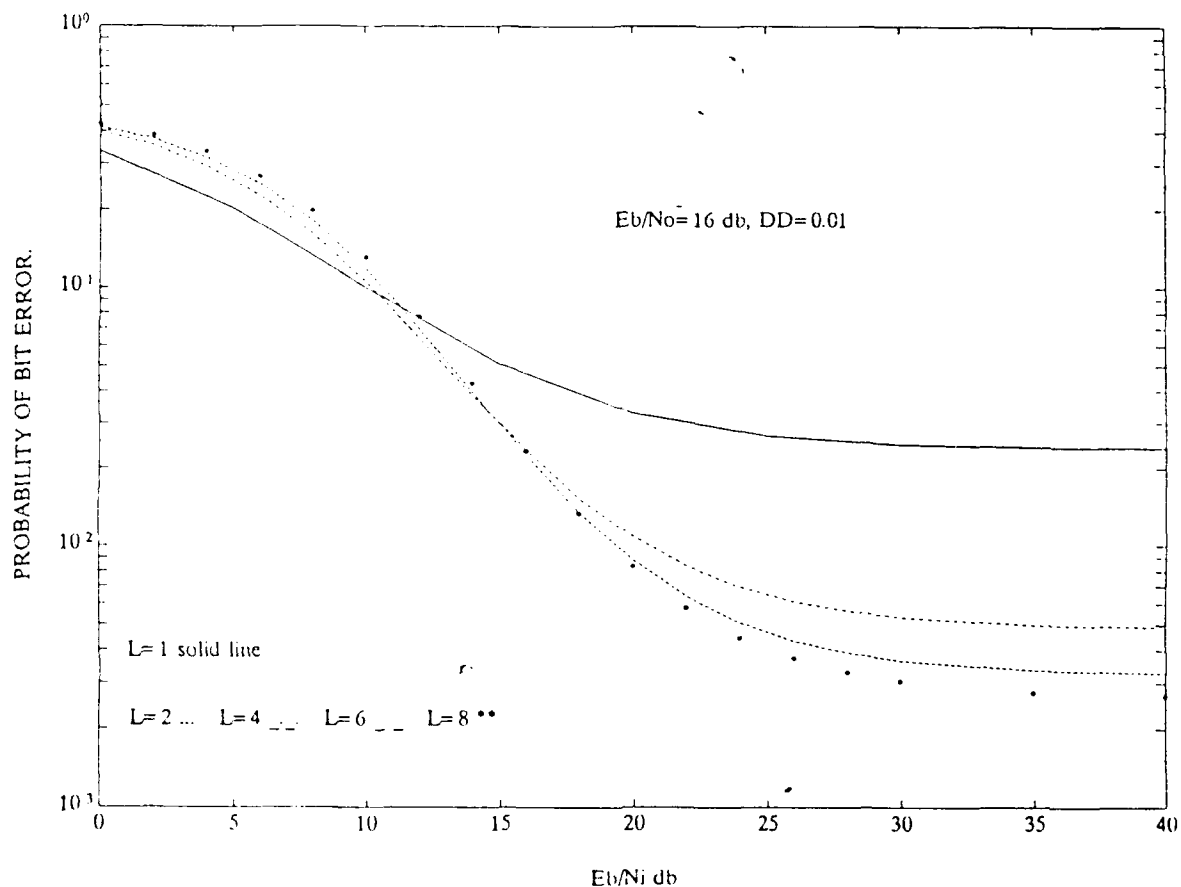
Figure 24. Square-Law Detector Linear Combining: Worst case performance of the linear combining square-law detector receiver with diversity combining, partial-band interference, and thermal noise in a fading channel for a relatively strong direct signal component ($A^2/2\sigma^2=10$) and $E_b/N_o=18$ dB.

Figure 25. Envelope Detector Linear Combining: Worst case performance of the linear combining envelope detector receiver with diversity combining, partial-band interference, and thermal noise in a fading channel for a strong direct signal component ($A^2/2\sigma^2=100$) and $E_b/N_c=18$ dB.
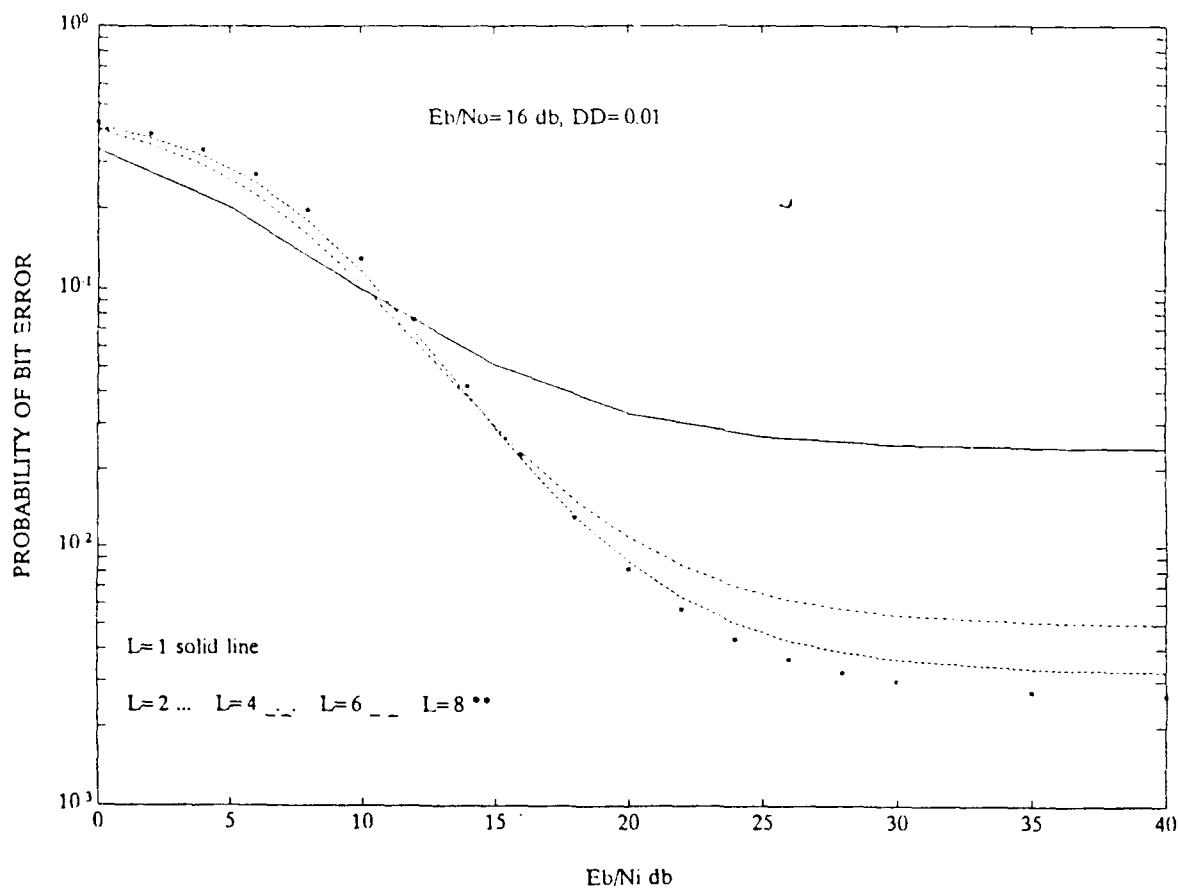
78

Figure 26. Square-Law Detector Linear Combining: Worst case performance of the linear combining square-law detector receiver with diversity combining, partial-band interference, and thermal noise in a fading channel for a strong direct signal component ($A^2/2\sigma^2=100$) and $E_b/N_o=18$ dB.
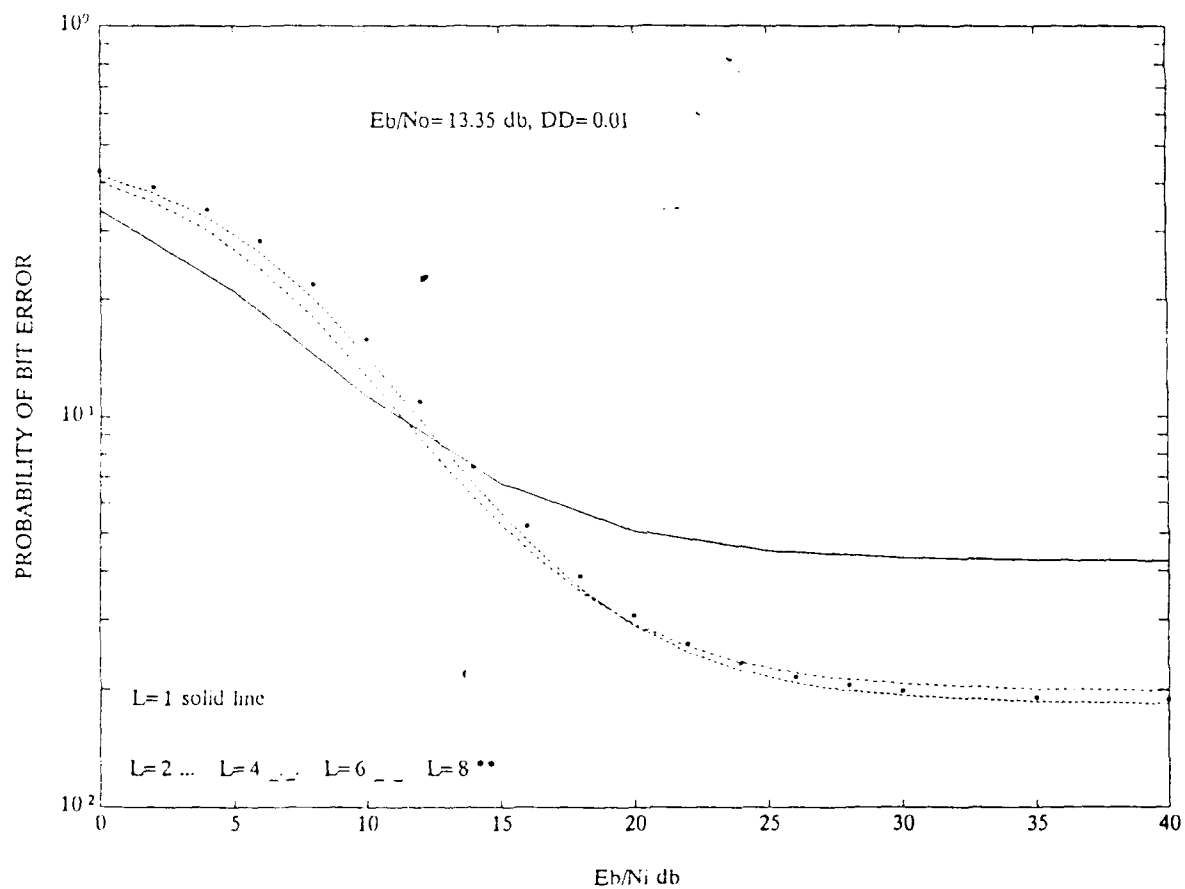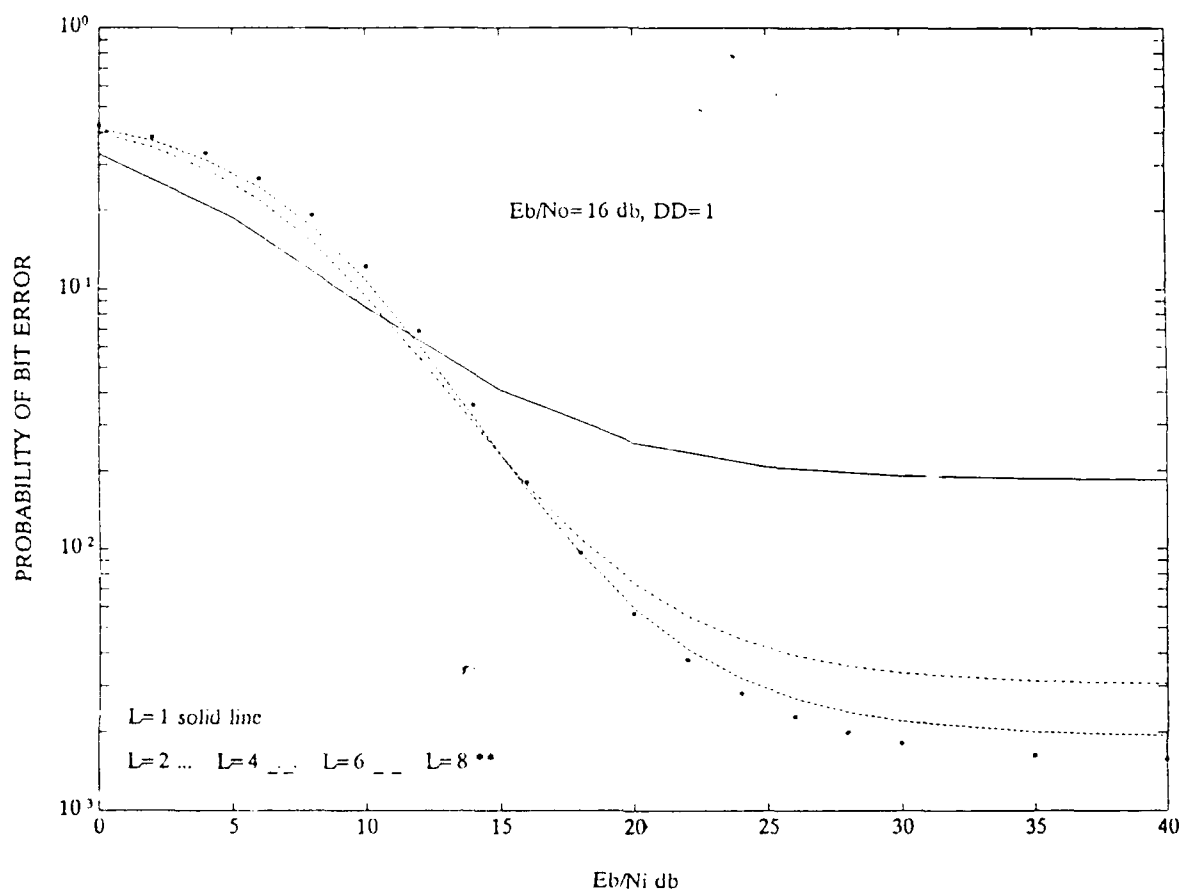
Figure 27. Envelope Detector Self-Normalization Combining:
Worst case performance of the self-normalization combining
envelope detector receiver with diversity combining,
partial-band interference, and thermal noise in a fading
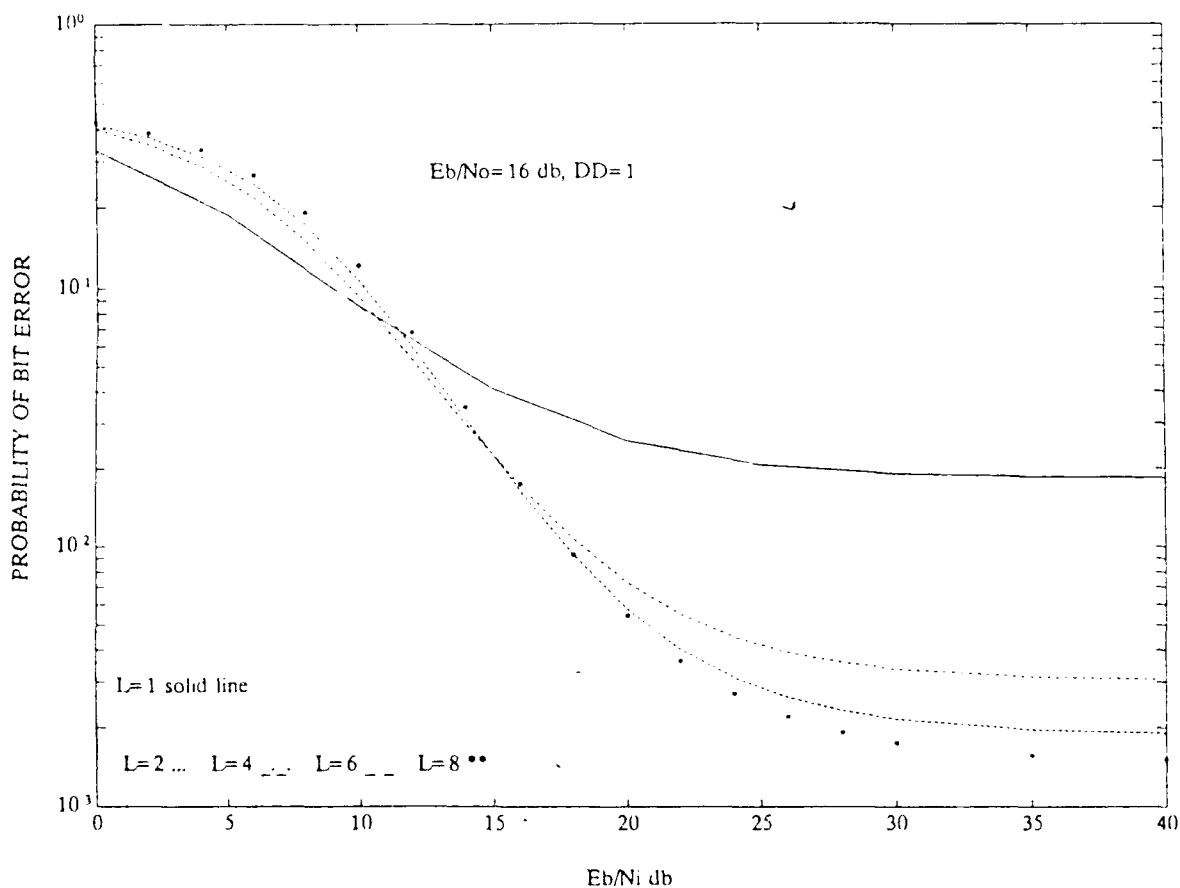channel for a diffuse signal ($A^2/2\sigma^2=0.01$) and $E_b/N_o=13.35$
dB.

Figure 28. **Square-Law Detector Self-Normalization**
Combining: Worst case performance of the self-normalization
combining square-law detector receiver with diversity
combining, partial-band interference, and thermal noise in a
fading channel for a diffuse signal ($A^2/2\sigma^2=0.01$) and
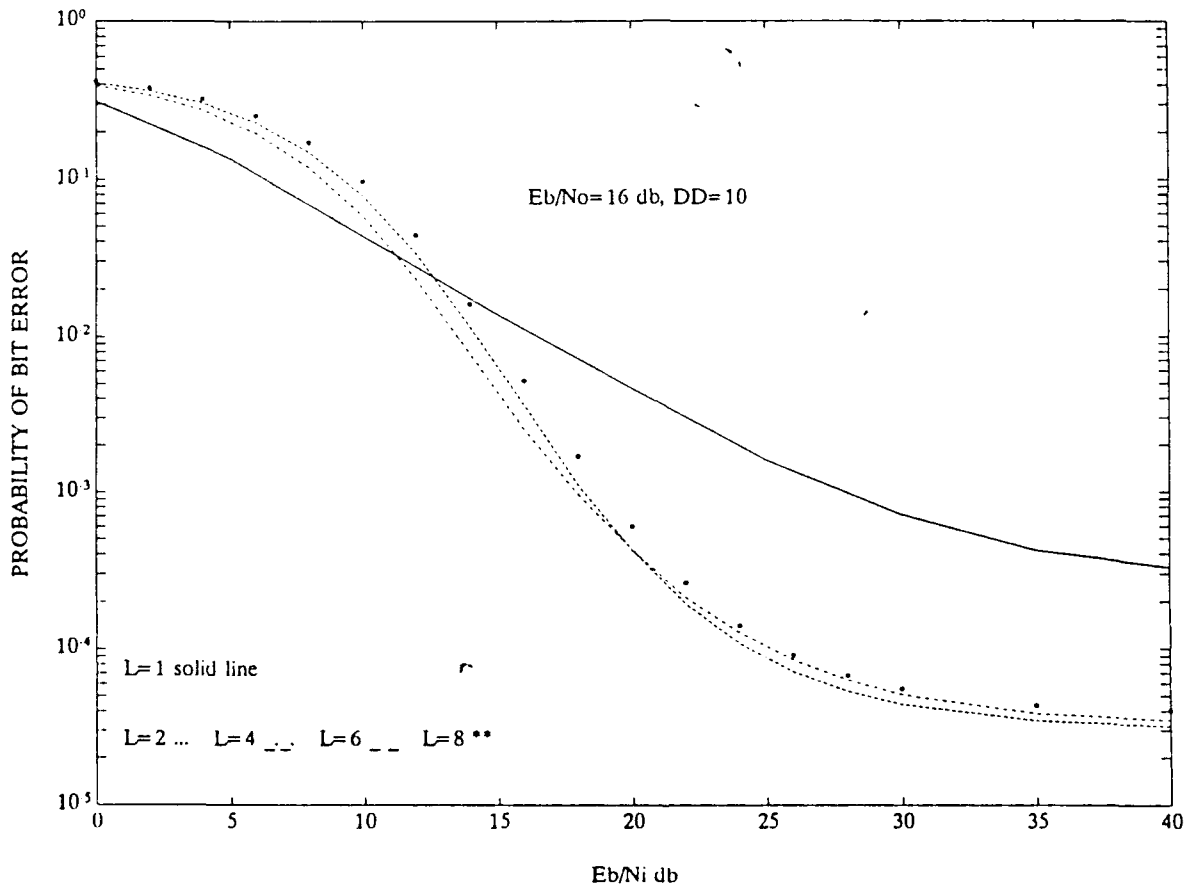$E_b/N_o=13.35$ dB.

81

Figure 29. Envelope Detector Self-Normalization Combining:
Worst case performance of the self-normalization combining
envelope detector receiver with diversity combining,
partial-band interference, and thermal noise in a fading
channel for a signal with equal direct and diffuse
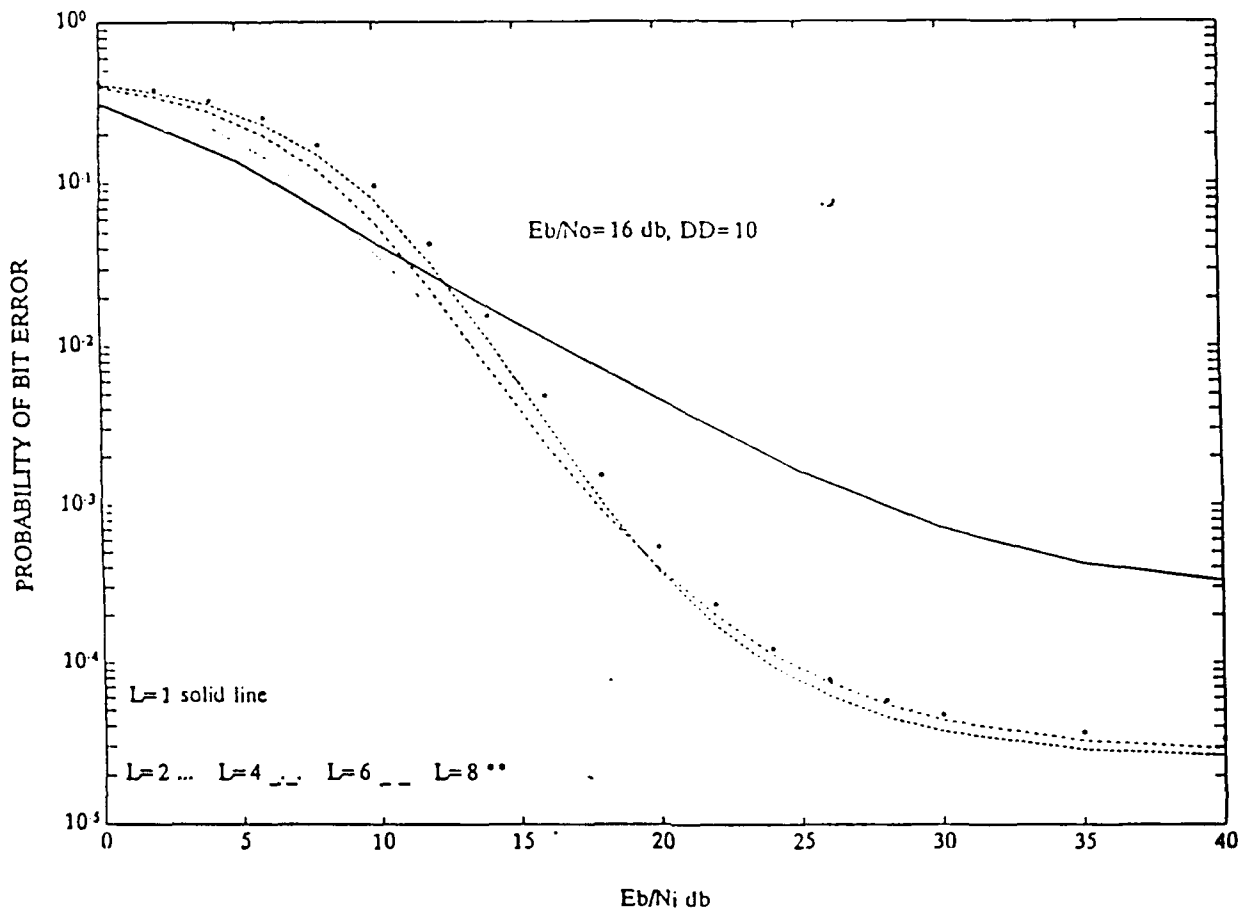components $(A^2/2\sigma^2=1)$ and $E_b/N_o=13.35$ dB.

82

Figure 30. Square-Law Detector Self-Normalization Combining: Worst case performance of the self-normalization combining square-law detector receiver with diversity combining, partial-band interference, and thermal noise in a fading channel for a signal with equal direct and diffuse components $(A_2/2\sigma^2=1)$ and $E_b/N_0=13.35$ dB.
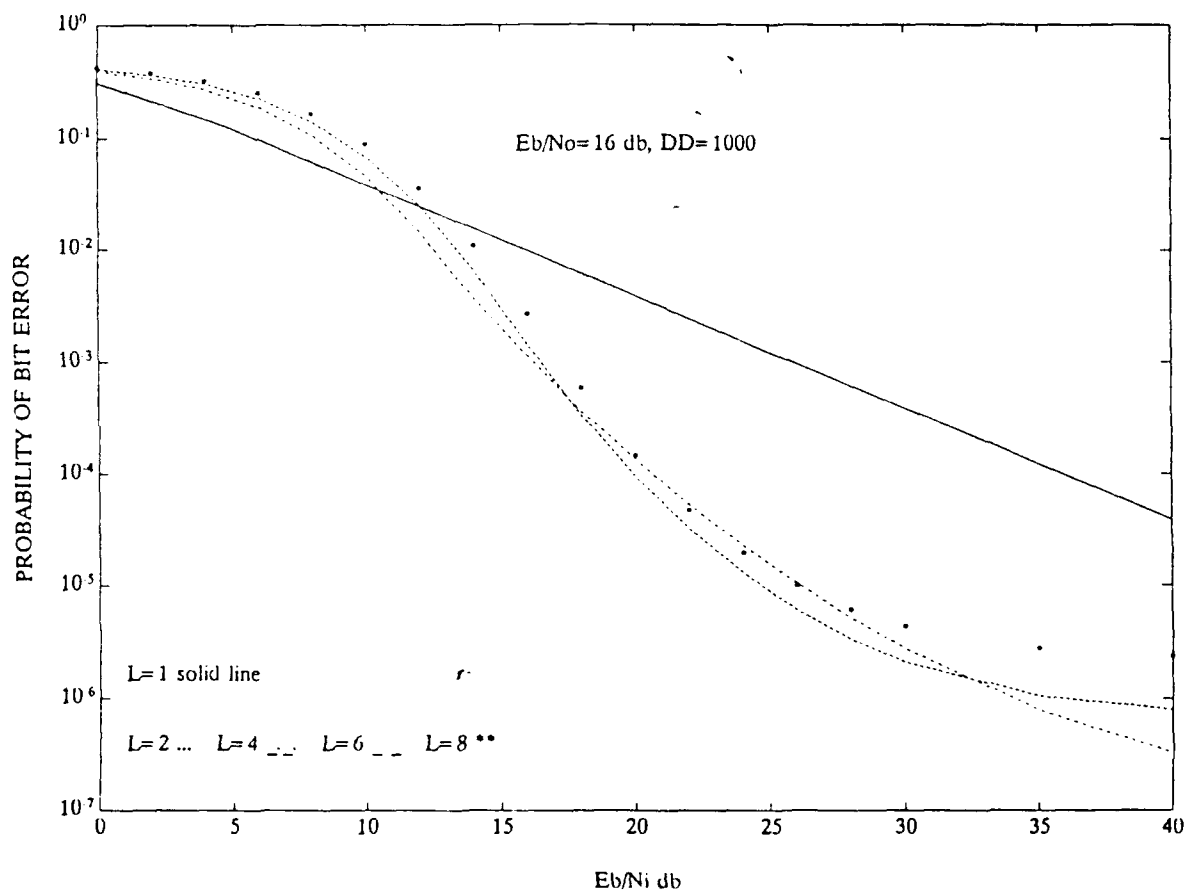
83

Figure 31. Envelope Detector Self-Normalization Combining:
Worst case performance of the self-normalization combining
envelope detector receiver with diversity combining,
partial-band interference, and thermal noise in a fading
channel for a relatively strong direct signal component
$(A^2/2\sigma^2=10)$ and $E_b/N_o=13.35$ dB.

84

PROBABILITY OF BIT ERROR

Eb/No=13.35 db, DD=10

L=1 solid line

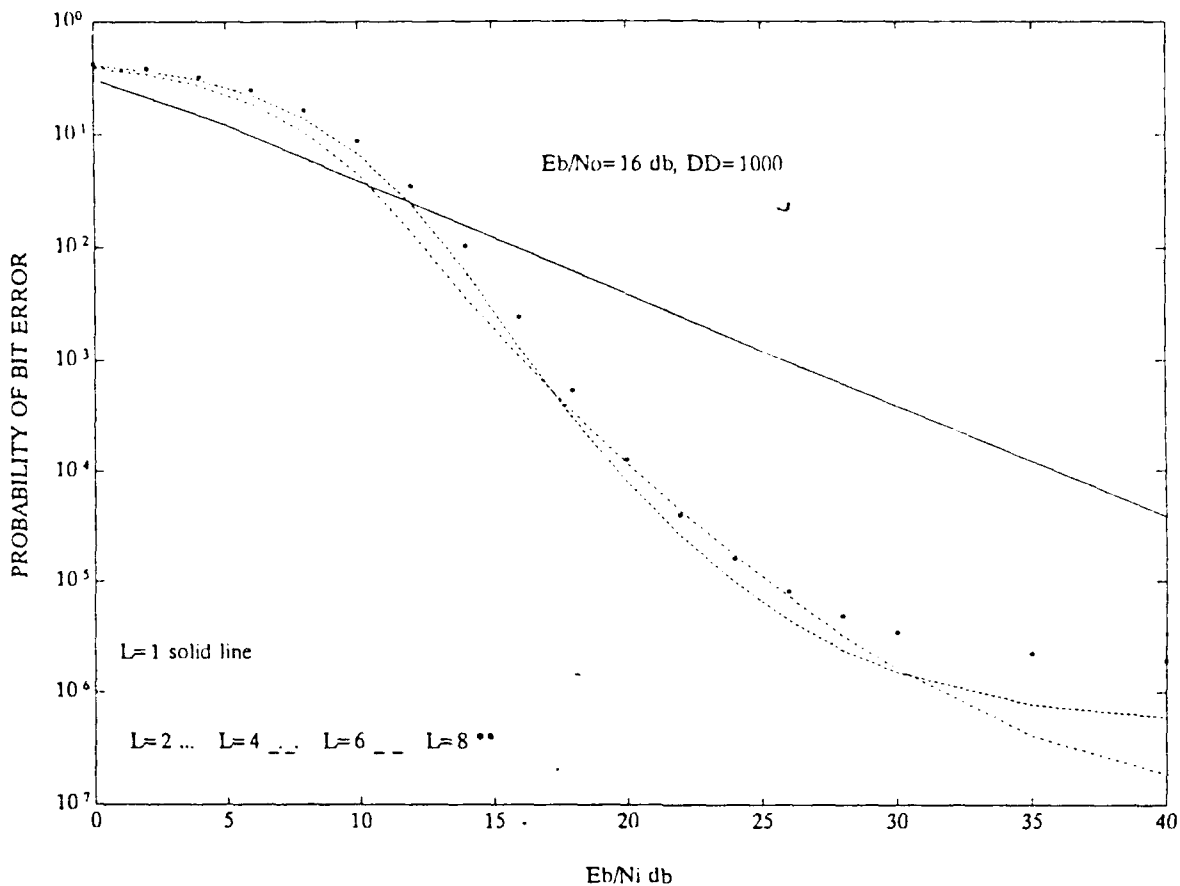L=2 ...   L=4 _._   L=6 _ _   L=8 ••

Eb/Ni db

Figure 32.   Square-Law Detector Self-Normalization
Combining: Worst case performance of the self-normalization
combining square-law detector receiver with diversity
combining, partial-band interference, and thermal noise in a
fading channel for a relatively strong direct signal
component $(A^2/2\sigma^2=10)$ and $E_b/N_o=13.35$ dB.

PROBABILITY OF BIT ERROR

Eb/No= 13.35 db, DD= 1000

L= 1 solid line

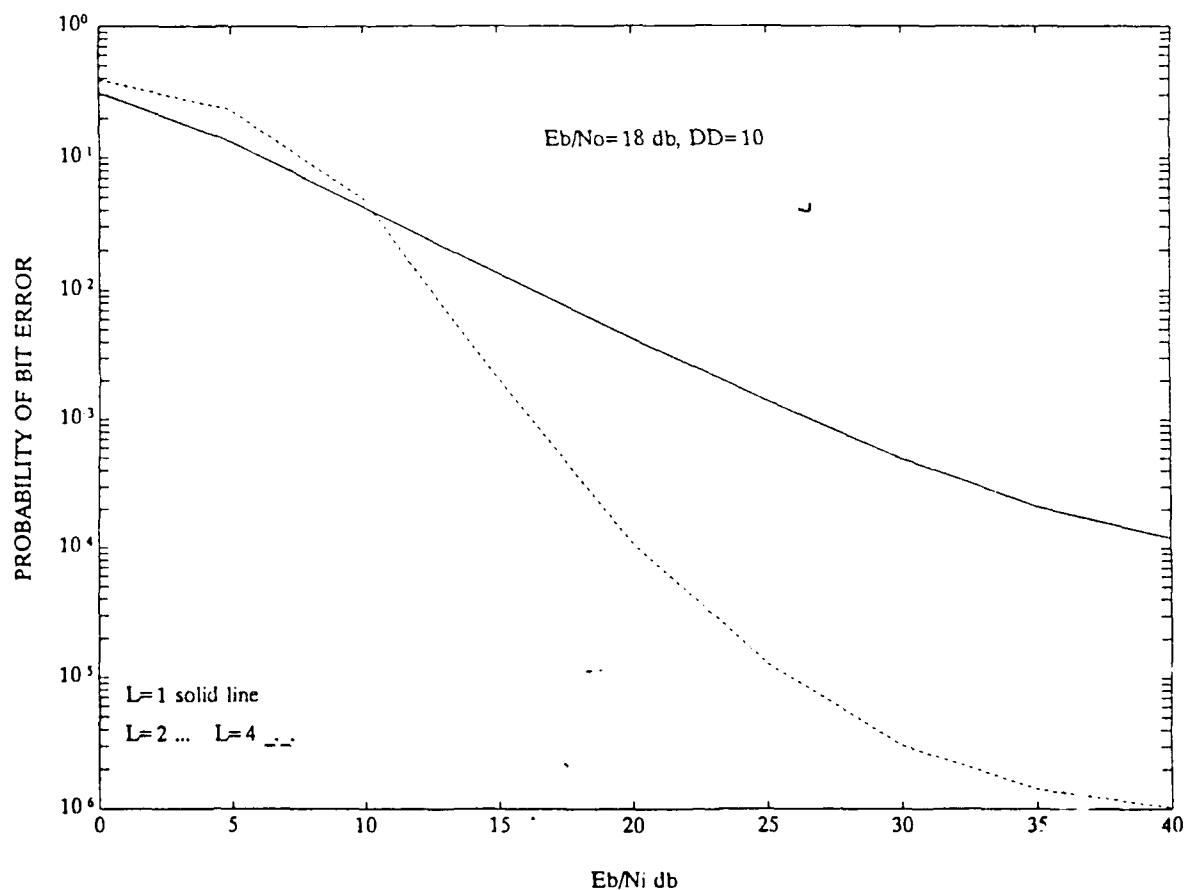L= 2 ...   L= 4 _._   L= 6 _ _   L= 8 ••

Eb/Ni db

Figure 33.   Envelope Detector Self-Normalization Combining:
Worst case performance of the self-normalization combining
envelope detector receiver with diversity combining,
partial-band interference, and thermal noise in a fading
channel for a strong direct signal component ($A^2/2\sigma^2$=1000)
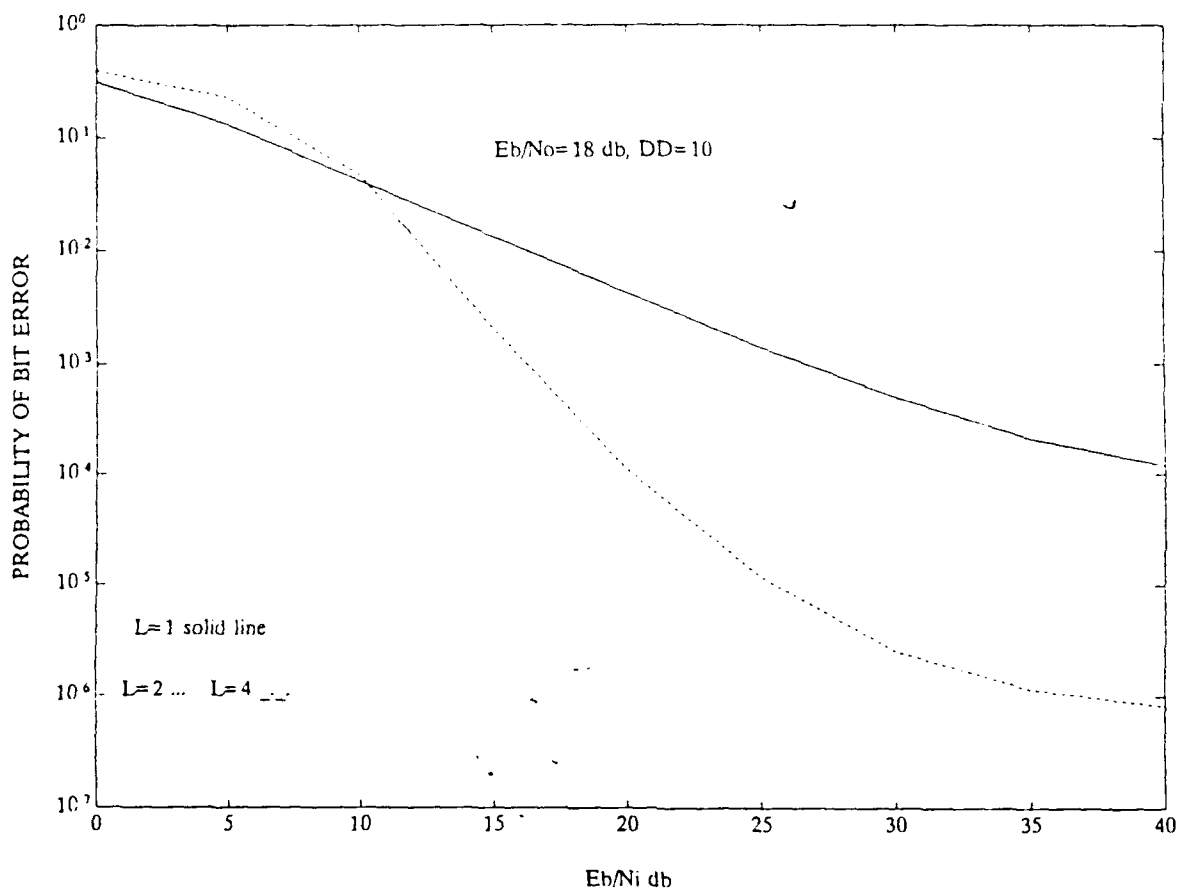and E_b/N_o=13.35 dB.

Figure 34. **Square-Law Detector Self-Normalization Combining:** Worst case performance of the self-normalization combining square-law detector receiver with diversity combining, partial-band interference, and thermal noise in a fading channel for a strong direct signal component $(A^2/2\sigma^2 = 1000)$ and $E_b/N_o = 13.35$ dB.
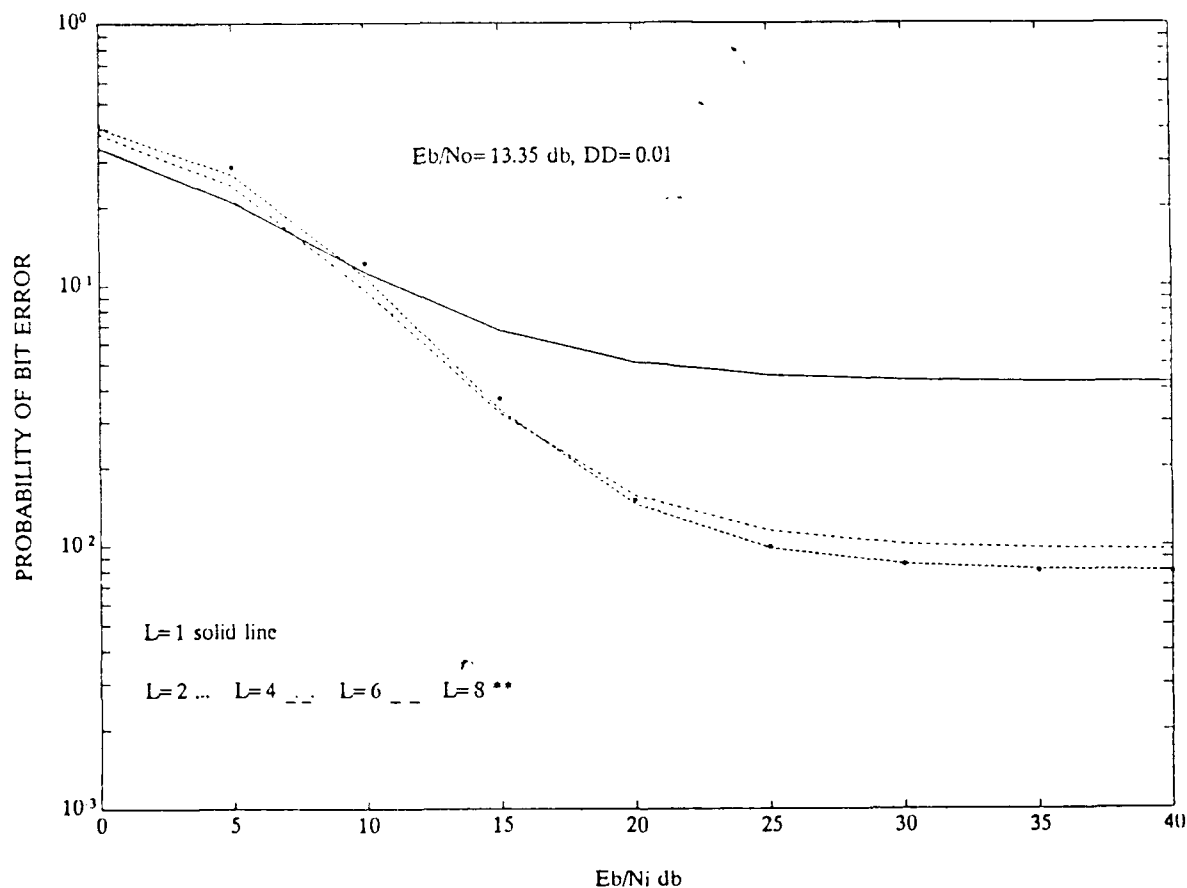
87

Figure 35. Envelope Detector Self-Normalization Combining:
Worst case performance of the self-normalization combining
envelope detector receiver with diversity combining,
partial-band interference, and thermal noise in a fading
channel for a diffuse signal $(A^2/2\sigma^2=0.01)$ and $E_b/N_o=16$ dB.

88

Figure 36. Square-Law Detector Self-Normalization

Combining: Worst case performance of the self-normalization

combining square-law detector receiver with diversity

combining, partial-band interference, and thermal noise in a

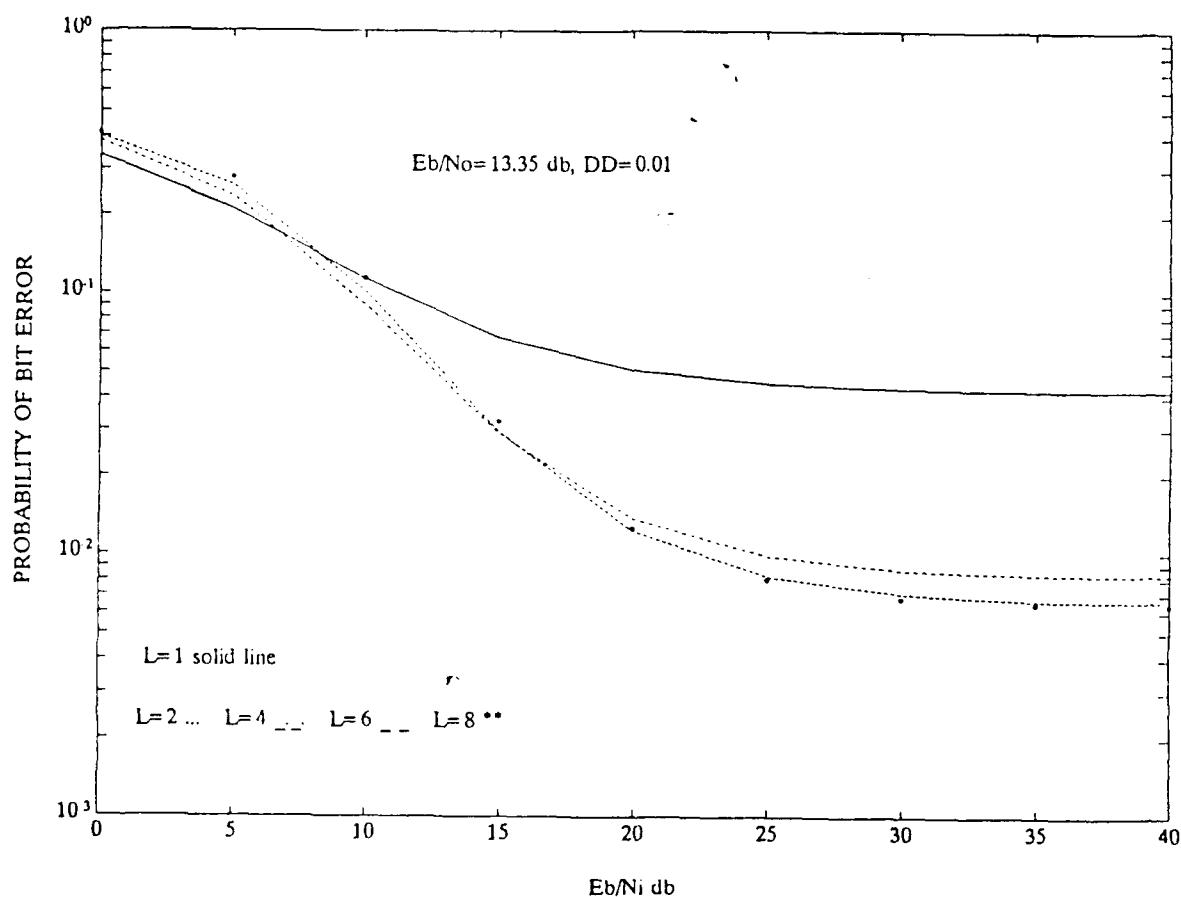fading channel for a diffuse signal ($A^2/2\sigma^2$=0.01) and

E_b/N_o=16 dB.

89

Figure 37. Envelope Detector Self-Normalization Combining:
Worst case performance of the self-normalization combining
envelope detector receiver with diversity combining,
partial-band interference, and thermal noise in a fading
channel for a signal with equal direct and diffuse
components $(A^2/2\sigma^2=1)$ and $E_b/N_o=16$ dB.

90

Figure 38. Square-Law Detector Self-Normalization Combining: Worst case performance of the self-normalization combining square-law detector receiver with diversity combining, partial-band interference, and thermal noise in a fading channel for a signal with equal direct and diffuse components $(A^2/2\sigma^2=1)$ and $E_b/N_o=16$ dB.
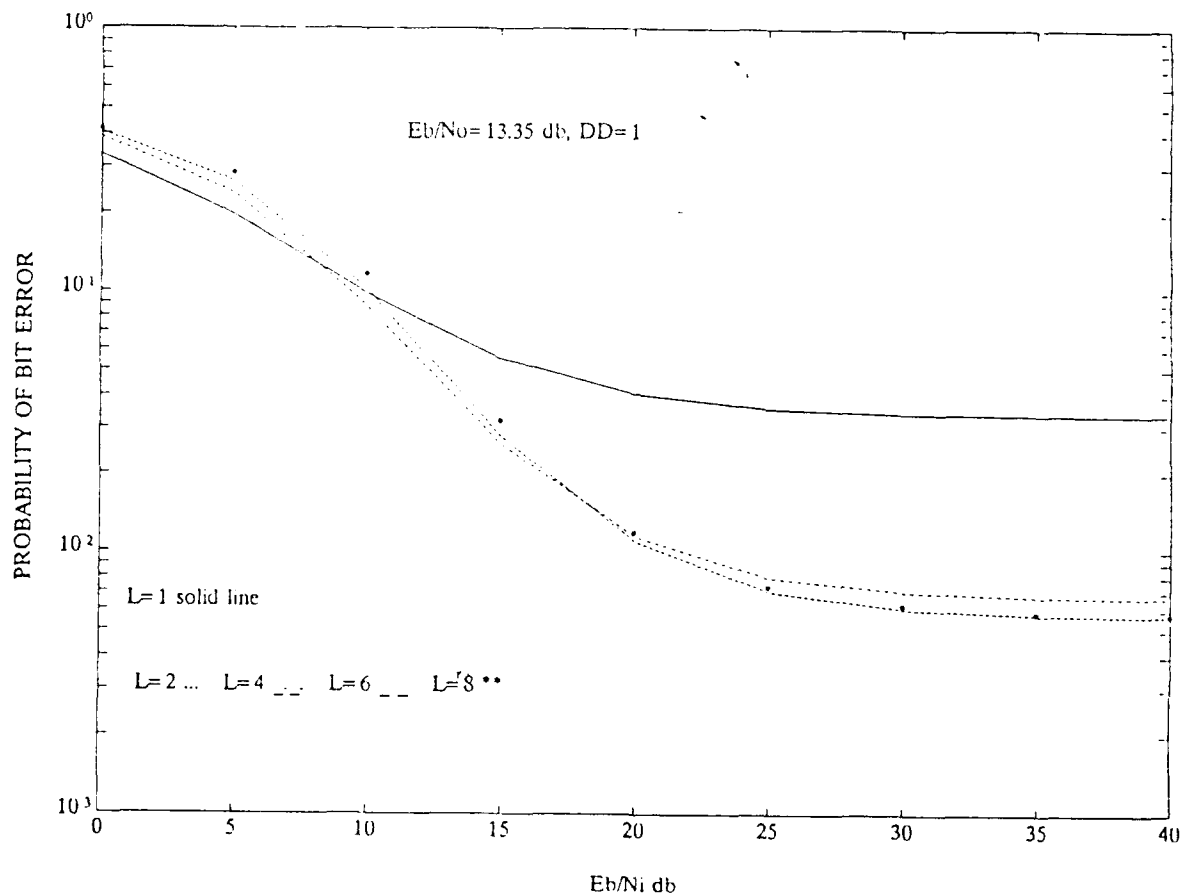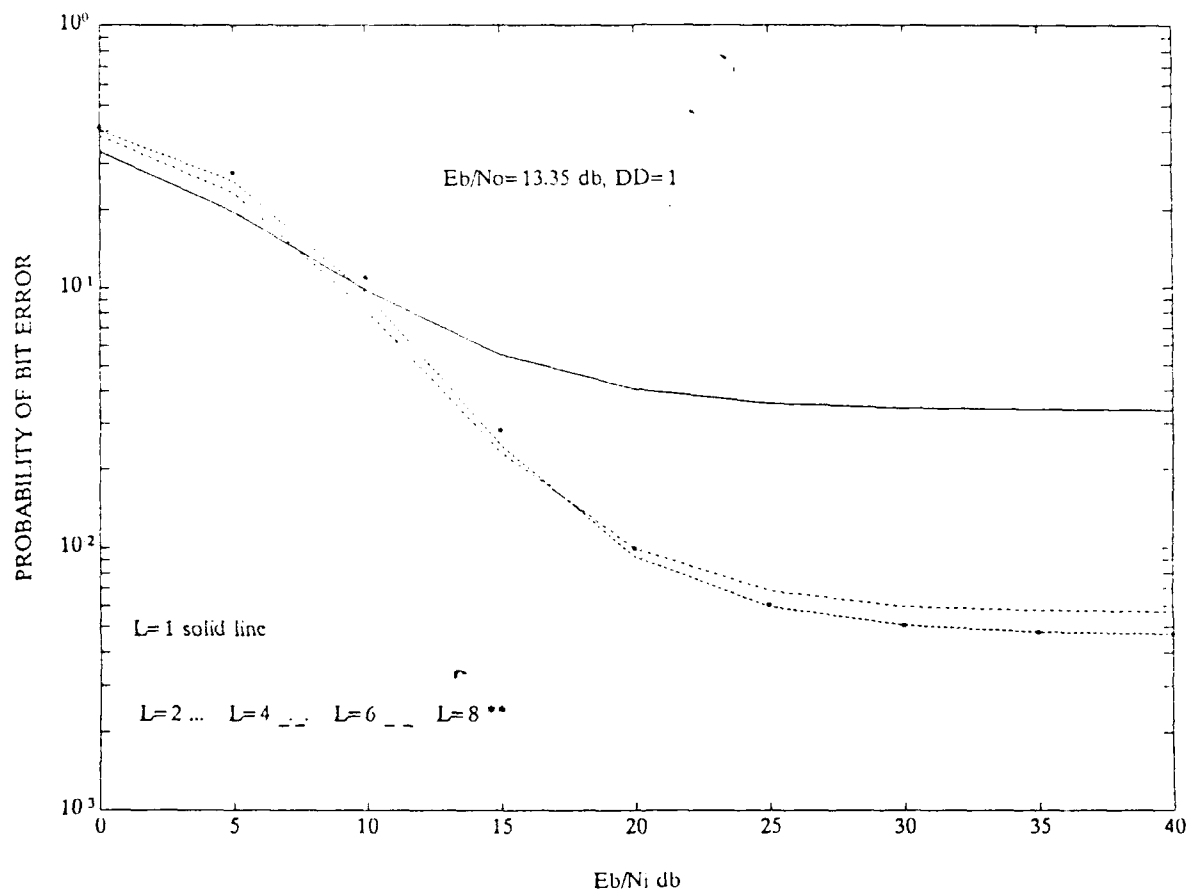
Figure 39. Envelope Detector Self-Normalization Combining: Worst case performance of the self-normalization combining envelope detector receiver with diversity combining, partial-band interference, and thermal noise in a fading channel for a relatively strong direct signal component $(A^2/2\sigma^2=10)$ and $E_b/N_o=16$ dB.

92

Figure 40. Square-Law Detector Self-Normalization Combining: Worst case performance of the self-normalization combining square-law detector receiver with diversity combining, partial-band interference, and thermal noise in a fading channel for a relatively strong direct signal component ($A^2/2\sigma^2=10$) and $E_b/N_o=16$ dB.
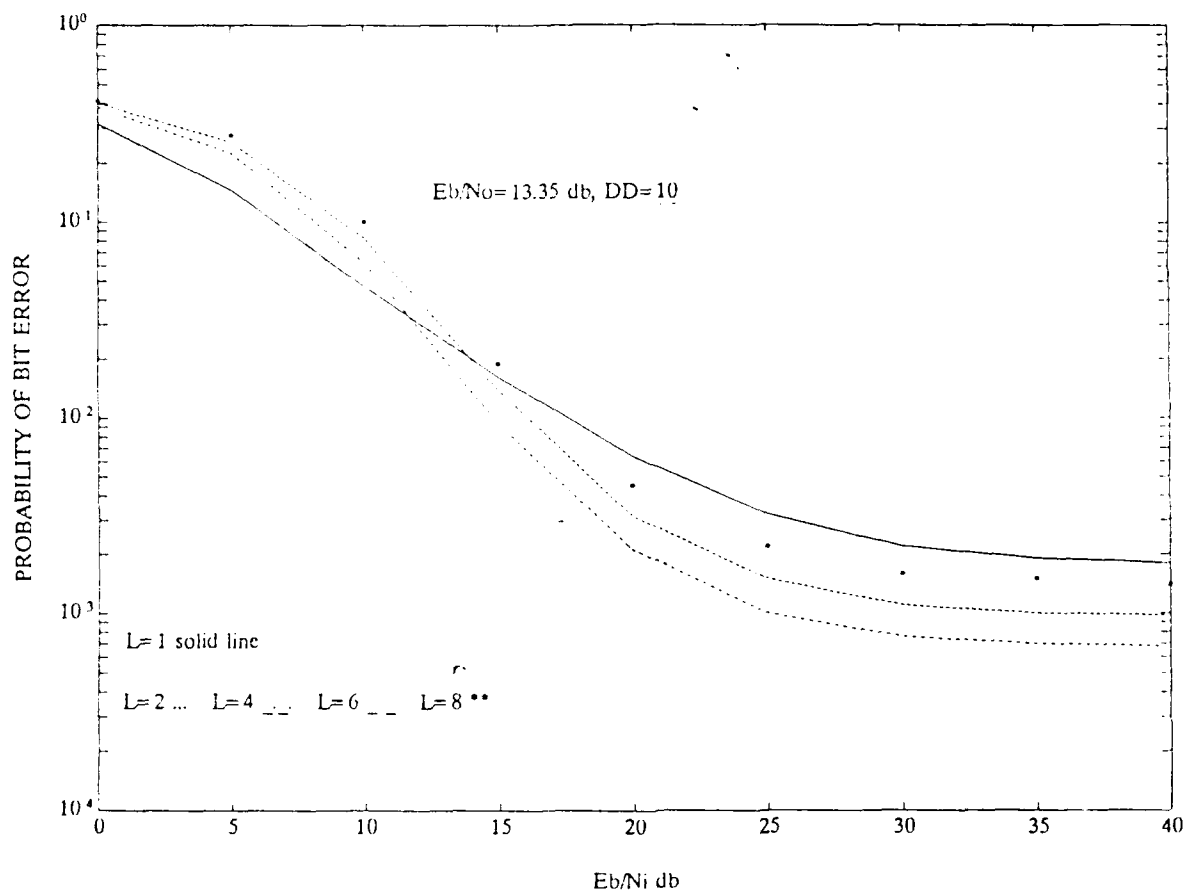
Figure 41. **Envelope Detector Self-Normalization Combining:** Worst case performance of the self-normalization combining envelope detector receiver with diversity combining, partial-band interference, and thermal noise in a fading channel for a strong direct signal component ($A^2/2\sigma^2=1000$) and $E_b/N_o=16$ dB.
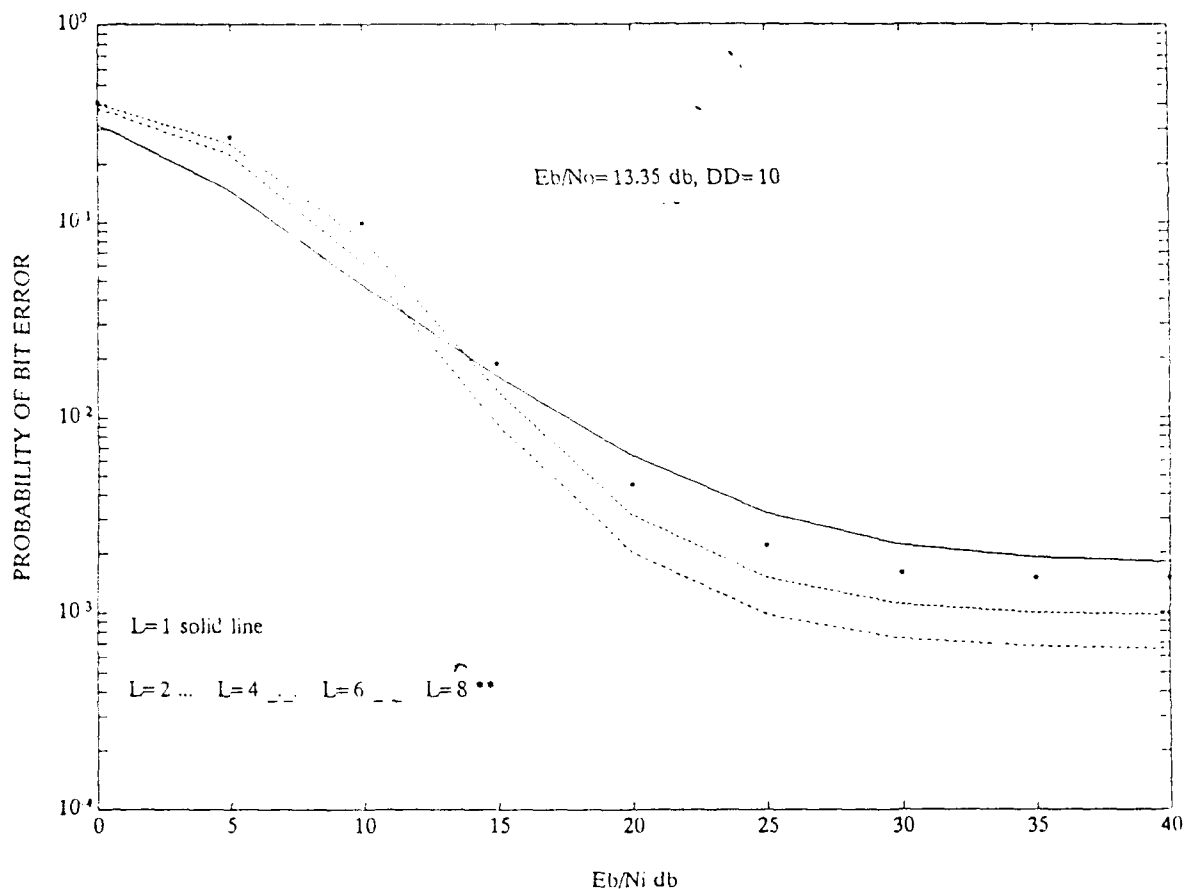
94

Figure 42. **Square-Law Detector Self-Normalization**

Combining: Worst case performance of the self-normalization combining square-law detector receiver with diversity combining, partial-band interference, and thermal noise in a fading channel for a strong direct signal component $(A^2/2\sigma^2=1000)$ and $E_b/N_o=16$ dB.

Figure 43. **Envelope Detector Self-Normalization Combining:** Worst case performance of the self-normalization combining envelope detector receiver with diversity combining, partial-band interference, and thermal noise in a fading channel for a relatively strong direct signal component $(A^2/2\sigma^2=10)$ and $E_b/N_o=18$ dB.
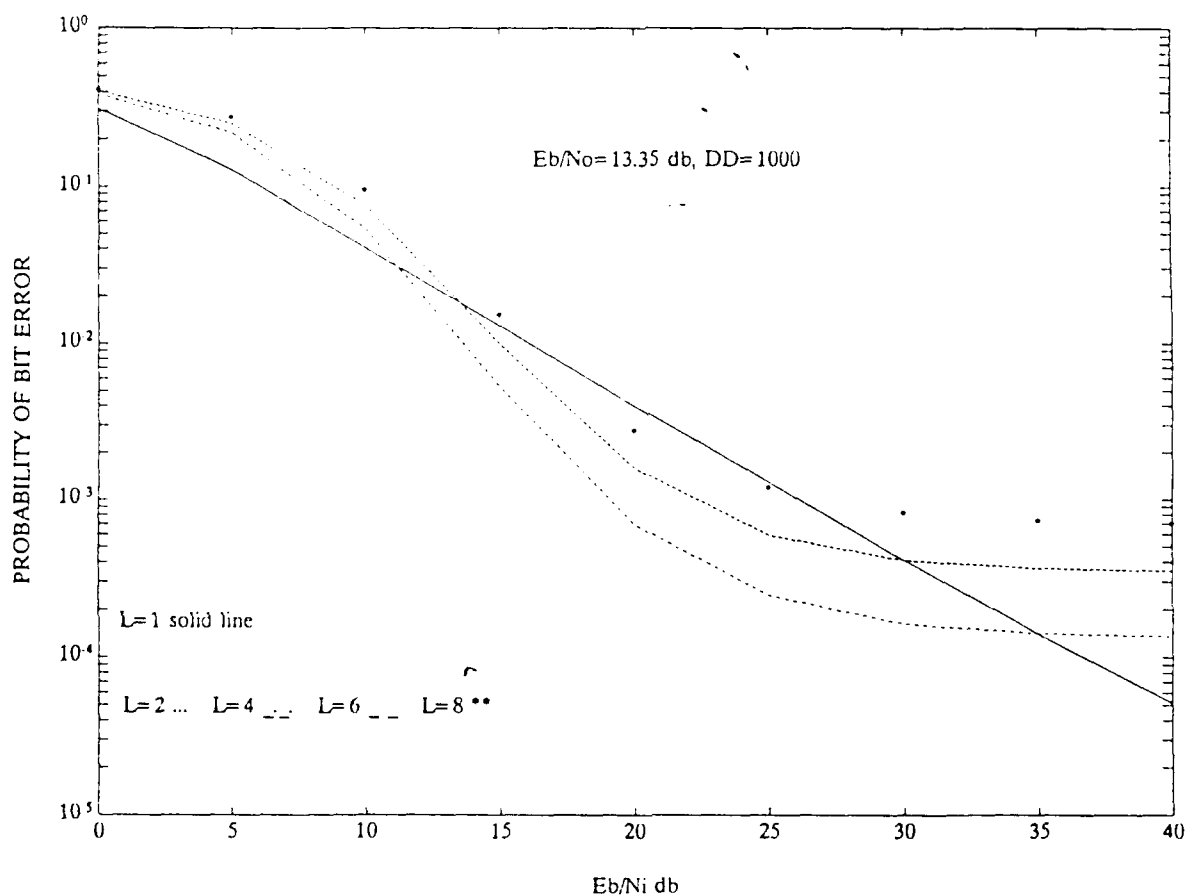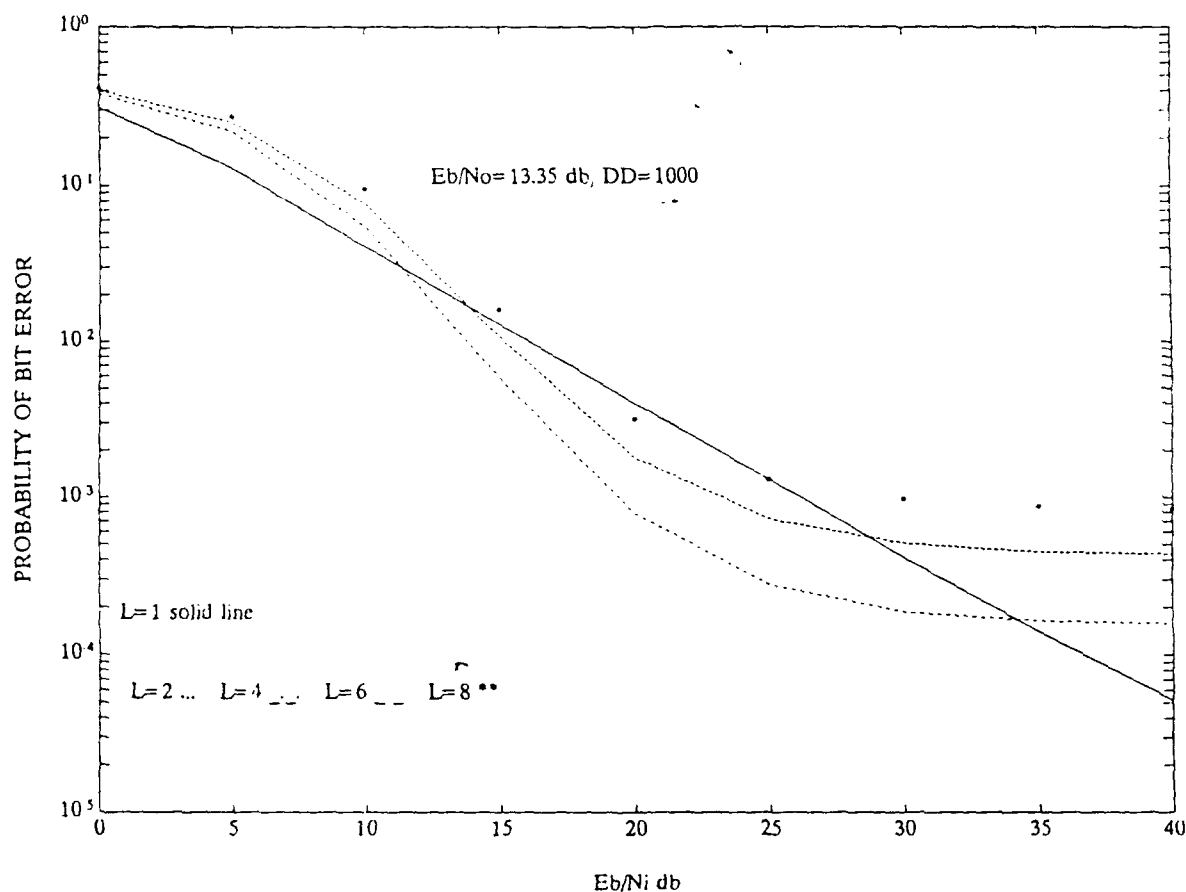
Figure 44. Square-Law Detector Self-Normalization Combining: Worst case performance of the self-normalization combining square-law detector receiver with diversity combining, partial-band interference, and thermal noise in a fading channel for a relatively strong direct signal component ($A^2/2\sigma^2=10$) and $E_b/N_o=18$ dB.

97

Figure 45. Envelope Detector Noise-Normalization Combining:
Worst case performance of the noise-normalization combining
envelope detector receiver with diversity combining,
partial-band interference, and thermal noise in a fading
channel for a diffuse signal $(A^2/2\sigma^2=0.01)$ and $E_b/N_o=13.35$
dB.

Figure 46. Square-Law Detector Noise-Normalization
Combining: Worst case performance of the noise-
normalization combining square-law detector receiver with
diversity combining, partial-band interference, and thermal
noise in a fading channel for a diffuse signal $(A^2/2\sigma^2=0.01)$
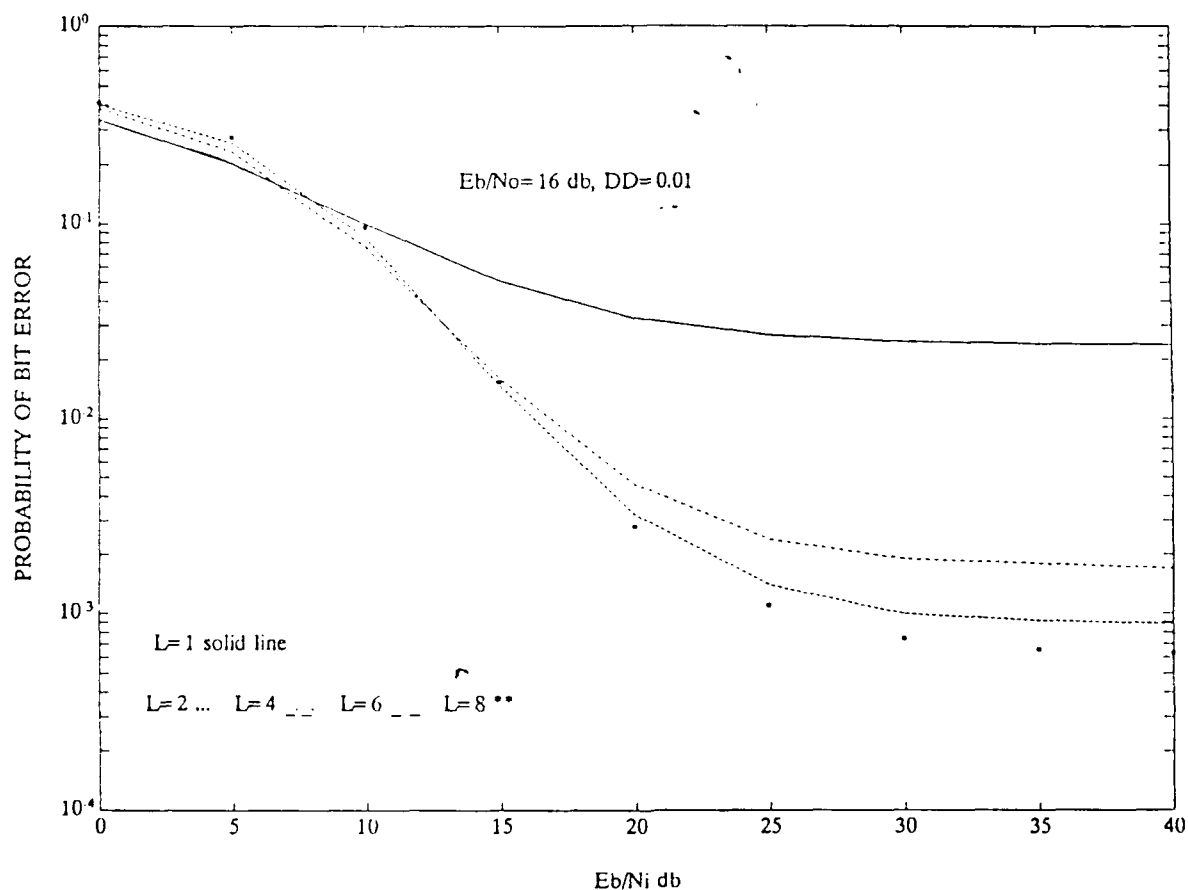and $E_b/N_o=13.35$ dB.

99

Figure 47. Envelope Detector Noise-Normalization Combining:
Worst case performance of the noise-normalization combining
envelope detector receiver with diversity combining,
partial-band interference, and thermal noise in a fading
channel for a signal with equal direct and diffuse
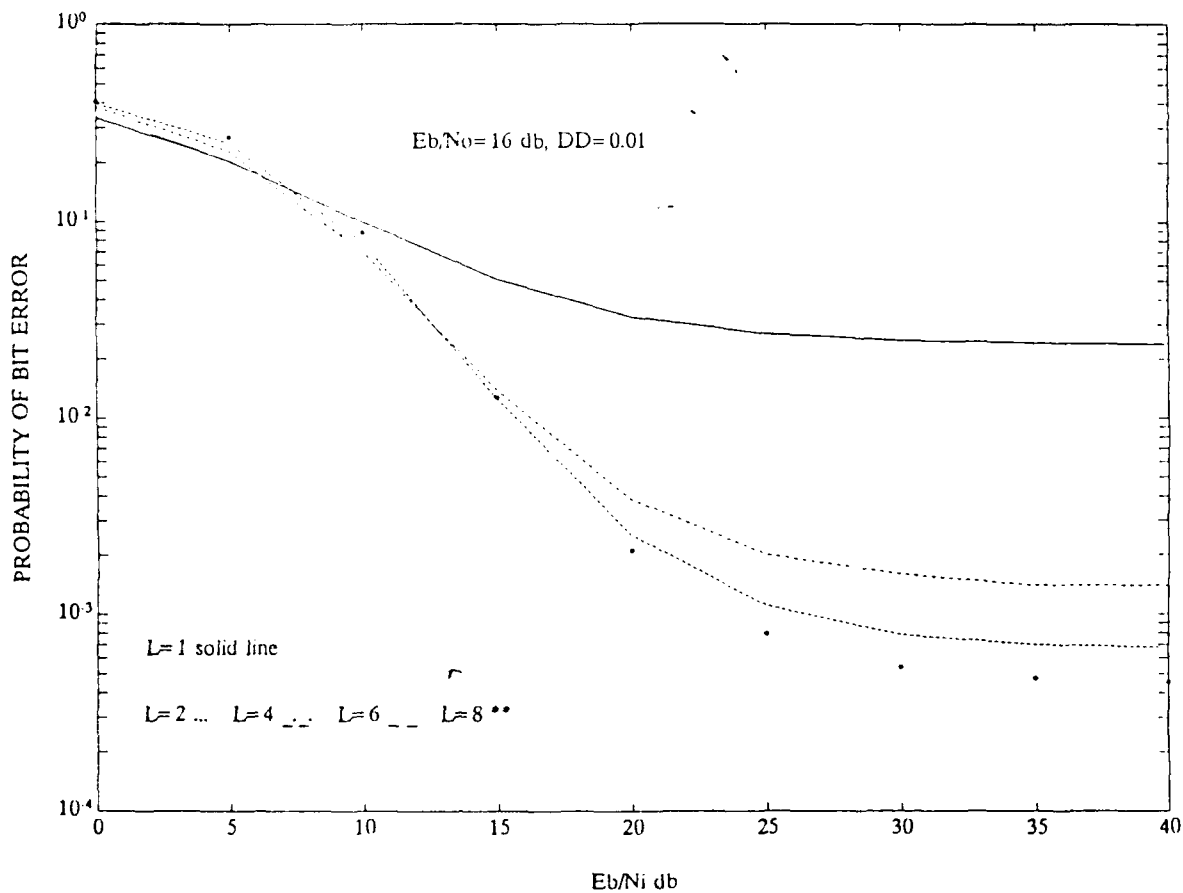components $(A^2/2\sigma^2=1)$ and $E_b/N_o=13.35$ dB.

100

Figure 48. Square-Law Detector Noise-Normalization
Combining: Worst case performance of the noise-
normalization combining square-law detector receiver with
diversity combining, partial-band interference, and thermal
noise in a fading channel for a signal with equal direct and
diffuse components $(A_2/2\sigma^2=1)$ and $E_b/N_o=13.35$ dB.

101

PROBABILITY OF BIT ERROR

10^0

10^{-1}

Eb/No= 13.35 db, DD=10

10^{-2}

10^{-3}

L= 1 solid line

L=2 ...   L=4 _._   L=6 _ _   L=8 ••

10^{-4}

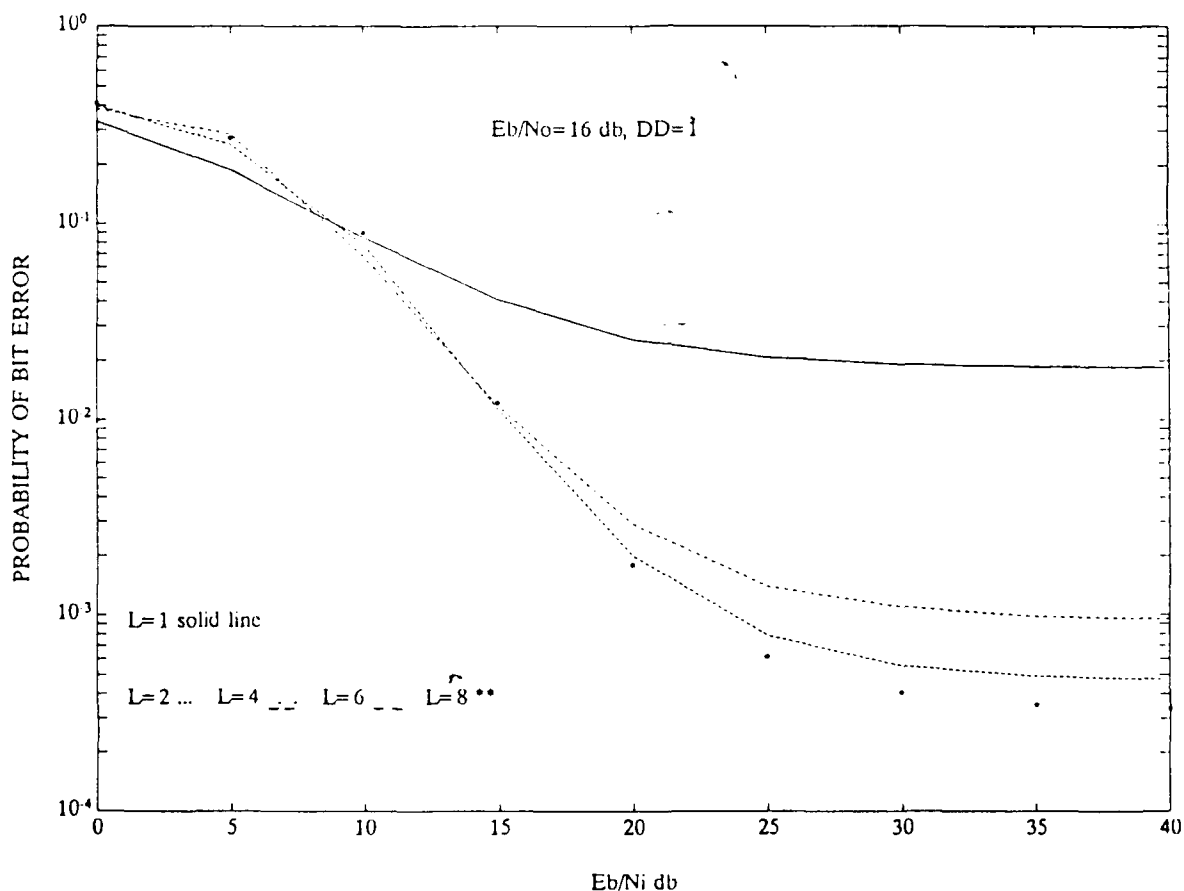0   5   10   15   20   25   30   35   40

Eb/Ni db

Figure 49.   Envelope Detector Noise-Normalization Combining:
Worst case performance of the noise-normalization combining
envelope detector receiver with diversity combining,
partial-band interference, and thermal noise in a fading
channel for a relatively strong direct signal component
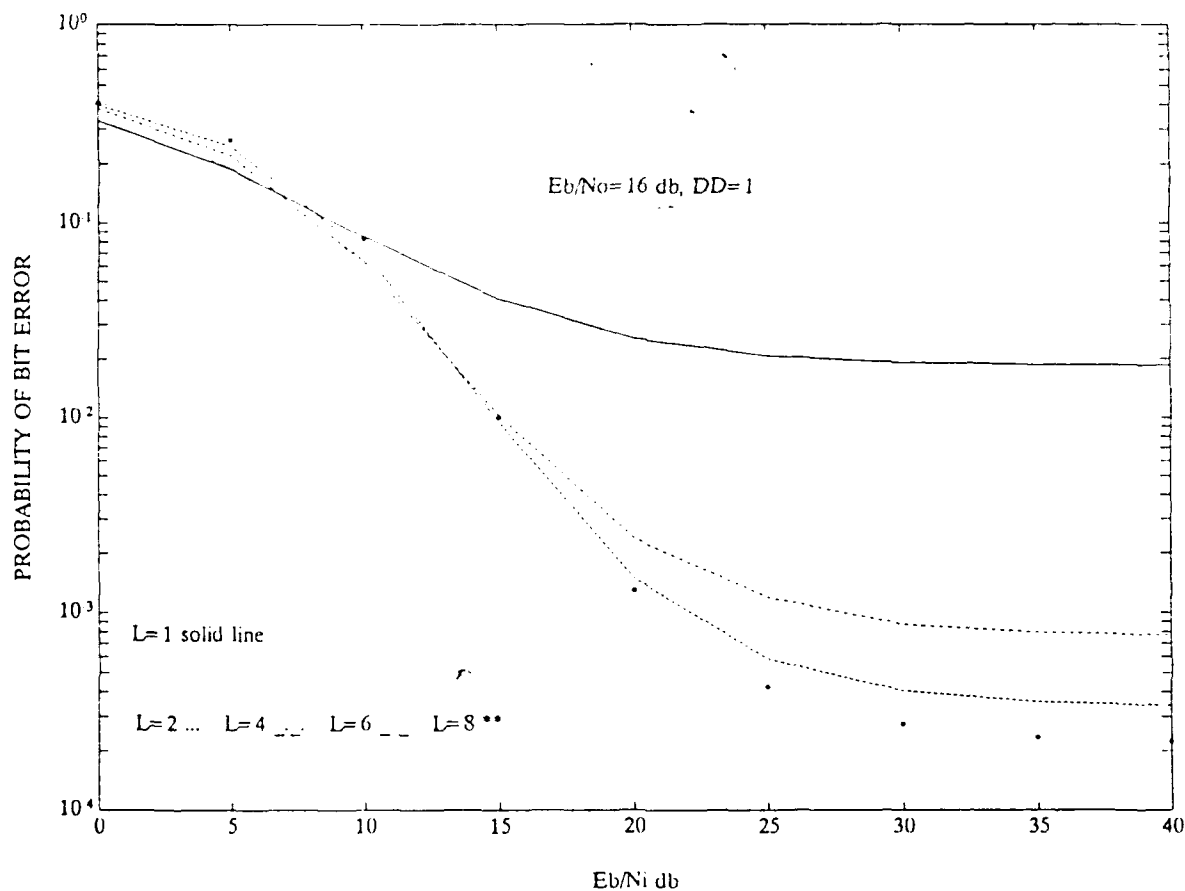$(A^2/2\sigma^2=10)$ and $E_b/N_o=13.35$ dB.

102

Figure 50. Square-Law Detector Noise-Normalization Combining: Worst case performance of the Noise-normalization combining square-law detector receiver with diversity combining, partial-band interference, and thermal noise in a fading channel for a relatively strong direct signal component $(A^2/2\sigma^2=10)$ and $E_b/N_o=13.35$ dB.
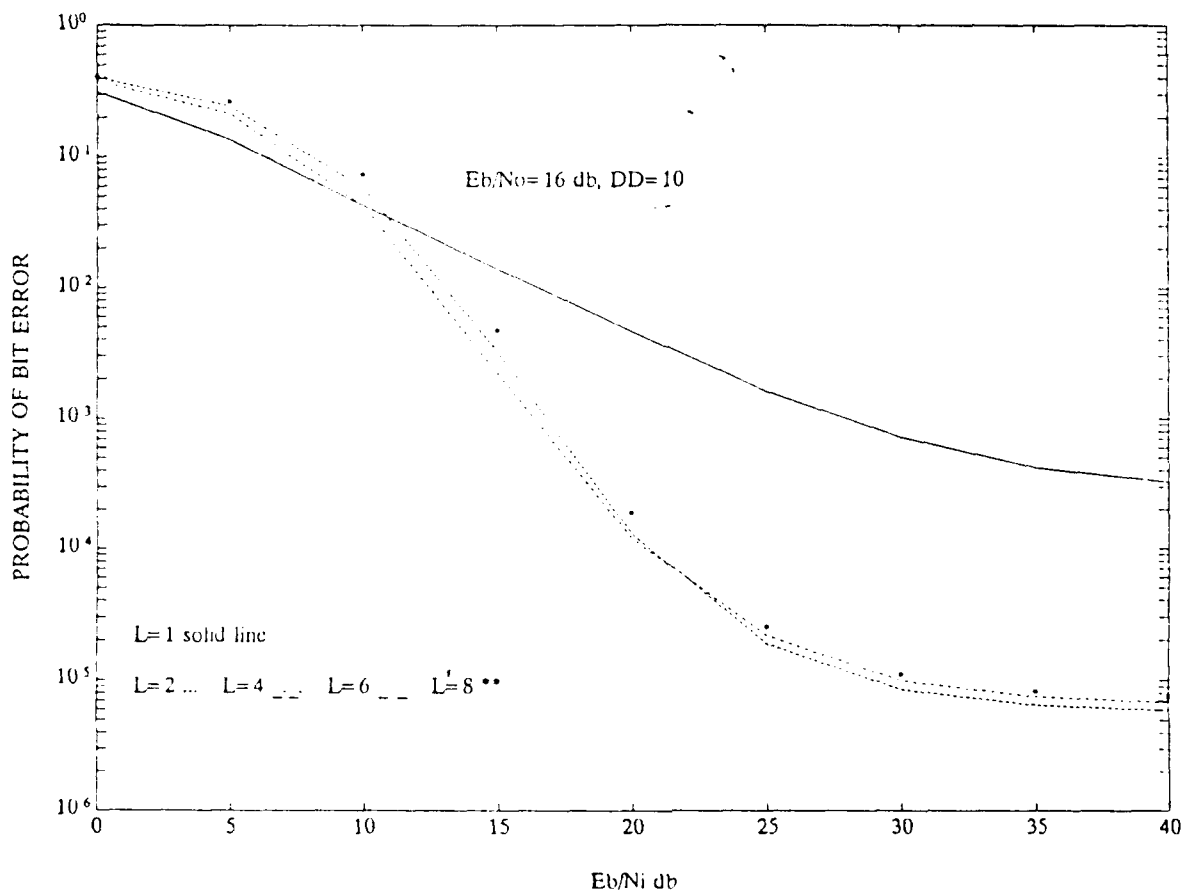
103

Figure 51. **Envelope Detector Noise-Normalization Combining:**
Worst case performance of the noise-normalization combining
envelope detector receiver with diversity combining,
partial-band interference, and thermal noise in a fading
channel for a strong direct signal component ($A^2/2\sigma^2=1000$)
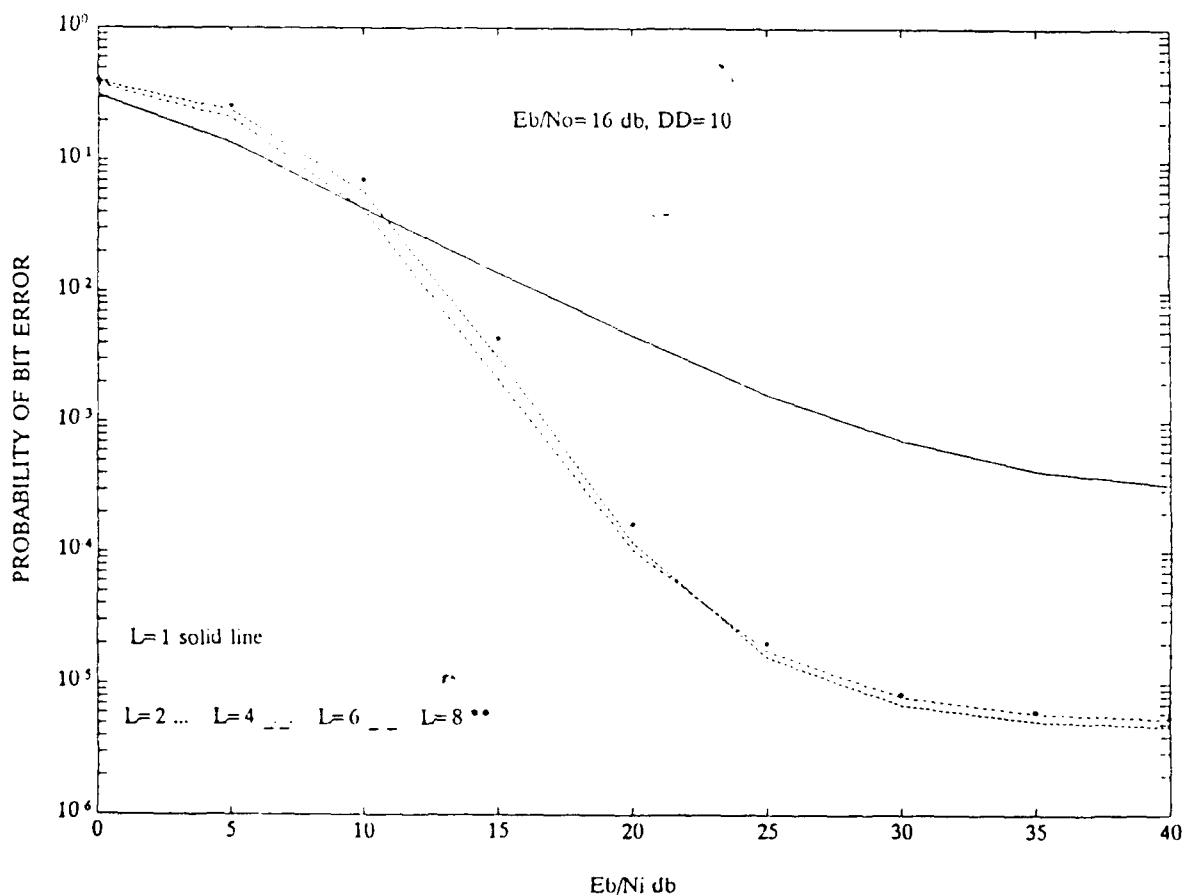and $E_b/N_o=13.35$ dB.

Figure 52. Square-Law Detector Noise-Normalization Combining: Worst case performance of the noise-normalization combining square-law detector receiver with diversity combining, partial-band interference, and thermal noise in a fading channel for a strong direct signal component $(A^2/2\sigma^2=1000)$ and $E_b/N_o=13.35$ dB.
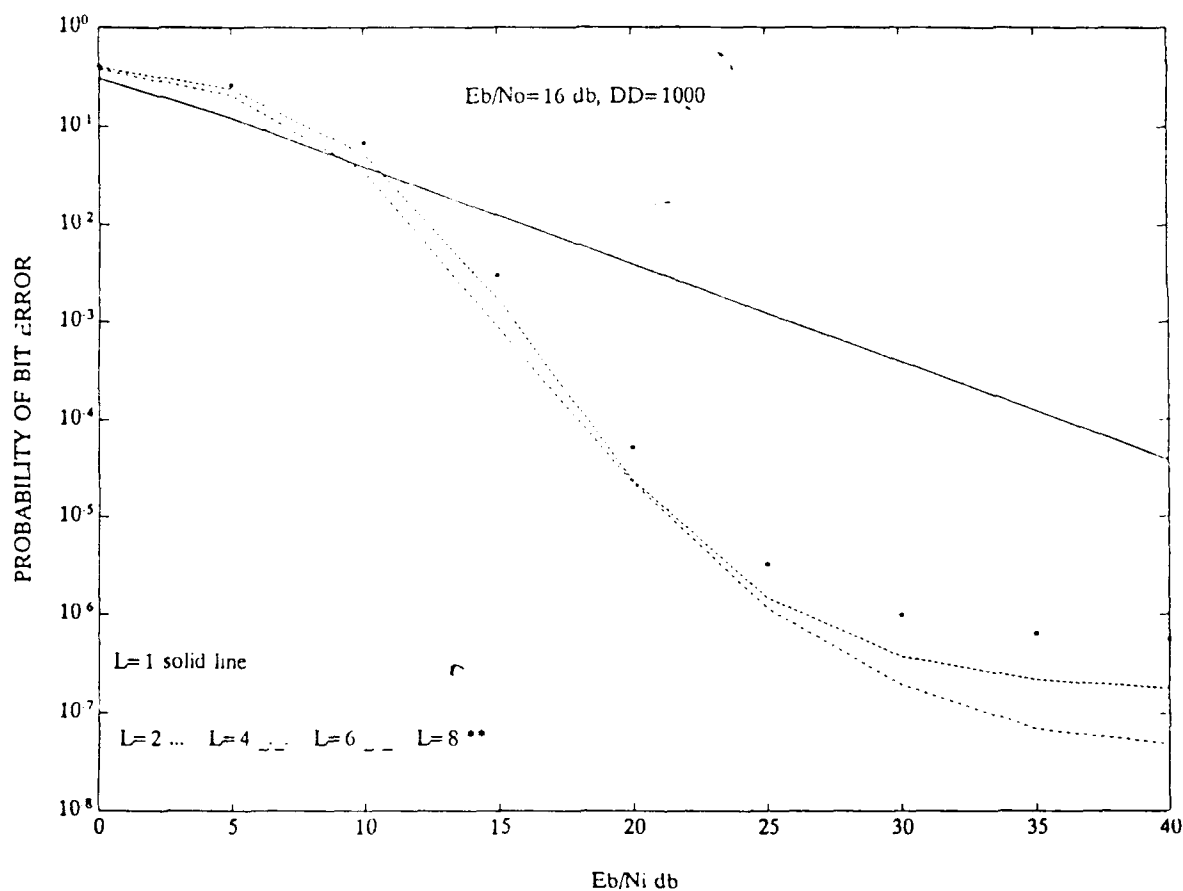
105

Figure 53. Envelope Detector Noise-Normalization Combining: Worst case performance of the noise-normalization combining envelope detector receiver with diversity combining, partial-band interference, and thermal noise in a fading channel for a diffuse signal ($A^2/2\sigma^2 = 0.01$) and $E_b/N_o = 16$ dB.
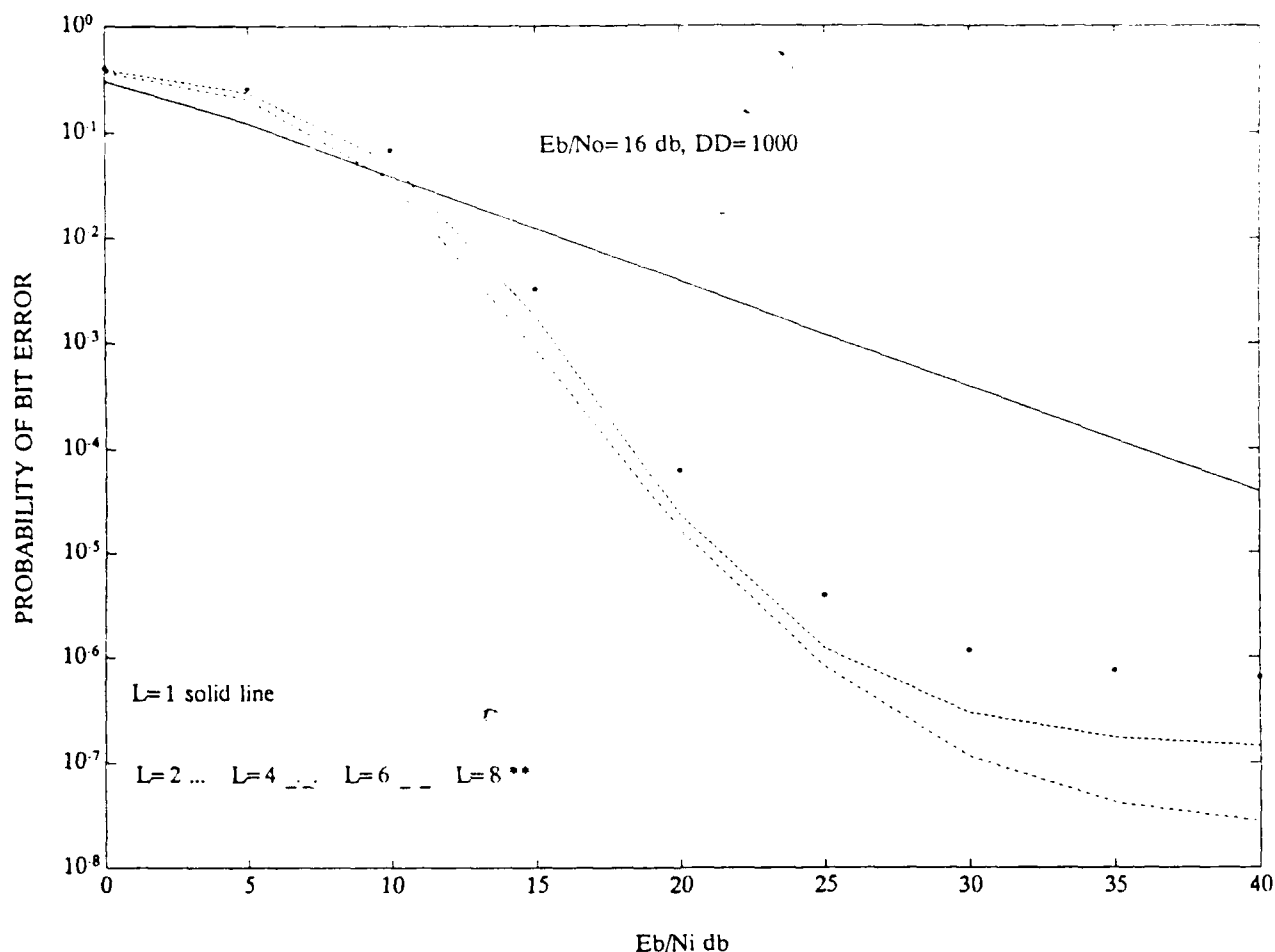
Figure 54. Square-Law Detector Noise-Normalization Combining: Worst case performance of the noise-normalization combining square-law detector receiver with diversity combining, partial-band interference, and thermal noise in a fading channel for a diffuse signal ($A^2/2\sigma^2=0.01$) and $E_b/N_o=16$ dB.
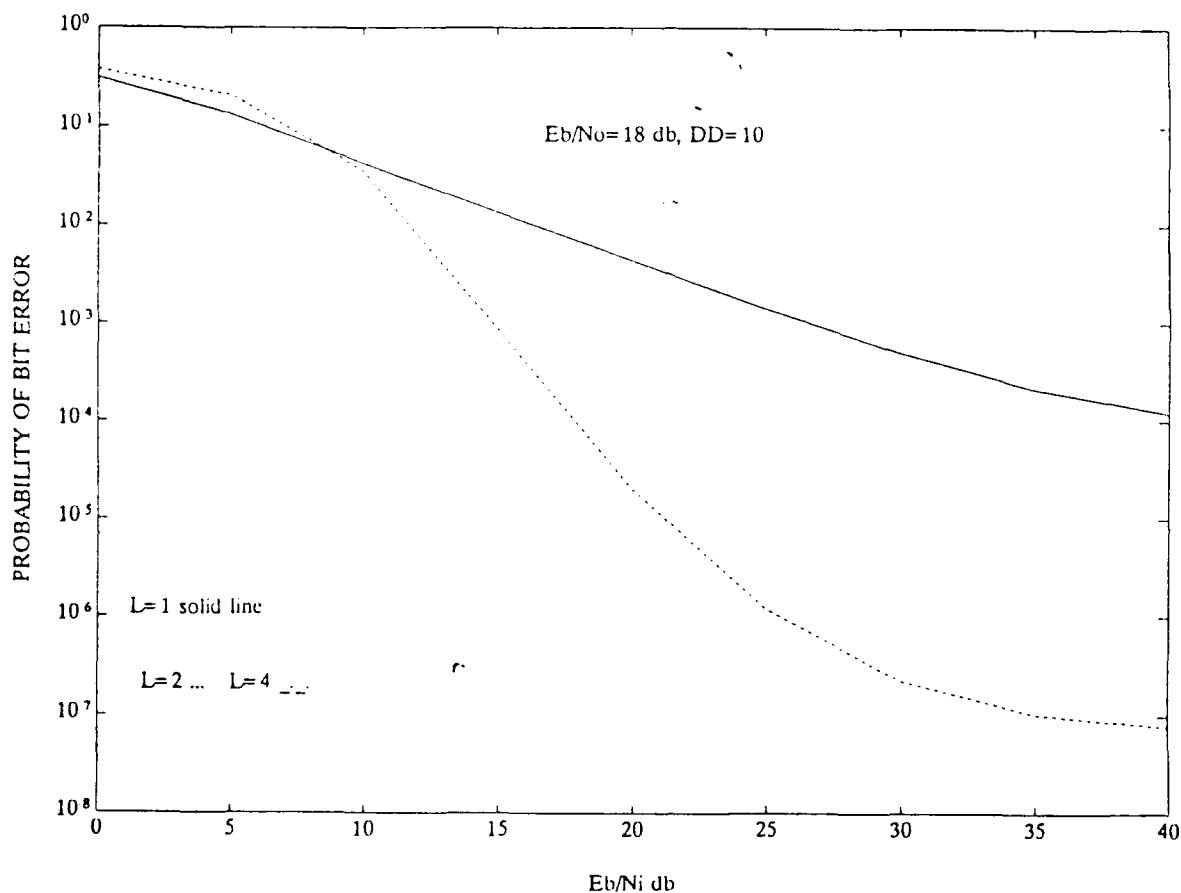
107

Figure 55. Envelope Detector Noise-Normalization Combining: Worst case performance of the noise-normalization combining envelope detector receiver with diversity combining, partial-band interference, and thermal noise in a fading channel for a signal with equal direct and diffuse components $(A^2/2\sigma^2=1)$ and $E_b/N_o=16$ dB.
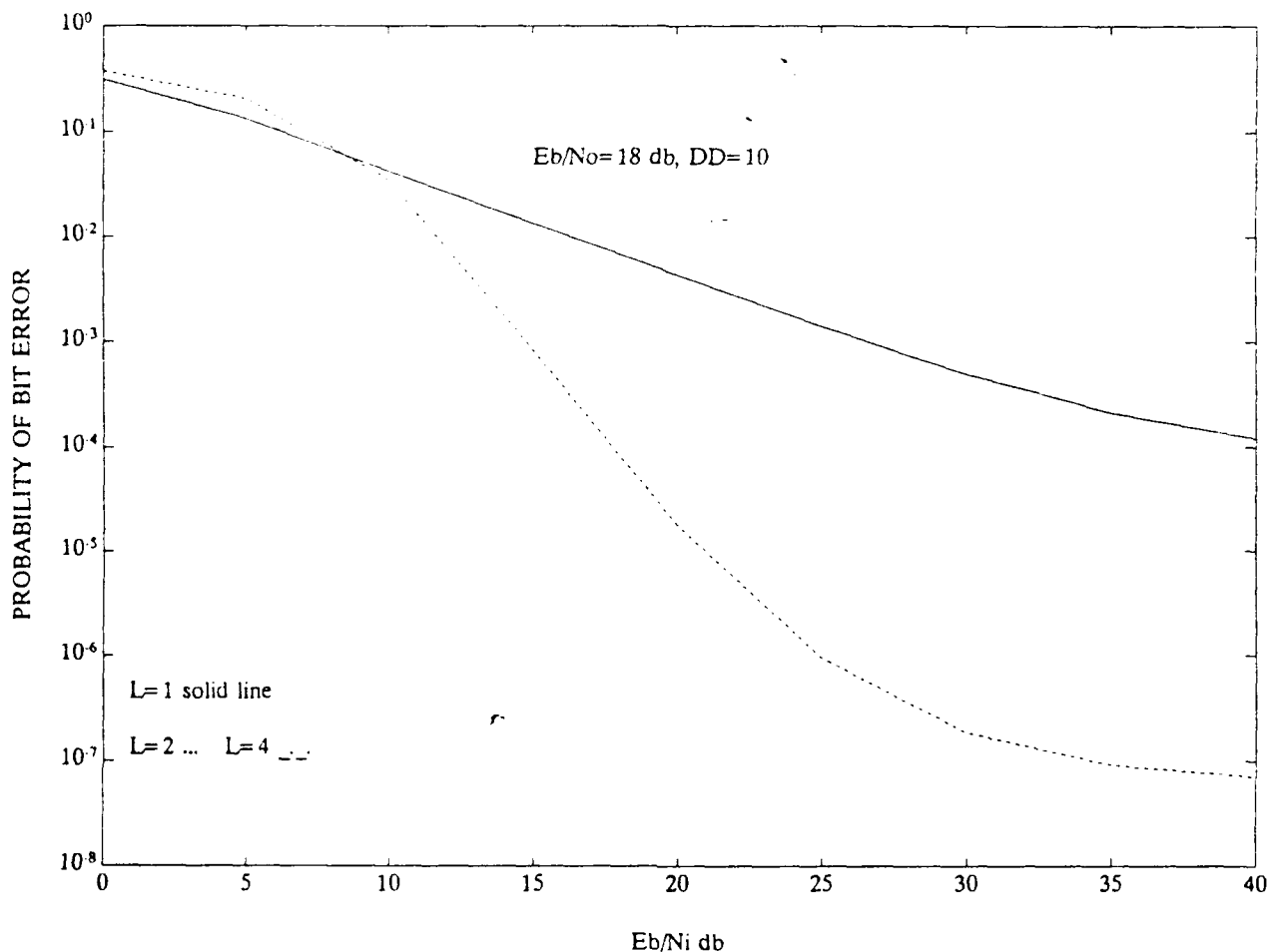
108

Figure 56. Square-Law Detector Noise-Normalization Combining: Worst case performance of the noise-normalization combining square-law detector receiver with diversity combining, partial-band interference, and thermal noise in a fading channel for a signal with equal direct and diffuse components $(A^2/2\sigma^2=1)$ and $E_b/N_o=16$ dB.

Figure 57. Envelope Detector Noise-Normalization Combining: Worst case performance of the noise-normalization combining envelope detector receiver with diversity combining, partial-band interference, and thermal noise in a fading channel for a relatively strong direct signal component $(A^2/2\sigma^2=10)$ and $E_b/N_o=16$ dB.

Figure 58. Square-Law Detector Noise-normalization
Combining: Worst case performance of the noise-
normalization combining square-law detector receiver with
diversity combining, partial-band interference, and thermal
noise in a fading channel for a relatively strong direct
signal component ($A^2/2\sigma^2=10$) and $E_b/N_o=16$ dB.

111

Figure 59. **Envelope Detector Noise-Normalization Combining:** Worst case performance of the noise-normalization combining envelope detector receiver with diversity combining, partial-band interference, and thermal noise in a fading channel for a strong direct signal component ($A^2/2\sigma^2=1000$) and $E_b/N_o=16$ dB.
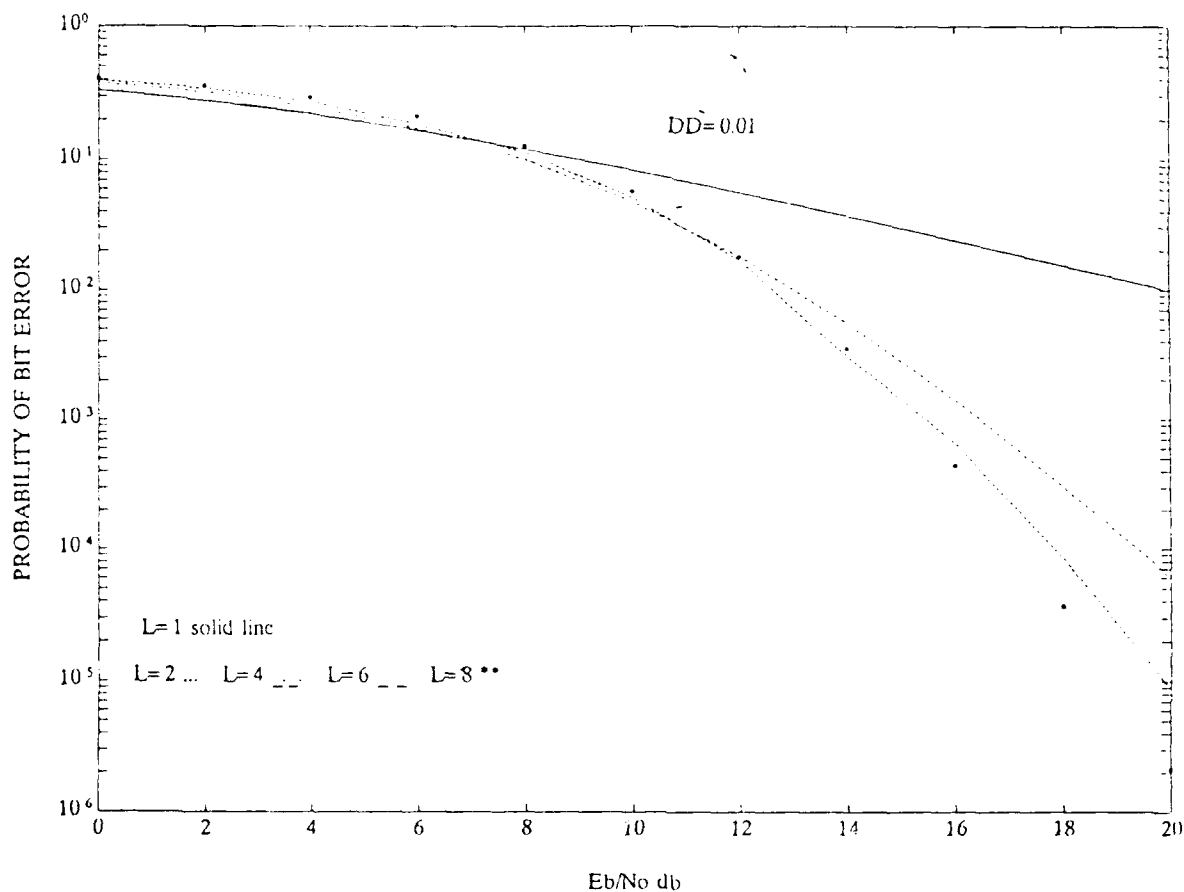
112

**Figure 60. Square-Law Detector Noise-Normalization
Combining:** Worst case performance of the noise-
normalization combining square-law detector receiver with
diversity combining, partial-band interference, and thermal
noise in a fading channel for a strong direct signal
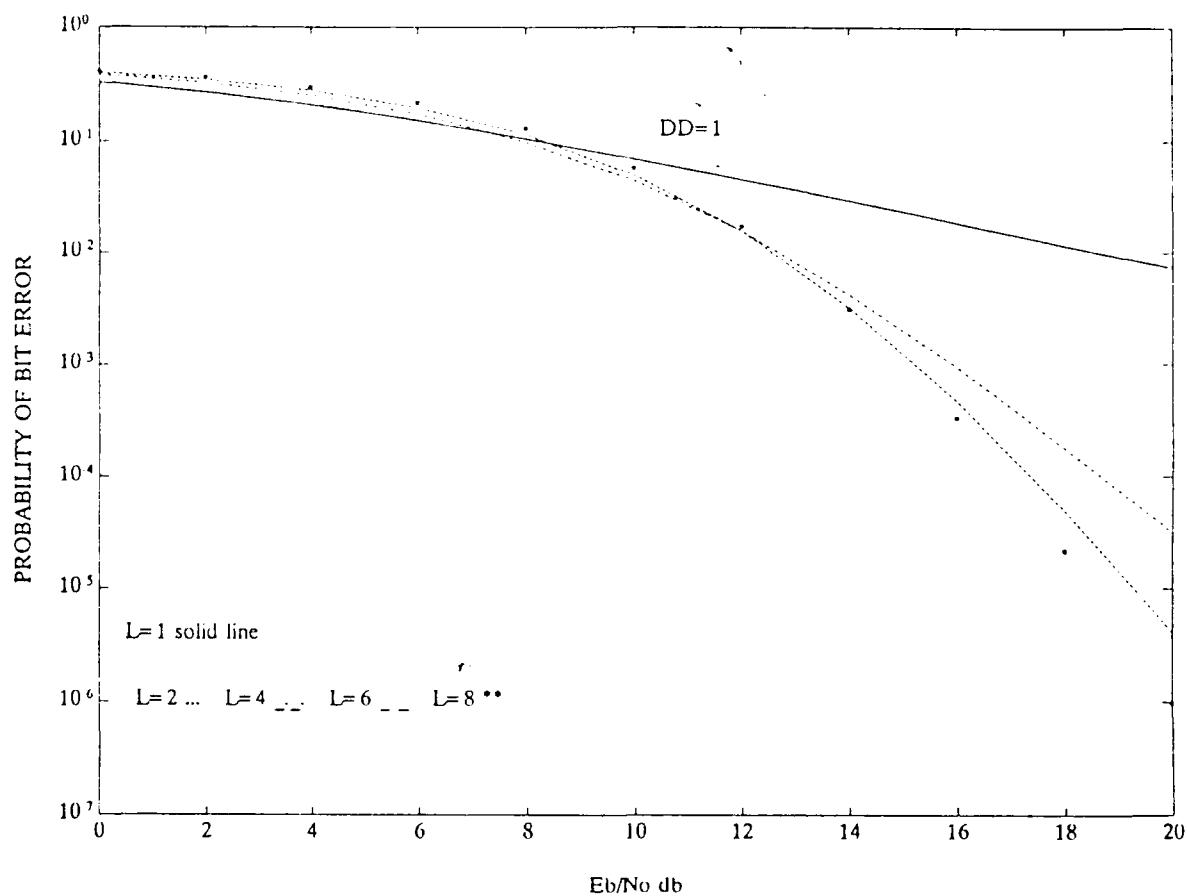component $(A^2/2\sigma^2 = 1000)$ and $E_b/N_o = 16$ dB.

113

Figure 61. Envelope Detector Noise-Normalization Combining:
Worst case performance of the noise-normalization combining
envelope detector receiver with diversity combining,
partial-band interference, and thermal noise in a fading
channel for a relatively strong direct signal component
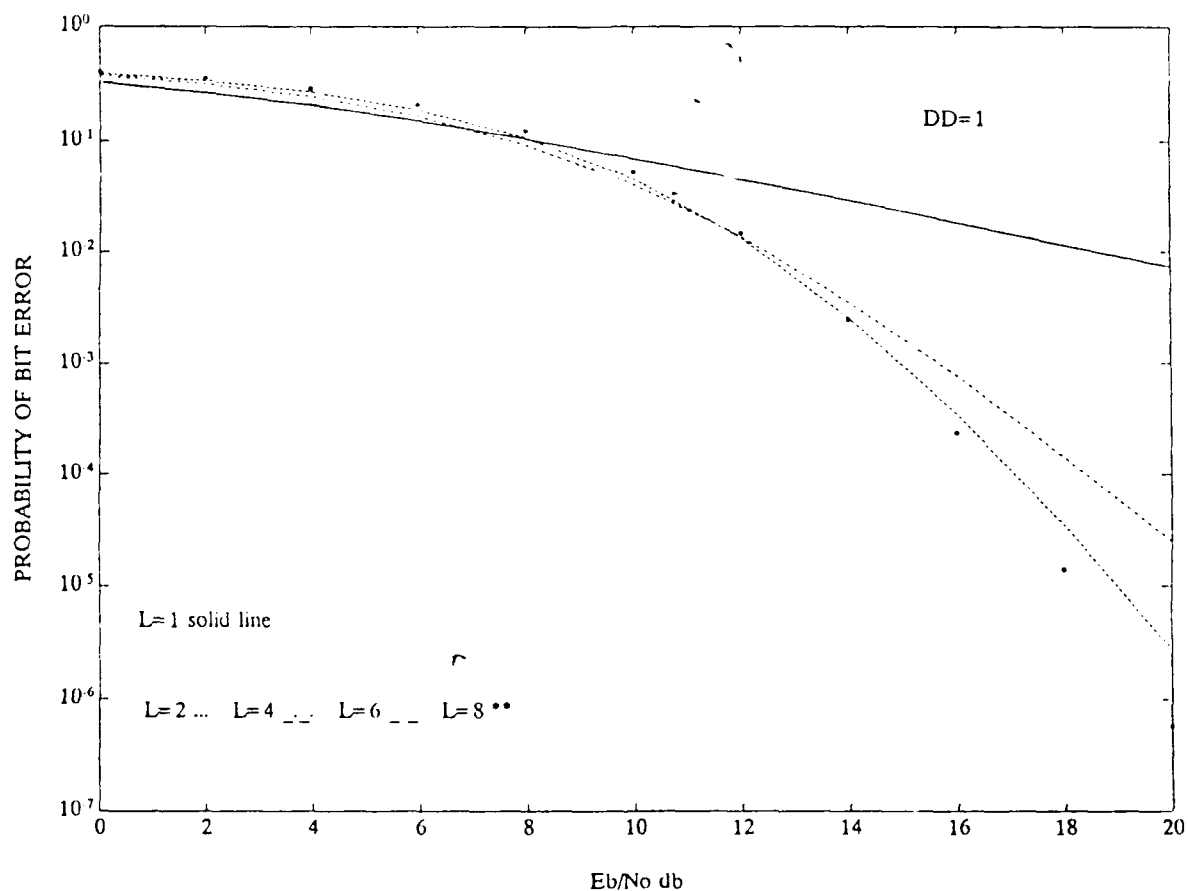$(A^2/2\sigma^2=10)$ and $E_b/N_o=18$ dB.

Figure 62. **Square-Law Detector Noise-Normalization**
Combining: Worst case performance of the noise-
normalization combining square-law detector receiver with
diversity combining, partial-band interference, and thermal
noise in a fading channel for a relatively strong direct
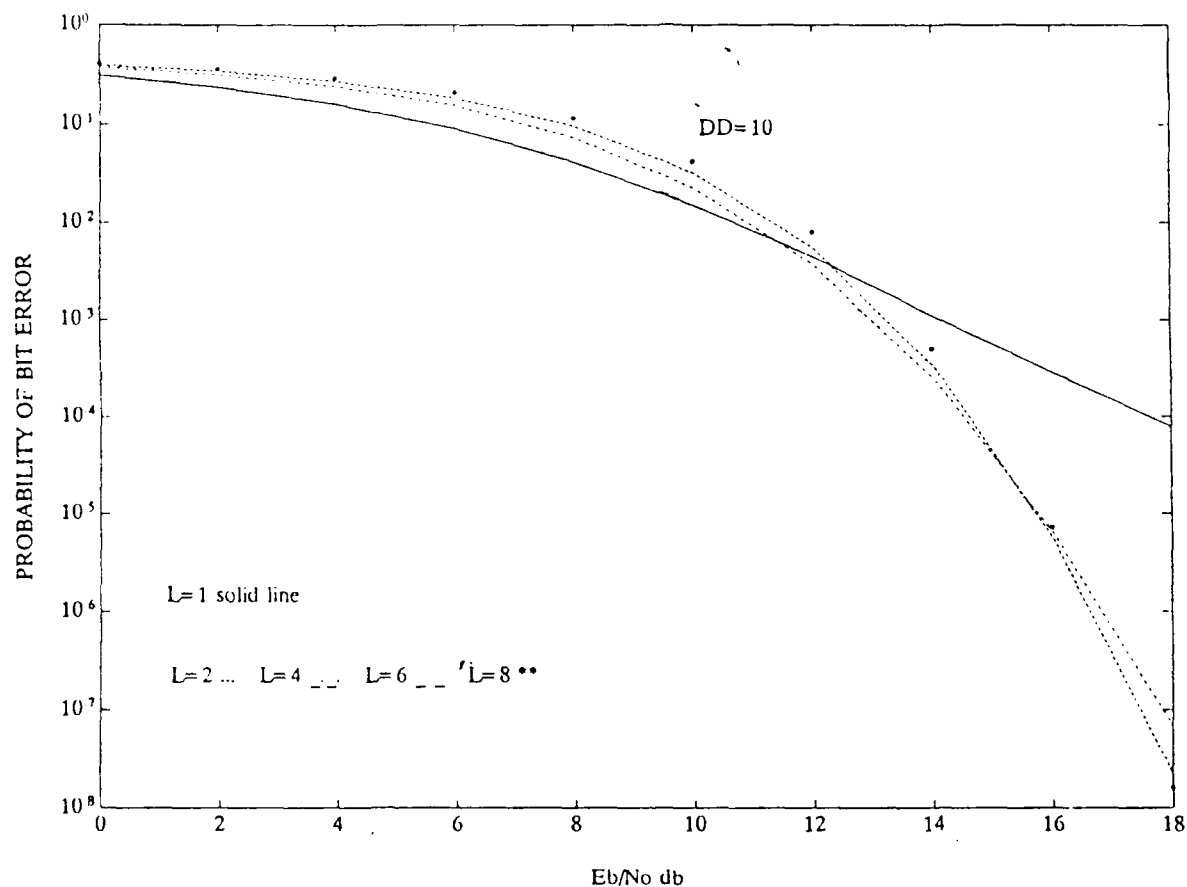signal component $(A^2/2\sigma^2=10)$ and $E_b/N_o=18$ dB.
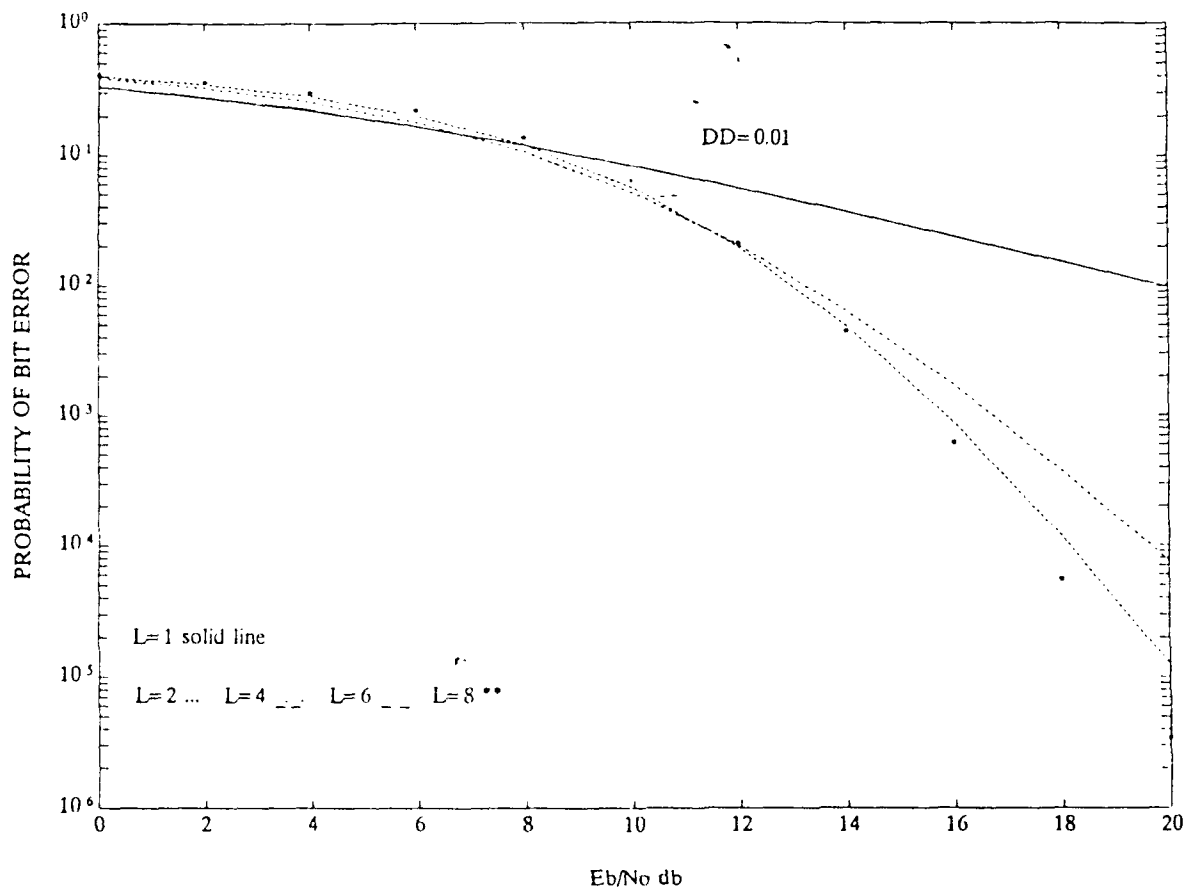
Figure 63. Envelope Detector Linear and Noise-Normalization Combining: Performance of the linear and noise-normalization combining envelope detector receiver with diversity combining, and thermal noise in a fading channel for a diffuse signal ($A^2/2\sigma^2=0.01$).
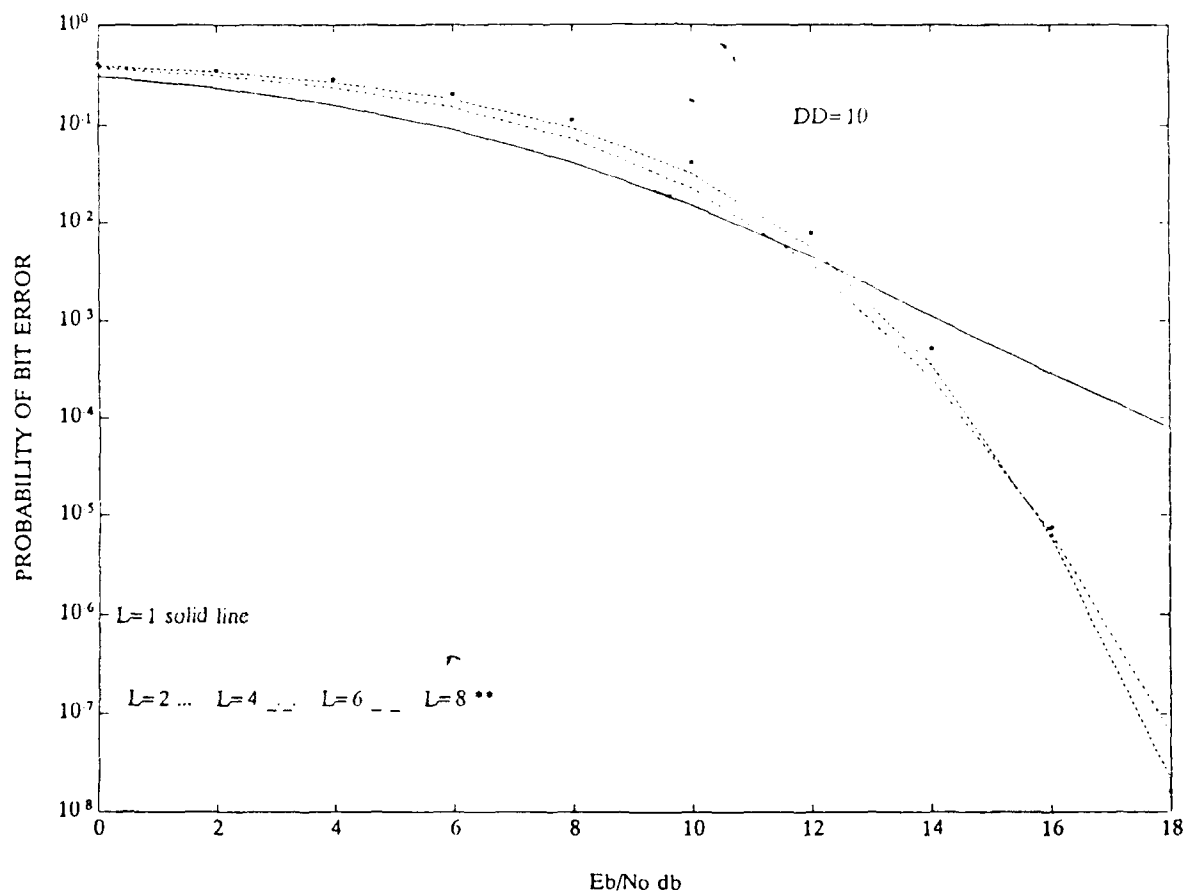
116

Figure 64. Square-Law Detector Linear and Noise-Normalization Combining: Performance of the linear and noise-normalization combining square-law detector receiver with diversity combining, and thermal noise in a fading channel for a diffuse signal $(A^2/2\sigma^2=0.01)$.
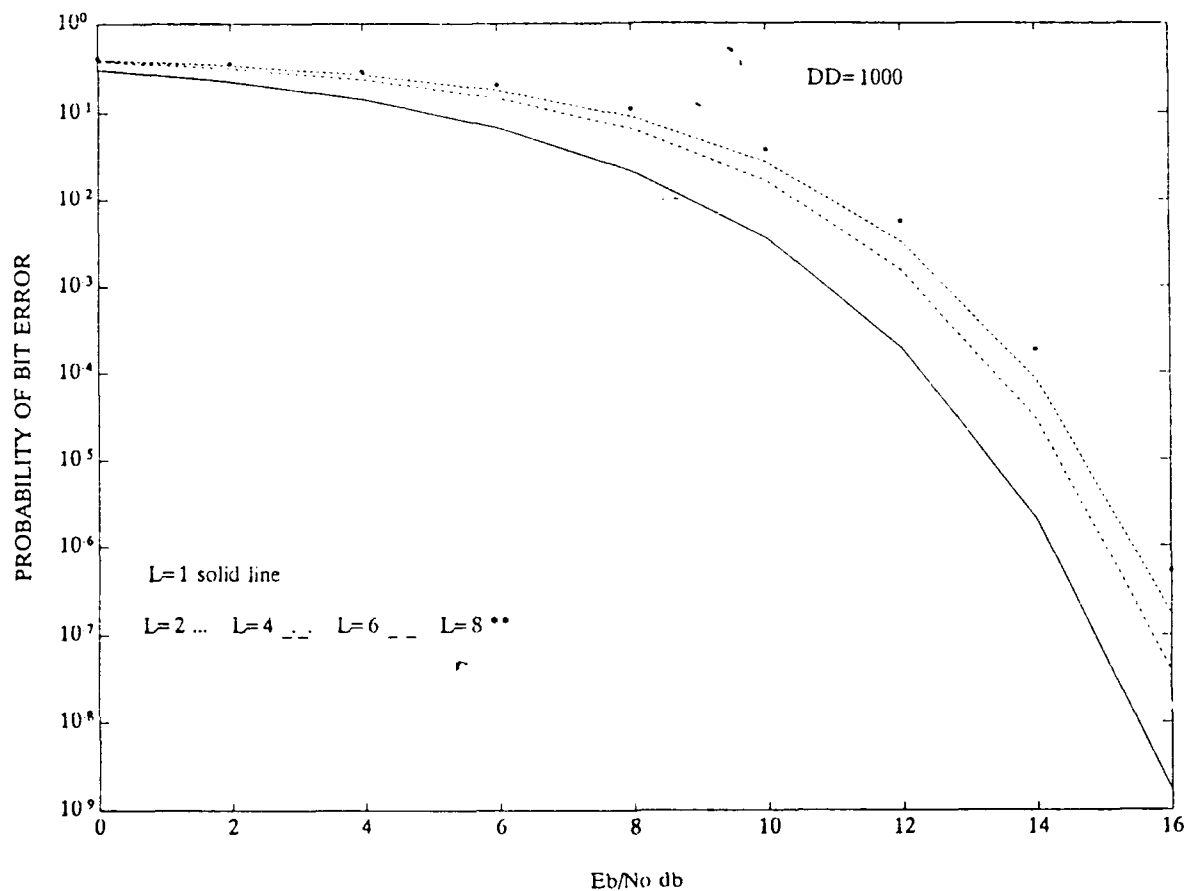
117

Figure 65. Envelope Detector Linear and Noise-Normalization Combining: Performance of the linear and noise-normalization combining envelope detector receiver with diversity combining, and thermal noise in a fading channel for a signal with equal direct and diffuse components $(A^2/2\sigma^2=1)$.
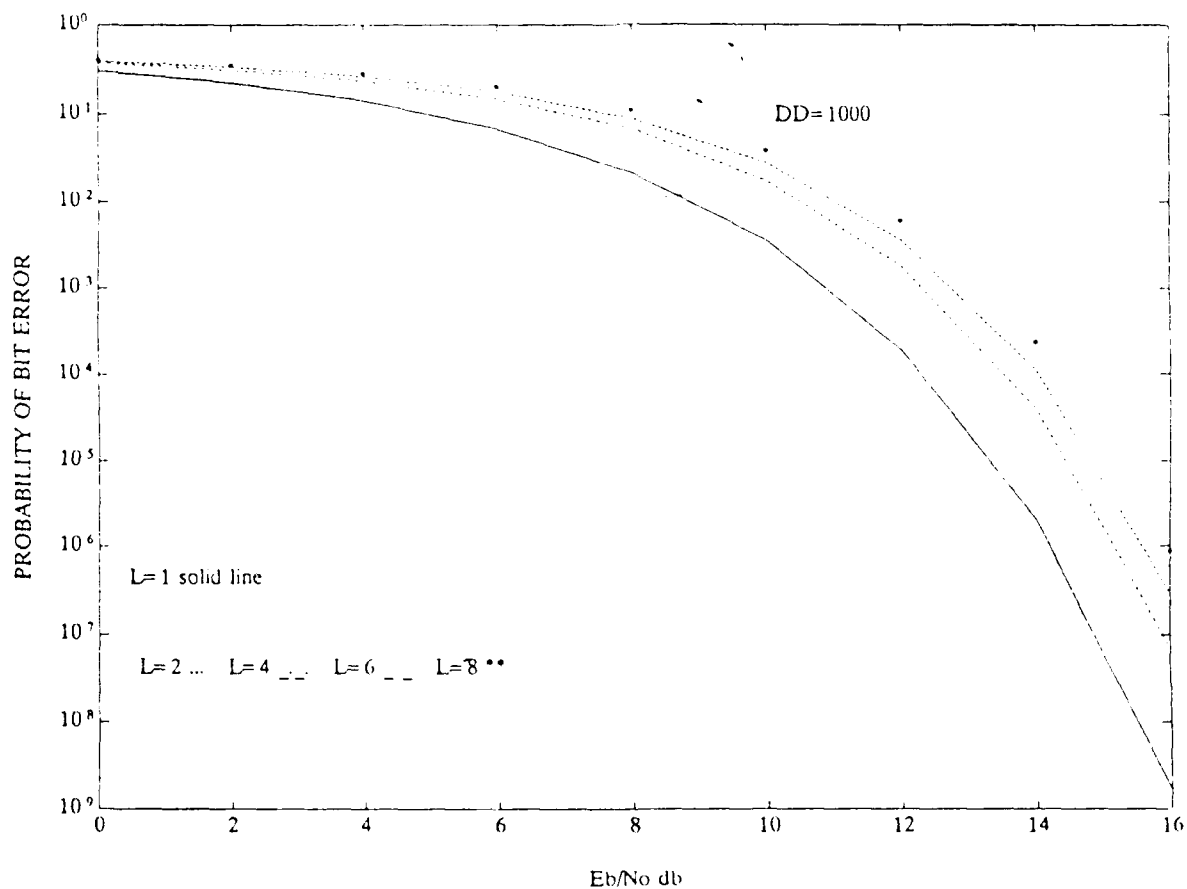
118

Figure 66. Square-Law Detector Linear and Noise-Normalization Combining: Performance of the linear and noise-normalization combining square-law detector receiver with diversity combining, and thermal noise in a fading channel for a signal with equal diffuse and direct components $(A^2/2\sigma^2=1)$.

119

Figure 67. **Envelope Detector Linear and Noise-Normalization Combining:** Performance of the linear and noise-normalization combining envelope detector receiver with diversity combining, and thermal noise in a fading channel for a relatively strong direct signal $(A^2/2\sigma^2=10)$.

120

Figure 68. Square-Law Detector Linear and Noise-Normalization Combining: Performance of the linear and noise-normalization combining square-law detector receiver with diversity combining, and thermal noise in a fading channel for a relatively strong direct signal $(A^2/2\sigma^2=10)$.
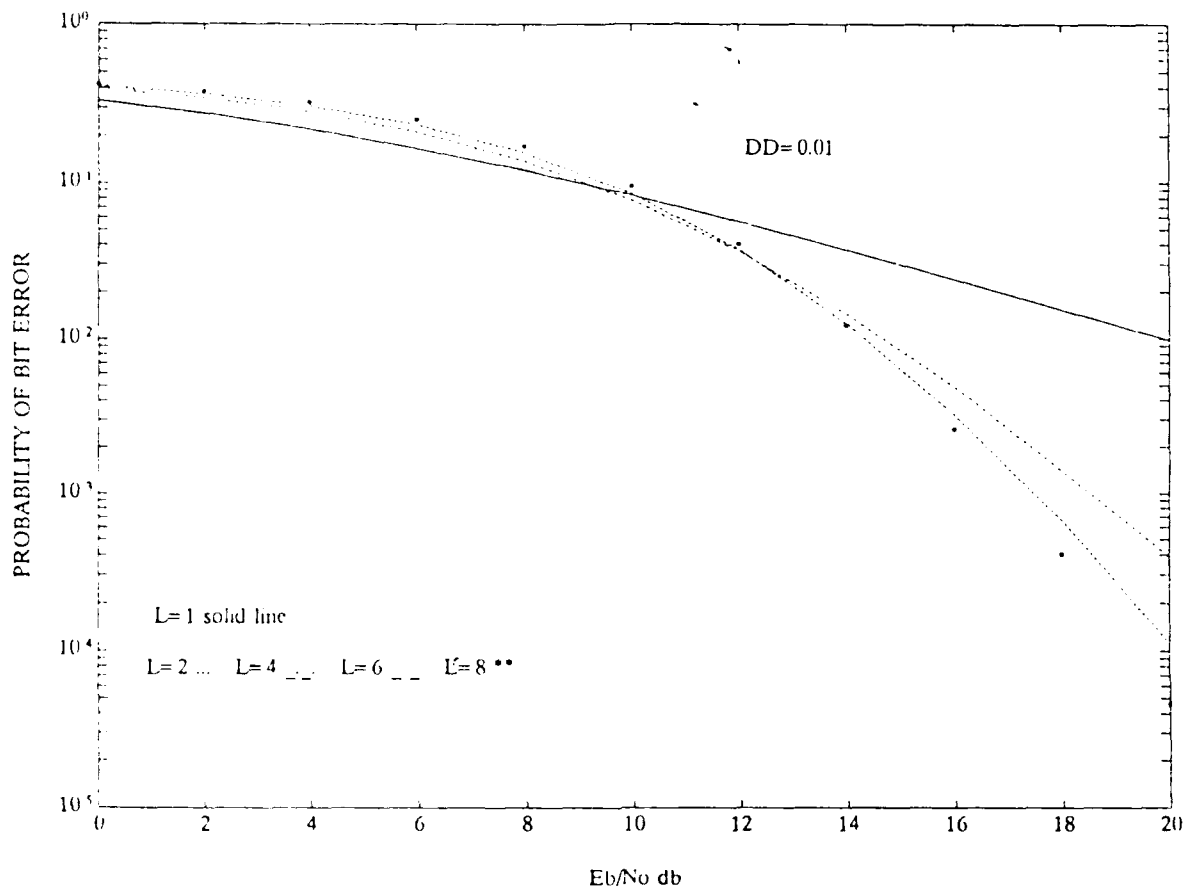
121

Figure 69. Envelope Detector Linear and Noise-Normalization Combining: Performance of the linear and noise-normalization combining envelope detector receiver with diversity combining, and thermal noise in a fading channel for a strong direct signal ($A^2/2\sigma^2=1000$).
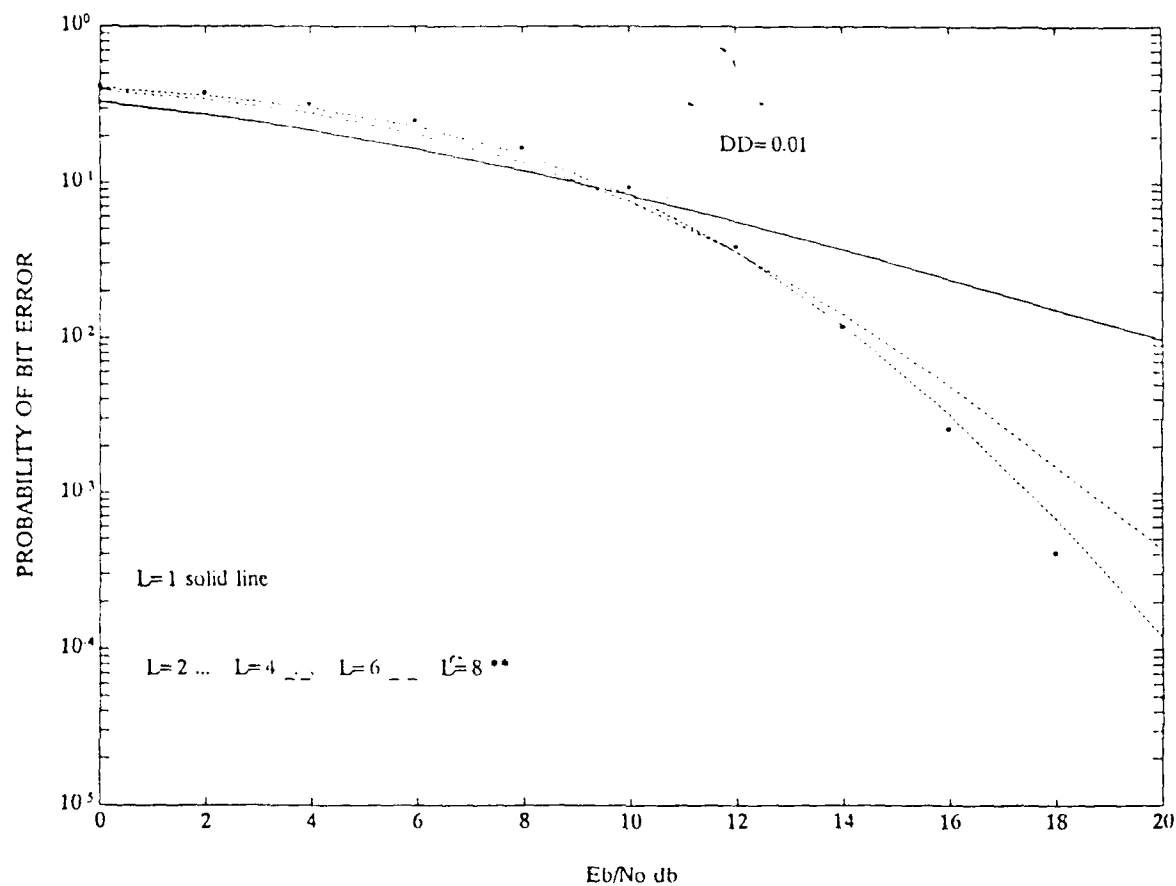
122

Figure 70. **Square-Law Detector Linear and Noise-Normalization Combining:** Performance of the linear and noise-normalization combining square-law detector receiver with diversity combining, and thermal noise in a fading channel for a strong direct signal $(A^2/2\sigma^2=1000)$.

123

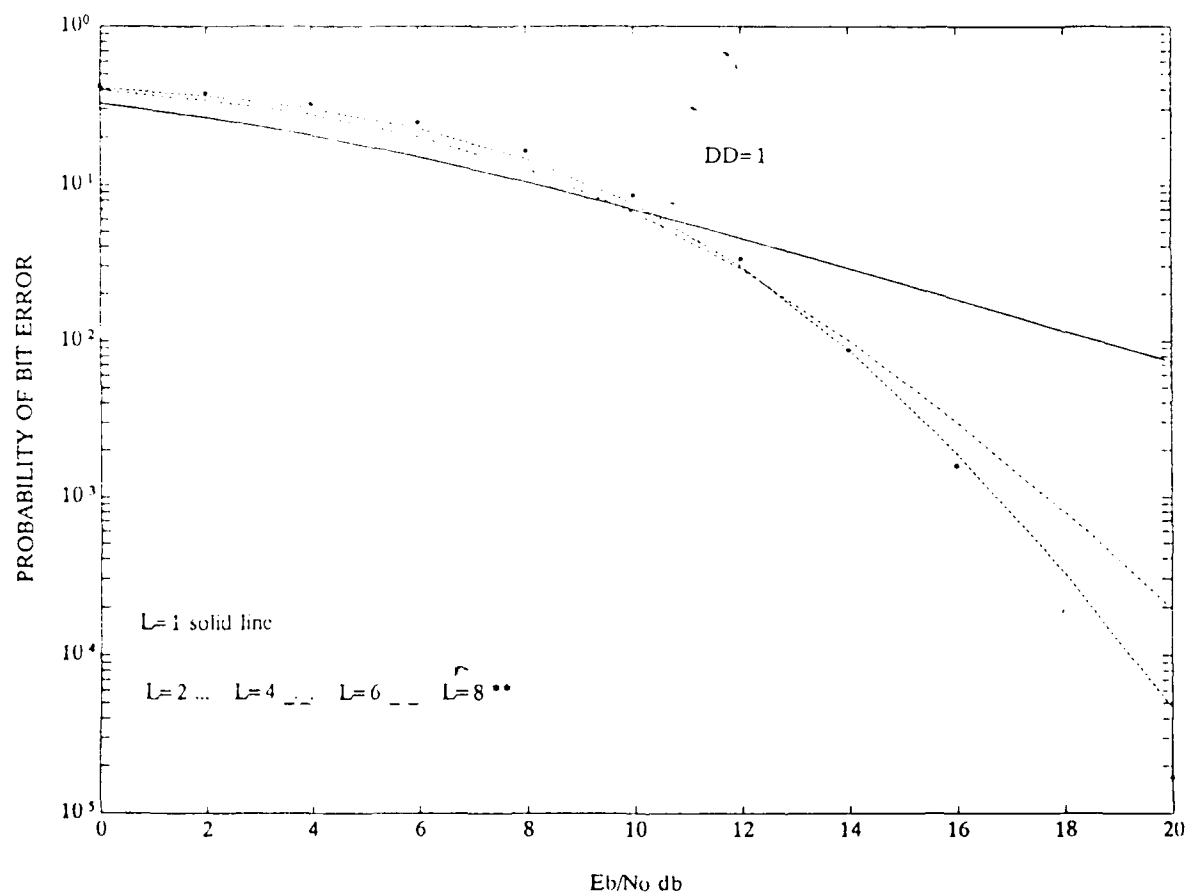**Figure 71. Envelope Detector Self-Normalization Combining:**
Performance of the self-normalization combining envelope
detector receiver with diversity combining, and thermal
noise in a fading channel for a diffuse signal
$(A^2/2\sigma^2=0.01)$.

Figure 72. Square-Law Detector Self-Normalization Combining: Performance of the self-normalization combining square-law detector receiver with diversity combining, and thermal noise in a fading channel for a diffuse signal $(A^2/2\sigma^2=0.01)$.

125

Figure 73. **Envelope Detector Self-Normalization Combining:**
Performance of the linear and self-normalization combining
envelope detector receiver with diversity combining, and
thermal noise in a fading channel for a signal with equal
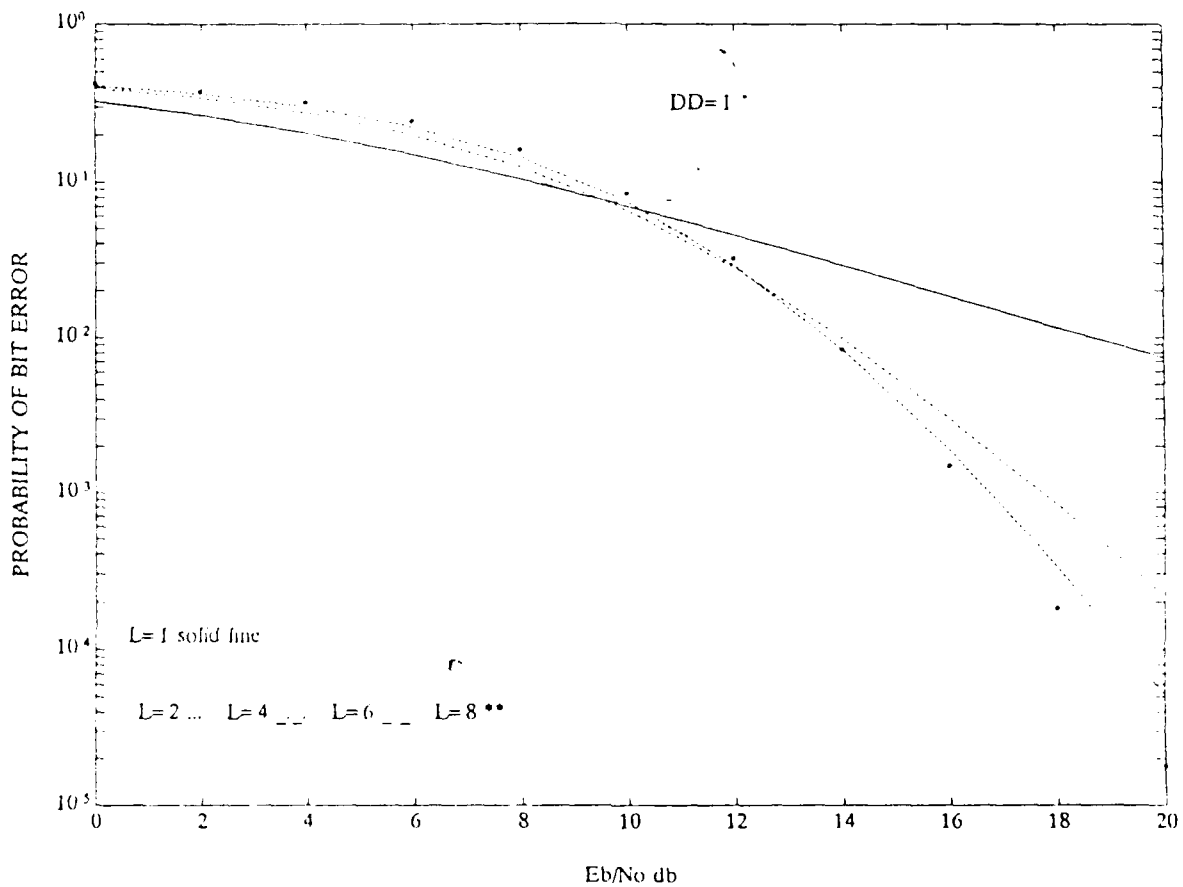direct and diffuse components ($A^2/2\sigma^2=1$).

126

Figure 74. Square-Law Detector Self-normalization
Combining: Performance of the self-normalization combining
square-law detector receiver with diversity combining, and
thermal noise in a fading channel for a signal with equal
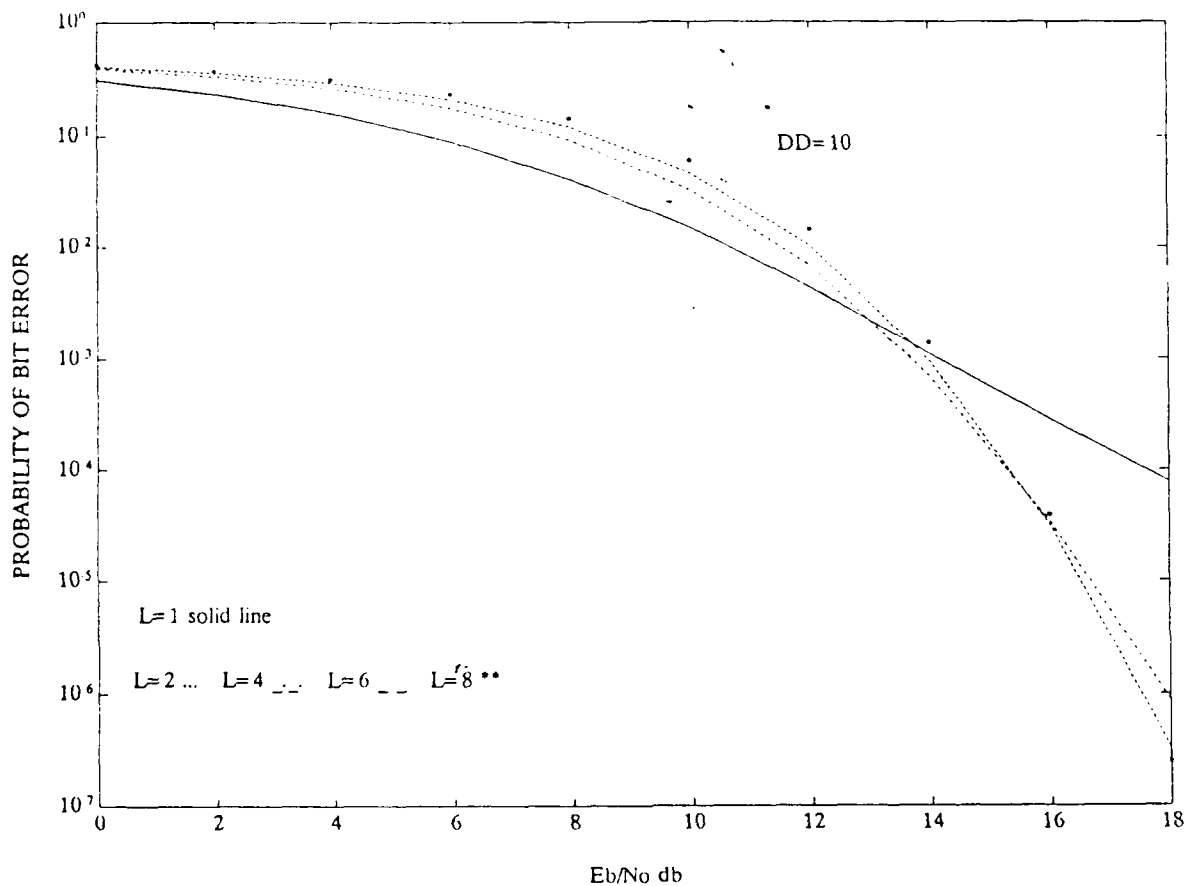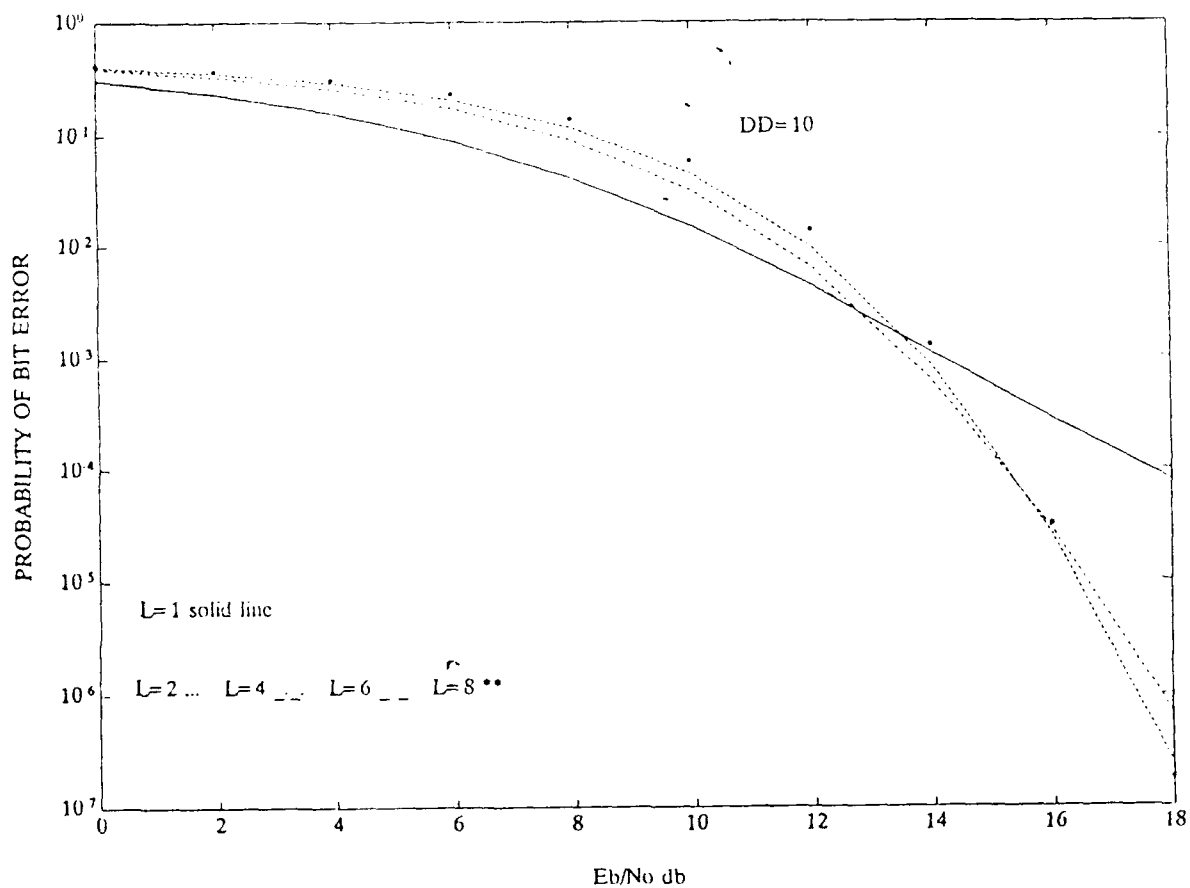diffuse and direct components $(A^2/2\sigma^2=1)$.

127

Figure 75. Envelope Detector Self-Normalization Combining:
Performance of the self-normalization combining envelope
detector receiver with diversity combining, and thermal
noise in a fading channel for a relatively strong direct
signal $(A^2/2\sigma^2=10)$.

128

Figure 76. Square-Law Detector Self-Normalization Combining: Performance of the self-normalization combining square-law detector receiver with diversity combining, and thermal noise in a fading channel for a relatively strong direct signal $(A^2/2\sigma^2=10)$.
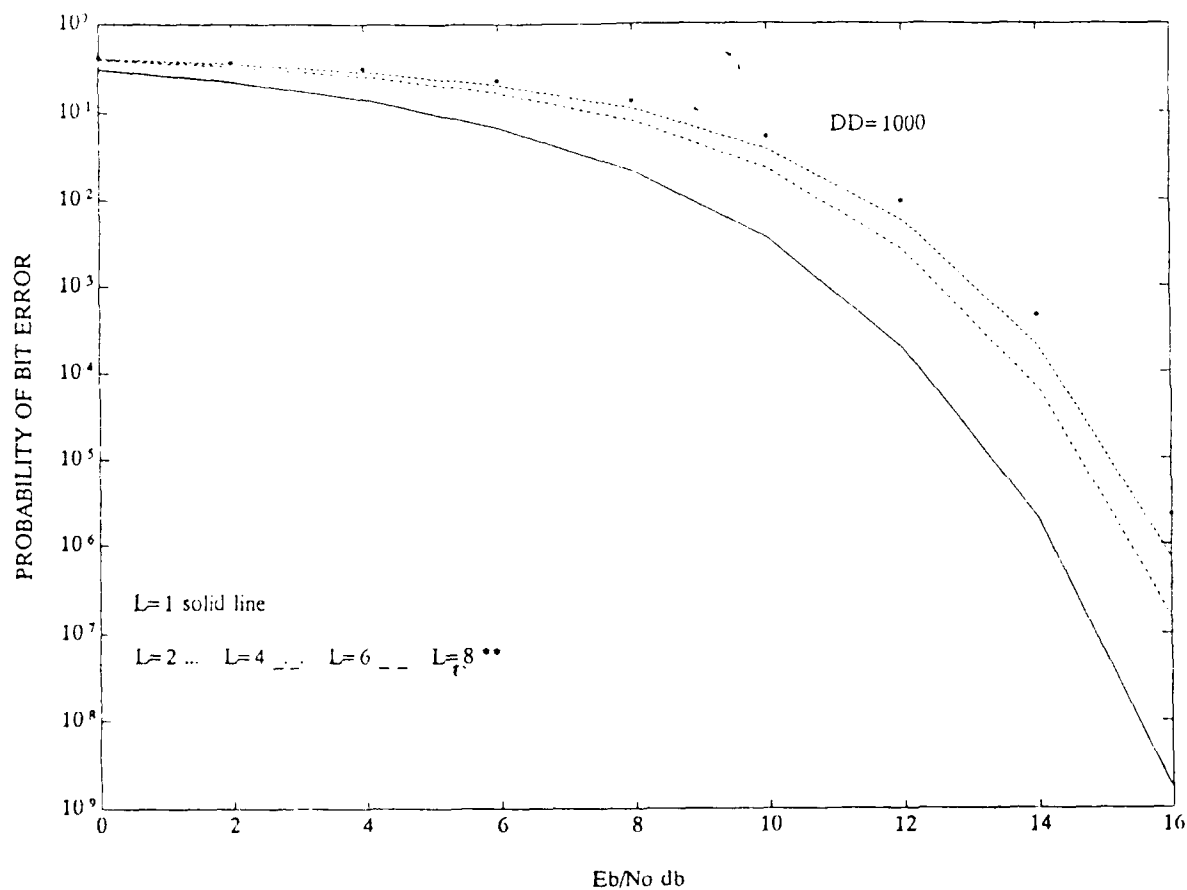
Figure 77. Envelope Detector Self-Normalization Combining: Performance of the self-normalization combining envelope detector receiver with diversity combining, and thermal noise in a fading channel for a strong direct signal $(A^2/2\sigma^2=1000)$.
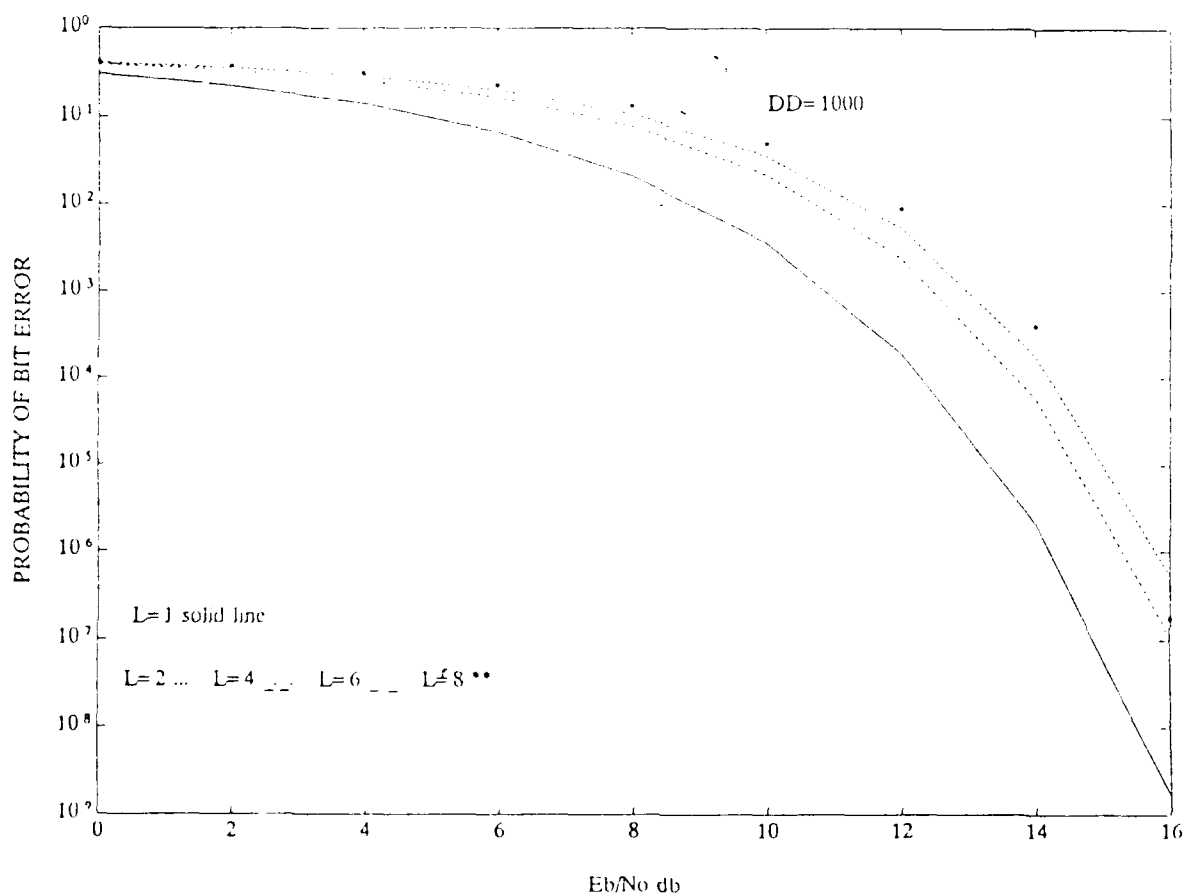
130

Figure 78. Square-Law Detector Self-Normalization

Combining: Performance of the self-normalization combining square-law detector receiver with diversity combining, and thermal noise in a fading channel for a strong direct signal $(A^2/2\sigma^2=1000)$.
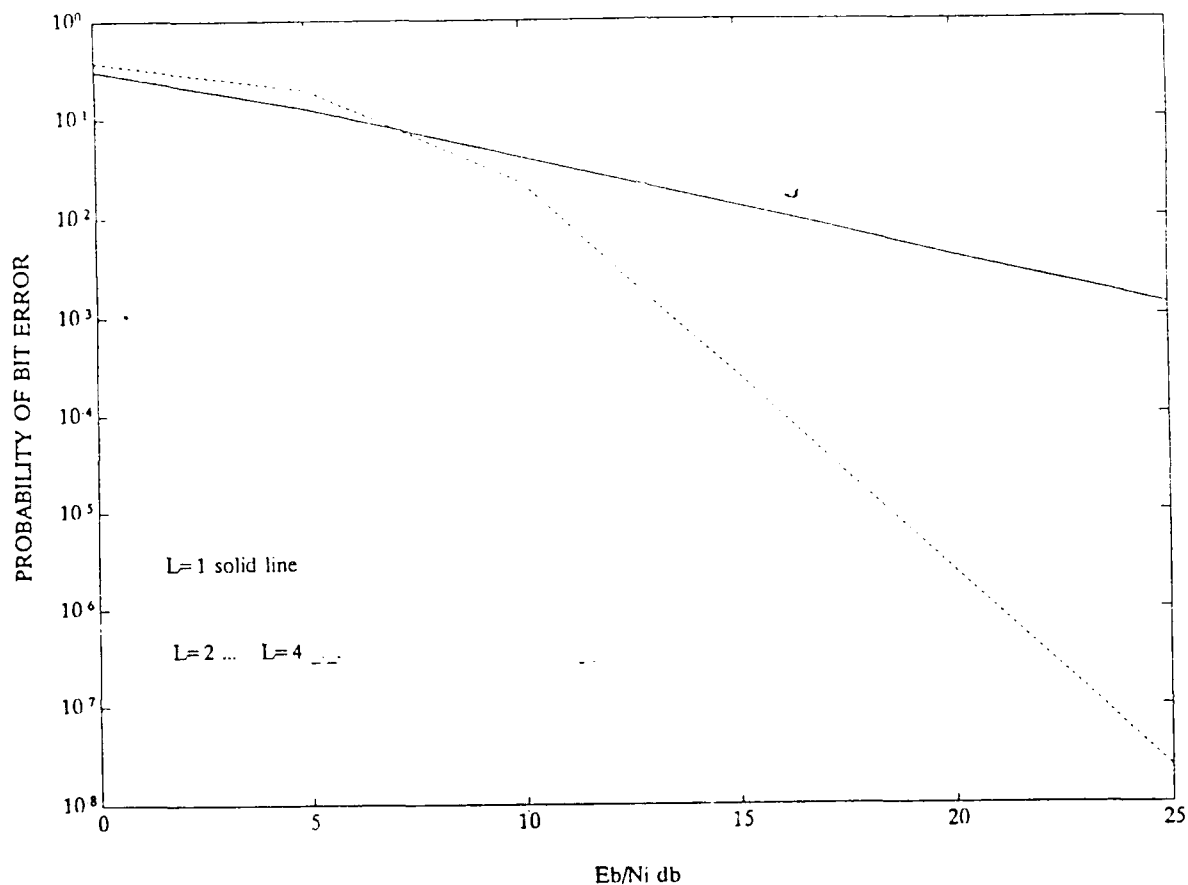
Figure 79. Envelope Detector Noise-Normalization Combining:
Performance of the noise-normalization combining envelope
detector receiver with diversity combining, and partial-band
interference in the absence of thermal noise, and in a
fading channel for a relatively strong direct signal
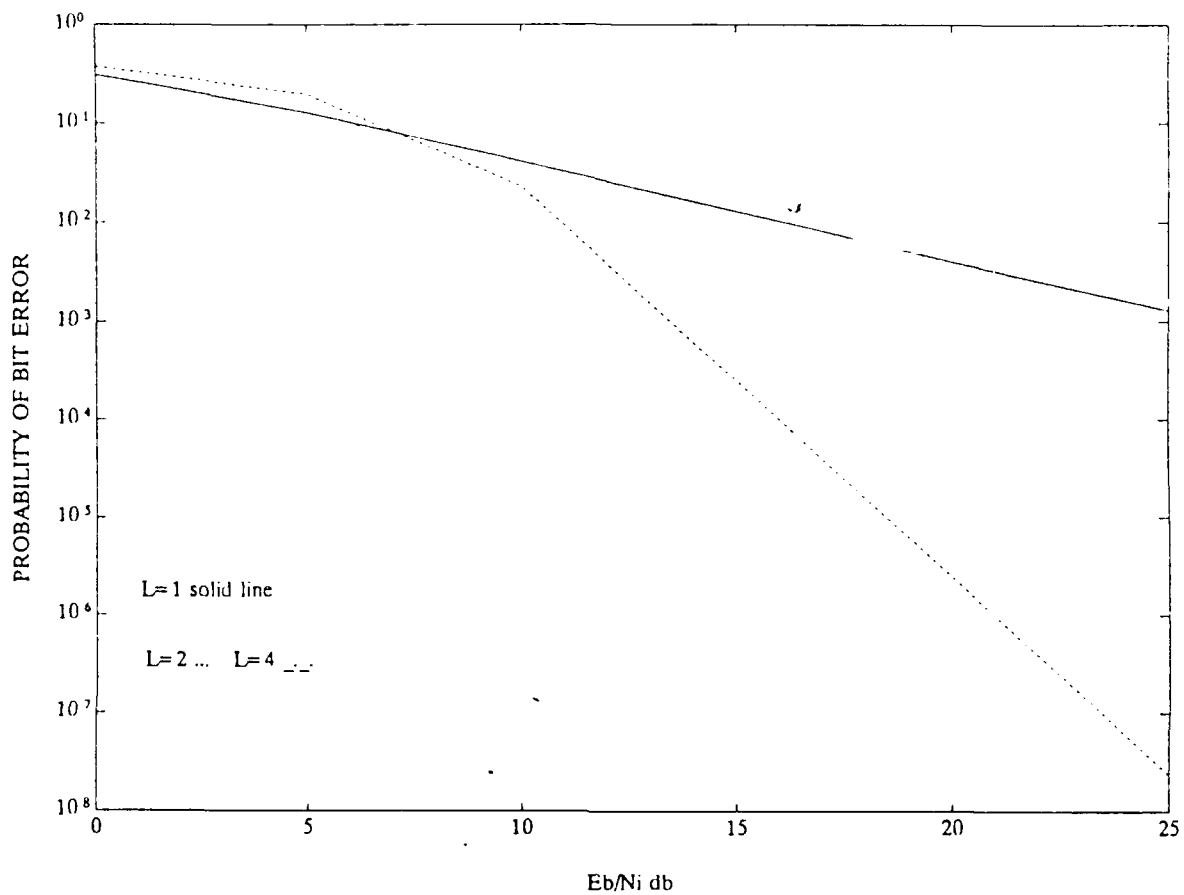$(A^2/2\sigma^2=10)$.

Figure 80. Square-Law Detector Noise-Normalization Combining: Performance of the noise-normalization combining square-law detector receiver with diversity combining, and partial-band interference, in the absence of thermal noise, and in a fading channel for a relatively strong direct signal $(A^2/2\sigma^2=10)$.
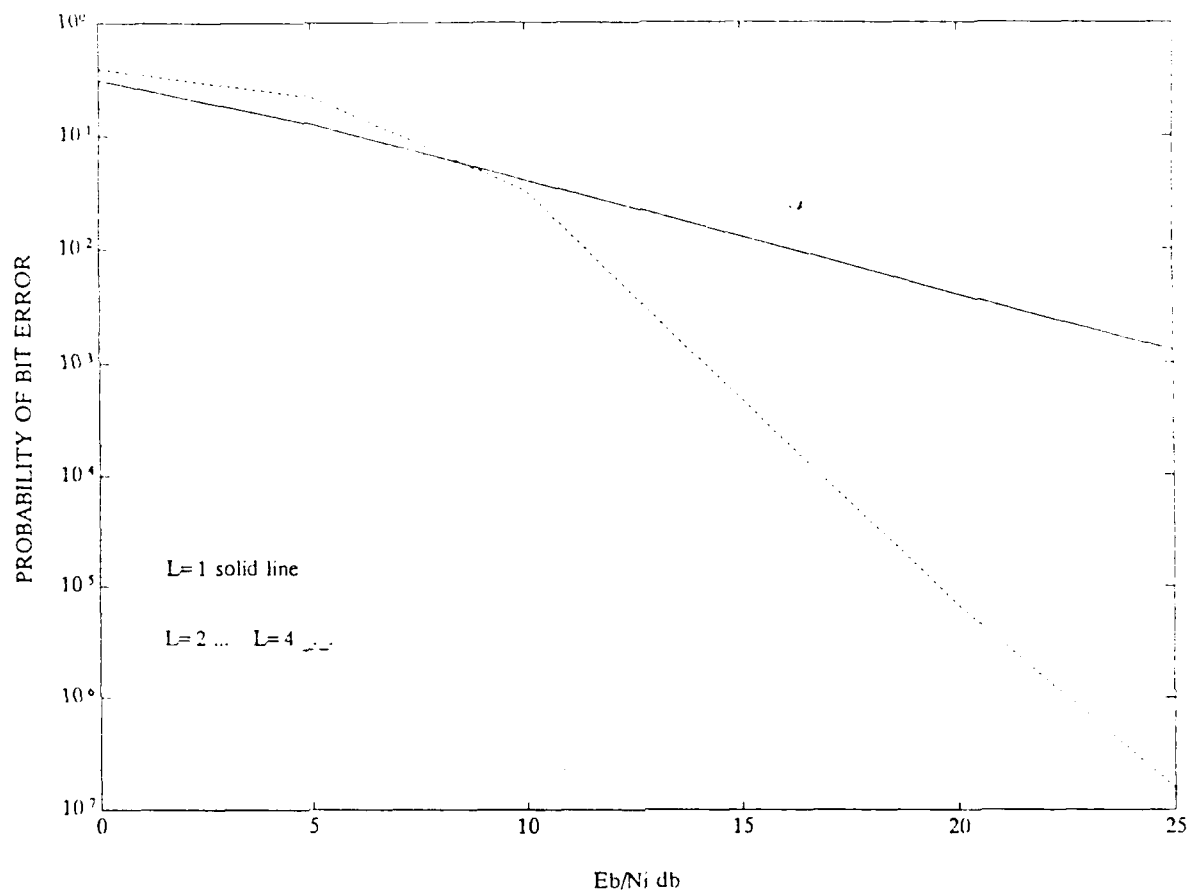
133

Figure 81. Envelope Detector Self-Normalization Combining:
Performance of the self-normalization combining envelope
detector receiver with diversity combining, and partial-band
interference in the absence of thermal noise, and in a
fading channel for a relatively strong direct signal
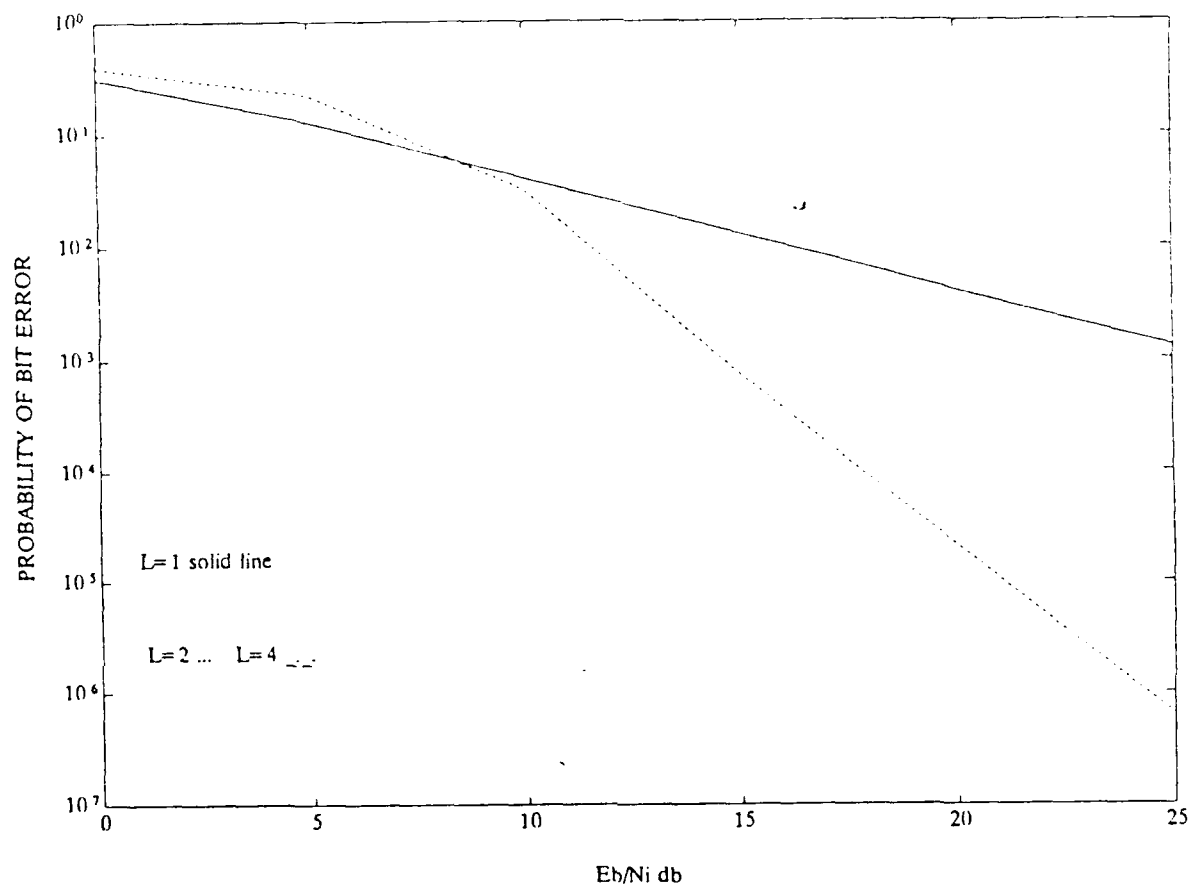$(A^2/2\sigma^2=10)$.

134

Figure 82. Square-Law Detector Self-Normalization Combining: Performance of the self-normalization combining square-law detector receiver with diversity combining, and partial-band interference, in the absence of thermal noise, and in a fading channel for a relatively strong direct signal $(A^2/2\sigma^2=10)$.

REFERENCES

1. R. C. Robertson, and T. T. Ha, 'Error Probabilities of Frequency-Hopped FSK with Self-Normalization Combining in a Fading Channel with Partial-Band Interference, ' IEEE Trans. Commun., forthcoming.

2. J. S. Lee, L. E. Miller, and Y. K. Kim, 'Probability of Error Analyses of a BFSK Frequency-Hopping System with Diversity Under Partial-Band Jamming Interference Part II: Performance of a Square-Law Nonlinear Combining Soft Decision Receivers, ' IEEE Trans. Commun., Vol. COM-32, no. 12, pp. 1245-1250, Dec. 1984.

3. R. C. Robertson, T. M. Clemons III, and T. T. Ha, 'Error Probabilities of Frequency Hopped MFSK with Noise-Normalization Combining in a Fading Channel with Partial-Band Interference, ' IEEE Trans. Commun., forthcoming.

4. J. S. Lee, R. H. French, and L. E. Miller, 'Probability of Error Analyses of a BFSK Frequency-Hopping System with Diversity Under Partial-Band Jamming Interference-Part I: Performance of Square-Law Linear Combining Soft Decision Receiver,' IEEE Trans. Commun., Vol. COM-32, no. 6, pp. 645-653, June 1984.

5. A. D. Whalen, Detection of Signals in Noise. New York: Academic Press, 1971.

6. G. N. Watson, 'A Treatise on the Theory of Bessel Functions, ' Macmillan, New York, 1945.

7. L. E. Miller, J. S. Lee, and A. P. Kadrichu, 'Probability of error analysis of a BFSK frequency-hopping system with diversity under partial-band jamming interference Part III: Performance of a square-law self-normalizing soft decision receivers, ' IEEE Trans. Commun., vol. COM-34, no. 7, pp. 669-675, July 1986.

8. G. A. Campbell, and R. M. Foster, 'Fourier Integrals for Practical Applications, Van Nostrad, Princeton, New Jersey, 1954.

9. J. S. Lee, L. E. MILLER, and R. H. French, 'The Analyses of Uncoded Performances for Certain ECCM Receiver Design Strategies for Multihops/Symbol FH/MFSK Waveforms, ' IEEE J. Sel. Areas Commun., vol. SAC-3, no. 2, pp. 611-621, Sep. 1985.

10.   W. C. Lindsey, 'Error Probabilities for Rician Fading Multichannel Reception of Binary and N-ary Signals, ' IEEE Trans. on Infor. Theory, Vol. IT-10, pp. 339-350, Oct. 1964.

11.   B. Solaiman,a. Glavieux, and A. Hillion, 'Error Probability of Fast Frequency Hopping Spread Spectrum with BFSK Modulation in Selective Rayleigh and Selective Rician Fading Channels,' IEEE Trans. Commun., Vol. 38, No. 2, pp. 223-240 Feb. 1990.